FLOOD RISK MAPPING USING ECONOMIC, ENVIRONMENTAL AND SOCIAL DIMENSIONS

A THESIS SUBMITTED TO
THE GRADUATE SCHOOL OF NATURAL AND APPLIED SCIENCES
OF
THE MIDDLE EAST TECHNICAL UNIVERSITY

BY

MURAT YEĞİN

IN PARTIAL FULFILLMENT OF THE REQUIREMENTS
FOR
THE DEGREE OF MASTER OF SCIENCE
IN
CIVIL ENGINEERING

NOVEMBER 2015

Approval of the thesis:

FLOOD RISK MAPPING USING ECONOMIC, ENVIRONMENTAL AND SOCIAL DIMENSIONS

submitted by **MURAT YEĞİN** in partial fulfillment of the requirements for the degree of **Master of Science in Civil Engineering Department, Middle East Technical University** by,

Prof. Dr. Gülbin Dural Ünver ____________________
Director, Graduate School of **Natural and Applied Sciences**

Prof. Dr. Ahmet Cevdet Yalçıner ____________________
Head of Department, **Civil Engineering**

Assoc. Prof. Dr. Elçin Kentel ____________________
Supervisor, **Civil Engineering Dept., METU**

Examining Committee Members:

Prof. Dr. Zuhal Akyürek ____________________
Civil Engineering Dept., METU

Assoc. Prof. Dr. Elçin Kentel ____________________
Civil Engineering Dept., METU

Assoc. Prof. Dr. Nuri Merzi ____________________
Civil Engineering Dept., METU

Assoc. Prof. Dr. İsmail Yücel ____________________
Civil Engineering Dept., METU

Assoc. Prof. Dr. Şahnaz Tiğrek ____________________
Civil Engineering Dept., Batman University

Date: 11.11.2015

I hereby declare that all information in this document has been obtained and presented in accordance with academic rules and ethical conduct. I also declare that, as required by these rules and conduct, I have fully cited and referenced all material and results that are not original to this work.

Name, Last name : Murat Yeğin

Signature :

ABSTRACT

FLOOD RISK MAPPING USING ECONOMIC, ENVIRONMENTAL AND SOCIAL DIMENSIONS

Yeğin, Murat

M.S., Department of Civil Engineering

Supervisor: Assoc. Prof. Dr. Elçin Kentel

November 2015, 147 pages

Flood is one of the most destructive natural hazards in Turkey. It is unavoidable but its impacts can be minimized by taking necessary precautions. Flood risk mapping is a developing concept and it is used to determine economically, environmentally and socially risky areas. European Council stipulated the member countries to prepare flood hazard maps showing extents of low, medium and high probability flood events. These maps should also be prepared for Turkey during the European Union harmonization process. For this purpose, this study aims to present a methodology for economic, environmental and social flood risk mapping and its demonstration on a case study. In this study, three risk dimensions (economic, environmental and social) are considered. Water depths are calculated using HEC-RAS while damages and risks are calculated in the ArcGIS environment. Water depths are used to calculate damages for each economic element at risk using depth-damage curves. Two different depth-damage curves from different countries are used in the calculations since depth-damage curves are not available for Turkey. Environmental and social risk maps are developed adapting a binary approach. In addition to this, vulnerability and resilience terms are integrated in these risk calculations. Finally, all three dimensions of risk are aggregated to develop overall risk maps. This procedure is demonstrated on part of Salkım Stream which is located in the Euphrates - Tigris Basin in the southern part of Turkey. Overall risk maps obtained for the study area successfully prioritized areas that require attention in terms of economic, environmental and social flood damages.

Keywords: Flood damage mapping, flood risk mapping, HEC-RAS, ArcGIS, vulnerability, resilience, depth-damage curves

ÖZ

EKONOMİK, ÇEVRESEL VE SOSYAL BOYUTLARI KULLANARAK TAŞKIN RİSK HARİTALANDIRILMASI

Yeğin, Murat

Yüksek Lisans, İnşaat Mühendisliği Bölümü

Tez Yöneticisi: Doç. Dr. Elçin Kentel

Kasım 2015, 147 sayfa

Türkiye'de taşkın en yıkıcı doğal afetlerden biridir. Taşkın önlenemez fakat gerekli tedbirler ile etkileri azaltılabilir. Taşkın risk haritalaması gelişmekte olan bir konsept olup, ekonomik, sosyal ve çevresel anlamda riskli alanları tespit etmek için kullanılmaktadır. Avrupa Birliği, taşkın yayılımı, su derinliği vb. değerleri gösteren düşük ihtimalli, orta ihtimalli ve yüksek ihtimalli taşkın tehlike haritalarının hazırlanmasını üye ülkeler için şart koşmaktadır. Avrupa Birliği'ne üye olma sürecinde bu haritalar Türkiye için de hazırlanmalıdır. Bu amaçla bu çalışma, örnek bir olay üzerinde taşkın risk haritalaması için bir metodoloji sunmayı hedeflemektedir. Bu çalışmada, üç risk (ekonomik, sosyal ve çevresel) boyutu dikkate alınmıştır. Su derinliklerini hesaplamak için HEC-RAS kullanılırken hasar ve riskler ArcGIS kullanılarak hesaplanmıştır. Bu su derinlikleri, derinlik-hasar eğrileri kullanılarak her bir risk elemanı için hasar hesaplanılmasında kullanılmıştır. Türkiye için geliştirilmiş derinlik-hasar eğrileri olmadığı için farklı ülkelerin kullandığı iki derinlik-hasar eğrisi hesaplamalarda kullanılmıştır. Çevresel ve sosyal risk haritaları iki değerli yaklaşım uyarlanarak geliştirilmiştir. Buna ek olarak hassasiyet ve direnç kavramları da hesaplara dahil edilmiştir. Son olarak, kapsamlı risk haritalarını geliştirmek için üç risk boyutu bir araya getirilmiştir. Bu prosedür Türkiye'nin güneyinde Fırat-Dicle Havzası'nda yer alan Salkım Deresi'nin bir kısmında uygulanmıştır. Çalışılan saha için elde edilen kapsamlı risk haritaları ekonomik, sosyal ve çevresel taşkın hasarı açısından dikkat edilmesi gereken yerleri başarılı bir şekilde öncelik sırasına koymuştur.

Anahtar Kelimeler: Taşkın hasar haritalaması, taşkın risk haritalaması, HEC-RAS, ArcGIS, hassasiyet, direnç, derinlik-hasar eğrileri

Dedicated to Kerem, Beren and my family

ACKNOWLEDGEMENTS

I would like to express my deep gratitude to my supervisor Assoc. Prof. Dr. Elçin Kentel for her invaluable and continuous contributions to this study. Every time I thought I could not accomplish this research, she encouraged and supported me. She made me believe that I can succeed everything if I want. This thesis could not be finished without her.

I am indebted to three most important women in my life at heart; to my mother Seyhan Yeğin for indulging my all whims and for her efforts to make me feeling good; to my sister Arzu Çelik for being my second mother and to my other sister Ayça Özkan for being the most important human that makes me who I am. I always feel their eternal love, support and confidence making me to move on. I am thankful to my father Mustafa Yeğin for his endless support too. I am also grateful to Hasan Çelik and Tolga Özkan for their motivation, especially to Tolga Özkan for being a brother instead of a sister's husband. This thesis would be meaningless without my family.

I want to thank to my special friends; to Sıla Gülgeç for being the partner of my dreams and being always with me despite living in the USA, to Hüseyin Erol and Bilgenur Keskin for their tremendous friendships and making me feel lucky, to Ayşe Önal for her precious and exact 'diagnoses', to İldem Kayışoğlu for making me smile everytime, to Ecem Gürkan for making the work hours very hilarious and tolerable and finally to Ferit Güvenir Yalçın for his insightful, unlimited and invaluable fellowship making me feeling great even in the bad times. They all have contributions to this study.

I would like to thank to Eser Project & Engineering employees for providing the material used in the study and I would like to express my gratitude to Erges Engineering Consulting employees for their toleration throughout the research.

TABLE OF CONTENTS

APPENDICES

LIST OF FIGURES

FIGURES

LIST OF TABLES

TABLES

LIST OF ABBREVIATIONS

1-D	One Dimensional
2-D	Two Dimensional
AHP	Analytic Hierarchy Process
ANP	Analytic Network Process
CAD	Computer Aided Design
CORINE	Coordination of information on the environment
DEA	Data Envelopment Analysis
DEM	Digital Elevation Model
EC	European Council
ELECTRE	The Eliminating and Choice Translating Reality
FESWMS	Finite Element Surface Water Modeling System
GAIA	Geometrical Analysis for Interactive Aid
GIS	Geographic Information System
HEC-RAS	Hydraulic Engineering Centers River Analysis System
HIS-SSM	Hoogwater Informatie Systeem-Schadeen Slachtoffer Module
ISO	International Organization for Standardization
Macbeth	Measuring Attractiveness by a Categorical Based Evaluation Technique
MAUT	Multi-Attribute Utility Theory
MCA	Multicriteria Analysis
PROMETHEE	Preference Ranking Organization Method for Enrichment Evaluations

SWMM	Storm Water Management Model
TOPSIS	Technique for Order Preference by Similarity to Ideal Solution
UK	United Kingdom
US	United States
UTADIS	Utilities Additives Discriminants

LIST OF SYMBOLS

$\alpha_i(h_r)$	Stage-damage function
D	Damage
D_i^j	Damage at cell j for return period TR_i
$D_{max,i}$	Maximum damage for an object or land use category i
ENR^j	Environmental risk at cell j
ER^j	Economic risk at cell j
fe^j	Flag to determine if an environmental element at risk exists at cell j
fs^j	Flag to determine if a social element at risk exists at cell j
fsl^j	Flag to determine range of the slope at cell j
fv^j	Flag to determine if vegetation cover or impervious surface exist at cell j
h_i^j	Water depth at cell j for return period TR_i
i	Index for the return period
m	Index for the risk dimension
n	Total number of risk dimensions
N	Total number of cells in the study area
$NOENR^j$	Normalized overall environmental risk at cell j
$NOER^j$	Normalized overall economic risk at cell j
$NOSR^j$	Normalized overall social risk at cell j
NOR_m^j	Normalized overall risk of risk dimension m at cell j
$OENR^j$	Overall environmental risk at cell j

OER^j	Overall economic risk at cell j
OSR^j	Overall social risk at cell j
P_i	Probability of the flood event which has a return period TR_i
Q_2	Discharge of a 2 year return period flood
Q_5	Discharge of a 5 year return period flood
Q_{10}	Discharge of a 10 year return period flood
Q_{25}	Discharge of a 25 year return period flood
Q_{50}	Discharge of a 50 year return period flood
Q_{100}	Discharge of a 100 year return period flood
Q_{500}	Discharge of a 500 year return period flood
Q_{1000}	Discharge of a 1000 year return period flood
R	Resilience factor
SR^j	Social risk at cell j
TR_i	Return period of a i year flood event
$TRisk^j$	Total risk at cell j
V	Vulnerability factor

CHAPTER 1

INTRODUCTION

Floods are one of the most common and destructive hazards in the world. It cannot be prevented but good flood forecasting and taking necessary flood protection measures may reduce its impacts. Hence exploring flood vulnerable areas gain importance from day to day. Flood mapping studies play crucial role to identify flood prone areas. There are different kinds of flood maps in the literature: flood danger maps, flood hazard maps, flood vulnerability maps, flood damage maps, flood risk maps etc. For obtaining flood maps, first hydraulic characteristics of the flood events should be calculated. European Union Flood Directive [2007/60/EC] forces the member states to prepare flood hazard maps and flood risk maps for low, medium and high probability floods. The Directive stipulates preparation of flood extent maps. Furthermore, water depth maps and water velocity maps are expected to be prepared where appropriate. The majority of the European Countries have flood extent maps: Flanders (Belgium), France, Switzerland, England, Romania, Slovakia, Hungary, Ireland, Lithuania, Czech Republic, Slovenia, Germany, Spain, Italy, Austria, Luxembourg, Poland, Norway, Portugal, Sweden, Croatia, Denmark and Latvia. On the contrary, limited number of European Countries have flood depth maps such as Flanders, Switzerland, Netherlands, Germany, Finland, Luxembourg and Poland. Moreover, very few countries have developed flood velocity maps. These maps can be used to minimize flood impacts by governments such as emergency planning, spatial planning, awareness raising, insurance, flood management etc. Since Turkey is a country where many floods have been experienced and high costs have been paid, preparation of these maps is also crucial for Turkey to decrease the effects of floods.

Majority of the studies focus on the economic impacts of floods because economic loss is the easiest to calculate and may be the most visible one. However, in addition to economic consequences, social and environmental consequences should also be included in the risk analysis since they might be more destructive than the economic consequences such as people's death, extinction of species and valuable natural resources, etc. It is very difficult to include these dimensions in the risk analysis but a number of approaches have been proposed in the literature. Although there is not an agreed and established method, binary approach is one of the commonly used ones to evaluate social and environmental dimensions of flood risk. To evaluate consequences of flood more accurately, new concepts might be introduced in the risk analysis such as vulnerability, exposure, resilience, coping capacity etc. These terms are used to identify elements with more significant or critical risks.

In the light of these information, this study initially aims to apply a method to generate overall risk maps including economic, environmental and social dimensions and demonstrate its application on a small village in Turkey. Another goal of this study is to include rarely used concepts such as vulnerability and resilience into the analysis. The study is expected to be a guide for flood risk mapping studies including social and environmental dimensions and help in prioritizing areas which require mitigation measures.

The following organization is adopted within this study. Chapter 2 presents literature review about flood mapping studies. Flood map types and elements at risk are introduced in detail in the same chapter. Finally, multicriteria decision analysis and various methods used in flood mapping studies are discussed. In Chapter 3, information about the study area is given such as population of the village, map of the studied area, hydraulic characteristics of the stream etc. Chapter 4 presents the methodology of the study step by step. In the first section, possible elements at risk at the study area are discussed. In the second section, the procedure of calculation of water depths is given. Then, obtaining of flood damage maps is presented. In the fourth section, steps for damage and risk calculations are given. In the next section the procedure of obtaining risk maps is presented. The integration of each risk map is given in section six while economic risk mapping with a different approach is explained in the last section. In Chapter 5, the results and discussion of the study is presented. Selected elements at risk, calculated water depths, flood damage maps, damage-exceedance probability curves, flood risk maps and integrated multicriteria risk maps are given in this chapter. Finally, Chapter 6 concludes the study by highlighting the major findings, discussing the limitations, and making suggestions for future researches and applications.

CHAPTER 2

LITERATURE REVIEW

Floods are one of the most destructive natural disasters. Annual deaths from various disasters in 57 nations from 1980 to 2002 are evaluated by Matthew E. Kahn (2003) (see Table 2.1). According to Table 2.1, floods are the third deathful natural disaster not only in the world but also in Turkey. Hence, creating flood maps has gained importance from day to day. The aim of this study is to create an integrated flood risk map for a selected basin in Turkey by using multicriteria decision-making analysis. The flowchart of the procedure that will be followed in this study is given in Figure 2.1.

Table 2.1: Natural Disaster Statistics for Sample Nations (Kahn, 2003)

Country	Average Deaths per Earthquake	Average Deaths per Extreme Temperature Event	Average Deaths per Flood	Average Deaths per Land Slide	Average Deaths per Wind Storm
Algeria	195.44	.	91.42	15.00	2.00
Argentina	3.00	7.25	9.71	.	4.56
Australia	7.67	6.83	5.44	14.00	1.74
Austria	.	0.00	3.71	23.25	1.07
Bangladesh	6.00	144.64	257.51	.	3574.08
Bolivia	41.67	7.50	32.39	37.25	4.00
Brazil	1.00	28.00	39.58	39.02	16.00
Canada	.	0.00	2.86	.	8.60
Chile	40.00	0.67	32.29	86.50	16.70
China	43.52	33.47	453.23	71.41	77.19
Colombia	194.52	.	46.13	76.68	9.00
Costa Rica	7.00	.	4.00	7.00	21.00
Denmark	.	0.00	.	.	2.71

Table 2.1. continued

Country	Average Deaths per Earthquake	Average Deaths per Extreme Temperature Event	Average Deaths per Flood	Average Deaths per Land Slide	Average Deaths per Wind Storm
Egypt	190.33	19.00	154.25	34.00	24.00
El Salvador	566.50	.	62.44	22.00	98.40
France	.	7.60	5.95	9.80	8.89
Greece	14.32	216.80	6.00	.	16.67
Guatemala	6.36	0.00	87.22	47.33	130.67
Haiti	.	.	17.90	0.00	243.71
Honduras	1.00	.	32.46	10.00	2953.80
Hong Kong	.	10.00	3.29	1.00	5.49
India	2898.46	316.82	371.92	86.05	294.76
Indonesia	100.76	.	52.00	49.64	0.67
Iran	1222.50	.	62.57	26.50	39.00
Ireland	.	.	1.00	.	7.00
Italy	267.04	5.00	26.96	15.25	7.33
Japan	246.38	.	47.39	26.11	16.16
Kenya	0.00	.	45.13	16.00	50.00
Korea Rep.	.	33.50	68.60	22.00	55.80
Madagascar	.	.	0.00	.	61.53
Malawi	9.00	.	52.30	.	.
Malaysia	.	.	9.43	38.00	90.67
Mexico	806.21	92.50	49.13	24.67	47.46
Mozambique	.	.	100.83	87.00	76.17
Nepal	404.50	30.00	227.41	116.25	19.30
New Zealand	1.00	0.00	0.17	.	2.00
Nicaragua	62.00	.	8.83	.	453.63
Nigeria	.	39.00	32.81	8.00	100.00
Pakistan	53.70	95.56	175.84	31.93	81.88
Panama	30.00	.	2.71	.	14.00
Papua N. G.	7.50	.	7.50	87.50	23.50
Peru	22.90	21.00	86.35	69.50	59.00
Spain	0.00	18.33	13.06	84.00	8.30
Sri Lanka	.	.	26.68	65.00	2.50
Switzerland	.	0.00	0.88	9.33	1.50

Table 2.1. continued

Country	Average Deaths per Earthquake	Average Deaths per Extreme Temperature Event	Average Deaths per Flood	Average Deaths per Land Slide	Average Deaths per Wind Storm
Spain	0.00	18.33	13.06	84.00	8.30
Sri Lanka	.	.	26.68	65.00	2.50
Switzerland	.	0.00	0.88	9.33	1.50
Taiwan	383.00	.	20.50	14.00	30.93
Tanzania	1.00	.	21.81	13.00	4.00
Thailand	.	.	80.93	39.00	50.08
Turkey	447.97	19.25	26.02	69.00	9.50
UK	0.00	16.00	1.22	.	10.18
United States	6.59	105.94	8.64	.	20.80
Venezuela	19.30	.	1016.97	96.00	54.00
Vietnam	.	.	122.85	85.83	212.99
Average	206.50	42.09	75.64	44.12	165.80

Note: The “.” indicates that the nation did not experience this natural disaster.

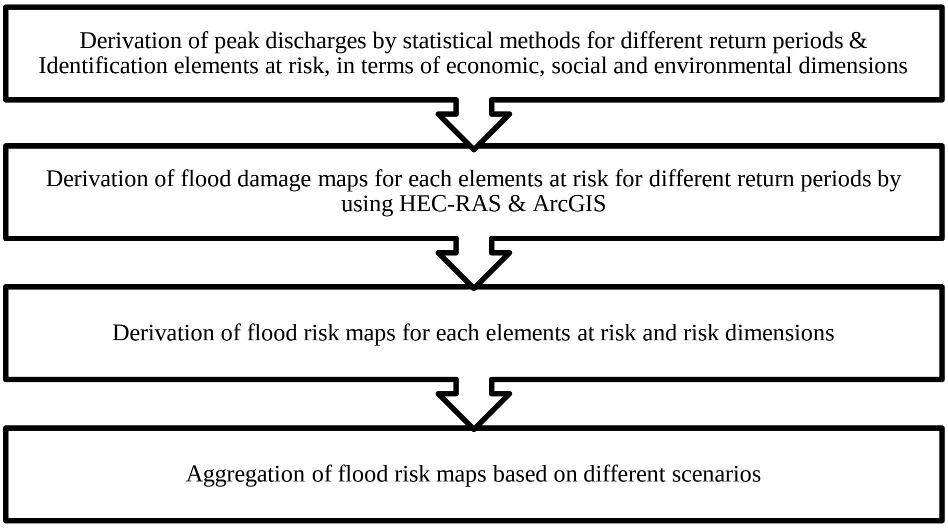

Figure 2.1: Flowchart of the Procedure

2.1 Flood Hazard Mapping

The intensity of flood events and the exceedance probabilities of associated events are used to illustrate flood hazards. The hazard map which shows the inundation area of a certain return period flood event is the most typical map type. An example flood hazard map is given in Figure 2.2 (Merz et al., 2007). In addition to inundation area; other characteristics of a flood such as flow velocities, water depths, durations of flood, rise rates, time of occurrences, contamination etc. can be used to create flood hazard maps. The inundated area can be used to determine which elements will be affected from that specific flood and they are called "elements at risk". Inundation depth has the most powerful influence on the amount of damage. Inundation duration is important for damages to buildings. On the other hand inundation velocity is important for the flash floods. Inundation rise rate is important for warnings and evacuation to reduce damage effects while the time of occurrence is important especially for agricultural products (FLOODsite, 2006).

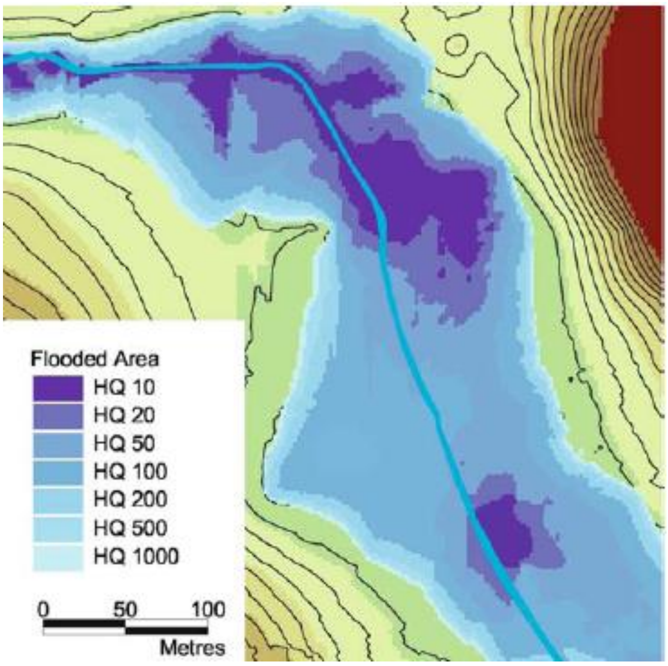

Figure 2.2: Flood Hazard Map which Shows the Inundation Area for Different Return Periods of Flood Events (Merz et al., 2007)

According to the European Flood Directive [2007/60/EC], flood hazard maps (i.e. flood extent or flood inundation maps) are mandatorily created by member states. Affected areas by floods with a low probability (extreme event), a medium probability (return period > 100 years) and a high probability (return period ≈ 10 years) have to be depicted on these maps. In addition to flood extent, water depth and flow velocity information are encouraged to be mapped when possible. The list of flood maps generated by European countries can be seen in Table 2.2 (De Moel et al., 2009). Commonly used flood parameters by European countries are flood extent, historical floods and water depth. Hence, in this study flood extent map will be generated and used to identify elements at risk in the study region.

Table 2.2: Types of Flood Maps Generated by European Countries (De Moel et al., 2009)

Country	Flood Map Type					
	Historical	**Flood Extent**	**Flood Depth**	**Rate of Rise**	**Velocity**	**Propagation**
Flanders	x	x	x	x		
France	x	x				
Switzerland		x	x			
Netherlands			x		x	
G. Britania		x				
Romania		x				
Slovakia		x				
Wallonia						
Hungary		x				x
Ireland	x	x				
Lithuania	x	x				
Czech Rep.	x	x				
Slovenia		x				
Estonia	x					
Greece	x					
Germany		x	x			
Spain	x	x				
Italy		x				
Finland	x		x			
Austria		x			x	
Luxembourg		x	x		x	

Tablo 2.2. continued

Poland		x	x			
Norway		x				
Portugal		x				
Sweden		x				
Crotia		x				
Denmark		x				
Latvia		x				

2.2 Flood Inundation Mapping

Flood inundated areas can be identified by one dimensional (1-D) or two dimensional (2-D) hydraulic models such as MIKE11, HEC-RAS, FLO-2D etc. Limited number studies have been conducted using 1-D and 2-D models for Turkey (Bozoğlu, 2015; Nimaev, 2015; Keskin, 2012; Şahin, 2012; Usul and Turan, 2006).

Nimaev (2015) compared the results of two different 2-D hydraulic models in his thesis study which are Lisflood-FP and MIKE 21. Lisflood-FP generated larger water depths while MIKE 21 concluded with higher inundated area. He concluded that the theoretical backgrounds of the models might be the underlying reason. In addition to this, Nimaev (2015) investigated the effects of scale and roughness on the results of the models. He concluded that the variation of these terms resulted in significant changes in the model results such as flood depths, velocities and inundation extents.

There are advantages and disadvantages of 1-D and 2-D models. A number of researchers studied these two different types of models and identified their strong and weak points.

FLOODsite (2006) compared one-dimensional models and two-dimensional models in their study and they stated advantages of 1-D hydraulic models over 2-D hydraulic models as follows:

- They are relatively simple and not extremely data-intensive.
- They are relatively fast.
- Implementation due to the GIS-coupling is relatively easy.

On the other hand, disadvantages of 1-D hydraulic models over 2-D hydraulic models are identified as follows:

- Owing to the method of combination of the cross-sections, they contain a certain degree of uncertainty
- Complex and highly detailed description of the flow process is not permitted.

Horritt and Bates (2002) compared one-dimensional models with two-dimensional models, including HEC-RAS, LISFLOOD-FP and TELEMAC-2D on a 60 kilometer reach of the river Severn. The results showed that, HEC-RAS and TELEMAC-2D produced acceptable results for inundated area while LISFLOOD-FP must be calibrated to produce acceptable results for inundated area.

Cook (2008) compared two-dimensional FESWMS model with one-dimensional model HEC-RAS for different digital elevation models. He stated that for the higher resolution digital elevation models (DEM), HEC-RAS produced similar inundation areas with FESWMS model when cross-sections were added to the simulations. On the other hand, for the lower resolution DEMs, inundation areas became similar when cross-sections were removed from HEC-RAS model. He stated that the advantage of HEC-RAS simulation was its fastness. On the other hand, the advantage of FESWMS simulation was its continuous floodplain.

Stepinski (2011) modeled floodplains under storm surge conditions by using both one-dimensional and two-dimensional models. HEC-RAS and XPSWMM were used in that study. She stated the advantages of HEC-RAS as effective riverine floodplain modelling, fast model run time and accepted use of the modeling engineering practice. On the other hand, she stated the advantage of XPSWMM as simulation riverine flooding with a 1D channel as well as overbank and overland flooding with a 2D model.

Fosu et al. (2012) used HEC-RAS in their study. River inundation and hazard mapping of Susan River was explored through the study. HEC-RAS was chosen based on the fact that it is an open source application and its geometric data input and simulation can be done in the GIS environment.

Hicks and Peacock (2005) studied the suitability of the unsteady flow simulation capability in HEC-RAS to the application of combined flood routing and flood level forecasting. This was explored through an example application to the Peace River in Alberta, for a significant open channel flood event that occurred in 1987. Despite the neglect of the large bed discontinuity at the Vermilion Chutes and estimation of channel resistance based on limited historical data rather on model calibration, HEC-RAS model provided good results in terms of discharges and water levels. Based on the case study conducted by Hicks and Peacock (2005), it can be deduced that flood level forecasting and flood routing can be easily performed by HEC-RAS.

İrvem and Topaloğlu (2012) evaluated flood risk of Orontes River Basin using Multicriteria Decision Analysis. Rainfall, topography, size of sub-watersheds and soil types were chosen for flood risk evaluation. The factors were ranked according to their relative importance to each other and multicriteria decision analysis was performed by adding the weighted flood rankings of the causative factors. The comparison between obtained flood map and the map, produced from field measurement, showed satisfactory results.

Vazifedoost et al. (2014) compared HEC-RAS and MIKE11 models in their study. They aimed to select the best hydraulic model for Tajan River Basin. Water depth and water level results by both models were similar to each other. They concluded that flood mapping by both hydraulic models were very close to each other.

A number of flood inundation studies have been performed in Turkey as well. Some recent ones are summarized here. Doğan et al. (2013) investigated flood inundation maps for Lower Sakarya River. The 100 year return period flood of last 113 km of the Lower Sakarya River were performed including dam break analysis of Yenice Dam. HEC-RAS was used to calculate water depths.

Usul and Turan (2006) produced flood inundation maps for Ulus Basin by using MIKE 11 hydraulic model. The highest water depths were obtained for observed 1991 flood, 25-year, 50-year and 100-year return period floods. The results were very close to each other. Furthermore Usul (n.d.) used HEC-RAS for the same basin and obtained very similar results with MIKE 11.

Uçar (2010) obtained flood hazard map by using GIS and a hydraulic model for Trabzon Değirmendere Basin in his master thesis. HEC-RAS was used as the hydraulic model. As a consequence he proposed structural and non-structural measures for the basin.

In addition to the above stated advantages, 1-D model HEC-RAS is open to public so it is used by many researchers in recent years (Brych et al., 2002; Salajegheh et al., 2009; Sredojevic and Simonovic, 2009; Ackerman et al., 2010; Lombard, 2011; Saville, 2011; Yerramilli, 2012; Nut and Plermkamon, 2013; Kute et al., 2014; Silva et al., 2014; Bashar et al., 2014). Thus, in this study HEC-RAS is selected to identify flood inundated areas. Digital elevation model, cross-sections through the watershed and flow data are the required inputs for identification of flood inundated areas by HEC-RAS.

2.3 Flood Risk Mapping

Risk analysis is used in different areas such as earthquake risk, flood risk, forest fire risk etc. However, the general definition and formulation of the risk is the same for all areas. According to ISO 31010, probability of a hazard and the consequences of that hazard create the related risk. Similarly, in the context of flood risk management, flood risk is defined in the European Flood Directive [2007/60/EC] as the combination of the probability of a flood event and of the potential adverse consequences to human health, the environment and economic activity associated with the event. Hence, flood risk can be formulated as follows:

$$Flood\ Risk\ =\ Probability\ x\ Consequence \tag{1.1}$$

In here, probability is the probability corresponding to the return period of the flood event and the consequence of the flood is the damage associated with the flood event. There are different methods to calculate flood damage in the literature. The objective of the study conducted by Meyer et al. (2009) was to provide an integrated assessment and mapping of economic, environmental and social flood risks. The damage was calculated differently for each dimension. The social damage was calculated for the population and for social hot spots. While affected number of people was calculated by intersecting population density map and inundation map, affected social hot spots were determined by a simple Boolean yes/no damage function. The economic risk, on the other hand, was calculated by depth-damage functions that are specific to different sectors. Finally, the environmental damage was calculated by a simple Boolean yes/no damage function.

Kubal et al. (2009) adapted multicriteria flood risk assessment approach - that was previously developed for the more rural Mulde river basin (Meyer et al. 2009), to Leipzig in Germany. The study focused on a specific urban-type set of economic, social and ecological flood risk criteria. These criteria were classified as binary and non-binary. Binary criteria were calculated by using Boolean 0 and 1 values. On the other hand, for all non-binary criteria, the damage function from HOWAS-database, the biggest database on flood damages in Germany, was used. The damage, D for water level h_w is calculated as follows:

$$D = \frac{27 * \sqrt{h_w}}{100} \tag{1.2}$$

Jonkman (2008) developed a model in the Netherlands for the estimation of damage caused by floods. In this model, only the modelling of direct and indirect economic damage were considered. The environmental damage and the social damage were not considered in the Jonkman's model. Direct economic damage was calculated by using:

$$D = \sum_{i}^{m} \sum\nolimits_{r}^{n} \alpha_i \,(h_r) * D_{max,i} * n_{i,r} \tag{1.3}$$

where $D_{max,i}$ is the maximum damage for an object or land use category i, i is the damage or the land use category, r is the location in flooded area, m is the number of damage categories, n is the number of locations in flooded area, h_r is the hydraulic characteristics of the flood at a particular location, $\alpha_i(h_r)$ is the stage-damage function that expresses the fraction of maximum damage for category i as a function of flood characteristics at a particular location r ($0 \leq \alpha_i(h_r) \leq 1$) and $n_{i,r}$ is the number of objects of damage category i at location r. The study area divided into grids and they were represented by r term. For each of the damage categories, a specific stage-damage function was estimated by using historical damage data and associated water depths.

Ozcan et al. (2008) aimed to determine risky areas in Sakarya sub-basin using remotely sensed data and GIS. They modeled the parameters of the basin using HEC-RAS. Risky areas were determined using 100-years return period flood. They calculated the total area under the risk and the classification of it (agricultural or residential).

The study conducted by Te Linde et al. (2011) estimated the current and future fluvial flood risk in 2030 for the Rhine basin based on various scenarios. The potential damage was calculated by using the damage model, Damage Scanner. The model was based on water depth and land use. Each land use category had its own damage functions. Furthermore, this model reflects direct tangible damages. Direct intangible damages are not included in the model. The model also includes 5% of indirect damages as a surcharge on direct damages. This model used stage-damage functions which were derived from HIS-SSM model, the standard damage model used in the Netherlands. The stage-damage function used by Ward et al. (2011) is given in Figure 2.3.

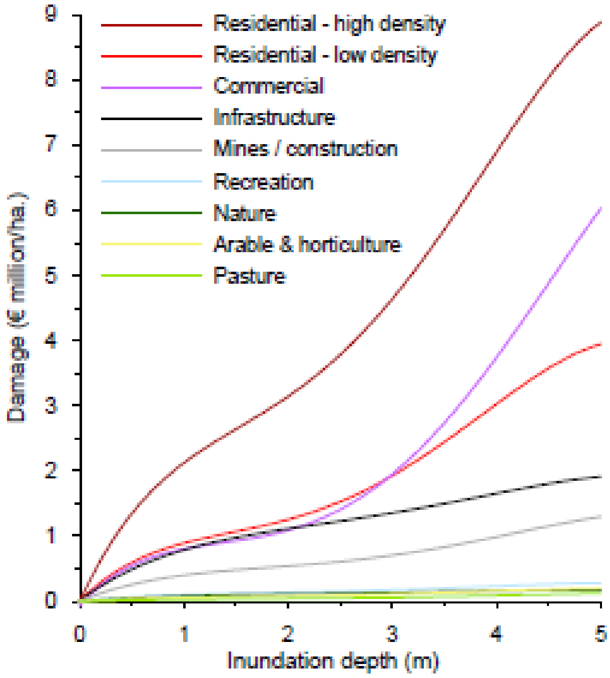

Figure 2.3: The Depth-Damage Curve (Ward et al. 2011)

De Moel and Aerts (2011) focused on effect of uncertainty on flood damage estimates. They covered uncertainty in land use, inundation depth, the value of elements at risk and damage models. In the study conducted by De Moel and Aerts (2011), three damage models were mentioned: Rhine Atlas, Flemish Method and Netherlands Later. CORINE land-cover data set was used by The Rhine Atlas

Method. Depth-damage curves and total value of elements at risk were derived by using German HOWAS database and experts from different sectors and countries. In this method, indirect damages, damages to vehicles and costs of emergency services were not considered. The Flemish Method was developed by Vanneuville et al. (as cited in Jongman et al., 2012). Flood losses were based on land-use classes and some objects. CORINE database and national database were the source of land-use information. The Netherlands Later Method was created by Klijn et al. (as cited in De Moel and Aerts, 2011) and 14 damage categories were considered. HIS-SSM output for various uniform inundation depths were used by deriving the depth-damage curves and values of elements at risks. These curves were derived by using a limited damage data and expert judgment. Consideration of indirect damages in this model is a big advantage. The depth-damage curves of these three models are given in Figure 2.4.

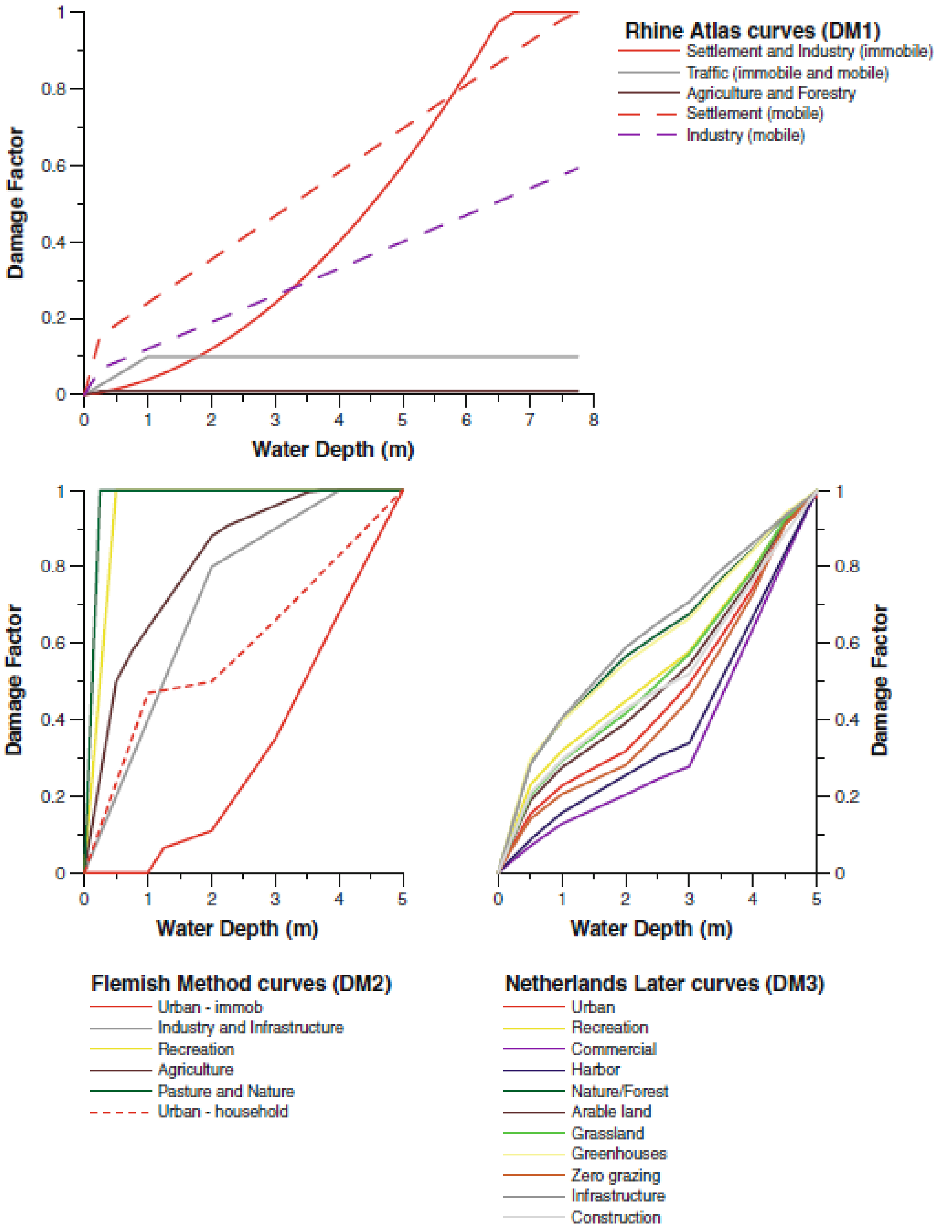

Figure 2.4: The Depth-Damage Curve Examples (De Moel and Aerts, 2011)

Keskin (2012) compared 1-D HEC-RAS hydraulic model and 2-D Flo-2D hydraulic model in his study for Dalaman Basin and tangible damages were calculated. He compared simulation time, inundation continuity and inundation area of the models. The simulation time of HEC-RAS is less than Flo-2D. Furthermore, he stated that 1-D models may produce discontinuous inundation area because they only simulate from cross section to cross section. On the other hand, 2-D models can produce continuous inundation area. While both models gave more or less same inundation extents, the resultant water depth values were different for these models. Tangible damages were classified into two categories: buildings and agricultural areas. Since there is no depth-damage curve for Turkey data from past flood events are used for damage estimation.

Based on literature review it can be deduced that four components were necessary to evaluate expected damage: inundation characteristics (flood velocity, inundation depth, inundation extent etc.), land use data, value of elements at risk (economic, social, environmental risks etc.) and depth damage functions. Inundation characteristics (flood duration, flow velocity, water depth etc.) are important inputs for damage evaluation. These parameters were explained detailed in Flood Hazard Map Part. Information on the location, number and type of properties which could be affected by a certain flood event (the elements at risk) needs to be gathered. This information is given by land use data and it can be data from field surveys or data from existing sources. Value of elements at risk is needed to measure damage in monetary terms. This information can be integrated in damage evaluation in two different ways. First, the total value of all elements at risk is estimated and using relative damage functions, the damaged share of this total value is calculated. Second, integrating this information into absolute damage functions, absolute damage depending on magnitude of inundation characteristics can be calculated. Finally depth/damage functions are used to obtain information on the susceptibility of elements at risk against inundation characteristics (FLOODsite, 2006). These elements are shown in Figure 2.5.

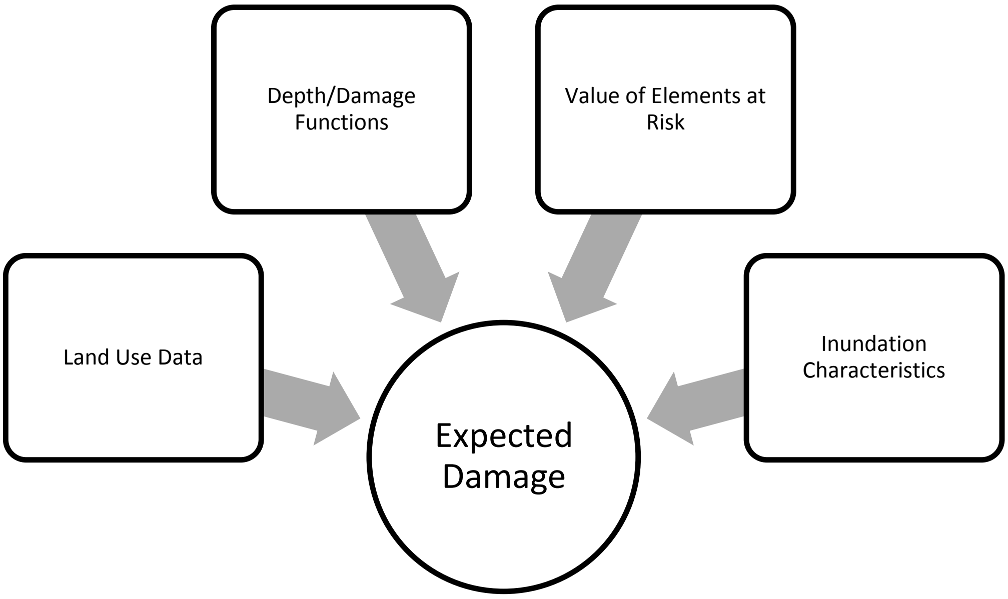

Figure 2.5: Evaluation of Expected Damage (Adapted from FLOODsite, 2006)

Unfortunately some of these components are rarely available for Turkey. For instance, no depth/damage functions are available for Turkey. Damage data associated with previous flood events are not collected and recorded either. Hence, it is impossible to produce depth/damage functions. Getting accurate inundation characteristics may be the most important part of expected damage evaluation. To be able to generate accurate results, detailed maps and accurate stream gauge measurements are needed and this data is not available for some parts of Turkey. In addition to depth/damage functions and inundation characteristics, determination of value of elements at risk may be difficult for Turkey as well. Economic damage may be calculated using data of local municipalities etc. However, calculation of ecological damage may be very difficult for some parts of Turkey due to lack of data, experience and background knowledge. Hence, selection of elements at risk for Turkey may be difficult due to limited data. On the other hand, land use data may be obtained from municipalities relatively easily.

2.4 Elements at Risk

The most important component of the damage evaluation is the selection of elements at risk. The term ‘elements at risk’ includes all elements of the human system, the built environment and the natural environment that are at risk of flooding in a given area (Merz et al., 2007). Population, civil engineering works, economic activities, environment are examples for elements at risk. Adverse consequences of flood-fatalities, injuries or psychological stress, destruction of civil engineering works, interruption of traffic or business, pollution- are experienced respectively. In the literature, three dimensions of risk are used in the flood risk mapping. These are economic, social and ecological dimensions (Kubal et al., 2009; Meyer et al., 2009; Balica et al., 2009; Kienberger et al., 2009). These dimensions are used to estimate the magnitude of damage. Flood damage may be monetary or non-monetary. The example of elements at risk which were used in the literature are summarized in Table 2.3.

The Flood Directive [2007/60/EC] identifies the elements at risk which should be included in flood risk maps as follows:

- Potentially affected number of inhabitants
- Potentially affected area of different types of economic activities
- Accidental pollution in case of flooding and potentially affected protected areas
- Other information which the Member State considers useful such as the indication of areas where floods with a high content of transported sediments and debris floods can occur and information on other significant sources of pollution.

Elements suggested by the European Council must be included in the flood risk maps of Union Members. However, some of these elements may be hard to obtain for Turkey. Potentially affected number of inhabitants and potentially affected area of different types of economic activities may be included in flood risk map for most parts of Turkey. On the other hand, information on significant sources of pollution may be harder to obtain.

Table 2.3: Elements at Risk Identified in the Literature

	Meyer et al. (2009)	**Kubal et al. (2009)**	**Balica et al. (2009)**	**Kienberger et al. (2009)**
Economic Dimension	Damages on assets	Transport Housing Commerce Administration Recreation Land value	Land use Proximity to river Closeness to inundation area % of urbanized area Cadastre survey	Housing Buildings Highways Roads Railways Power plants
Ecological Dimension	Erosion potential Accumulation potential Biotopes vulnerable to inundation	Potential pollution Erodibility Trophic level Biodiversity Forest	Ground WL, Land Use, Over used area Degrated area, Unpopulated land area Types of vegetation % of urbanized area Forest change rate	Assets (forests, reservoirs etc.) "Silent" land cover (lakes, glaciers etc.)
Social Dimension	Number of people affected Social hot spots	Population Children Elderly people Social hot spots	Population density, Population in flood area Closeness to inundation area Population close to coastal Population under poverty % of urbanized area, Rural population Cadastre survey, Cultural heritage % of disable	Population with respect to age distribution

2.5 Multicriteria Decision Analysis

People should make decisions in their business lives and most of the time there is not a perfect solution which fully satisfies all the criteria. Hence, multicriteria analysis (MCA) methods (or multicriteria decision analysis methods) have been developed to support decision maker in their choices. MCA places the decision maker at the center of the process and it does not provide the same solution for everybody. Mathematics, management, informatics, psychology, social science and economics are involved in MCA. Any problem in which a significant decision is needed to be made can be solved by MCA (Ishizaka and Nemery, 2013).

There are four main types of decisions which is identified by Roy (1981): the choice problem, the sorting problem, the ranking problem and the description problem. The aim of the choice problem is to select best option or reduce the options. The options with similar behaviors or characteristics are grouped and based on these groups, necessary measures may be taken. This is called the sorting problem. Ordering options from best to worst by scores is called the ranking problem. The goal of the description problem is to describe options and their consequences. MCA problems and methods are summarized in Table 2.4.

Table 2.4: MCA Problems and Methods (Adapted from Ishizaka and Nemery, 2013)

Problems	**Methods**
Choice Problems	AHP, ANP, MAUT, MACBETH, PROMETHEE, ELECTRE I, TOPSIS, Goal Programming, DEA
Ranking Problems	AHP, ANP, MAUT/UTA, MACBETH, PROMETHEE, ELECTRE III, TOPSIS, DEA
Sorting Problems	AHPSort, UTADIS, FlowSort, ELECTRE-Tri
Description Problems	GAIA, FS-Gaia

Plenty of literature is found on multicriteria analysis application in different fields. (Bana and Costa, 1990; Vincke, 1992; Belton and Stewart, 2002; Meyer et al, 2008; Kubal et al, 2009; Kühmaier and Stampfer, 2012; Adunlin et al., 2014; Ahmadi et al, 2014; Abudeif et al, 2015). The mathematical core of the analysis can be found in Handbook of Multicriteria Analysis (Zopounidis and Pardalos, 2010). Decision Analysis-Methods and Software (Ishizaka and Nemery, 2013) is another recent reference in which methods like Multi Attribute Utility Theory, Analytical Hierarchy Process etc. are explained in detailed together with necessary software. Furthermore, GIS and Multicriteria Decision Analysis (Malczewski, 1999) is another good reference which covers GIS and MCA simultaneously.

In the context of flood risk management, multicriteria analysis was rarely used. Evaluation of long-term flood risk management options in the Netherlands with MCA was studied by Brouwer and van Ek (2004). They combined and integrated environmental, economic and social impact assessment in order to help decision-makers in the context of flood control policy. Cost-benefit analysis and MCA were used together. Equal weighting procedure was selected as the MCA method. Finally, the outcomes of both methods were compared and they concluded that MCA is more sensitive than the cost-benefit analysis in terms of non-monetary terms.

Bana et al. (2004) evaluated alternative flood control measures in the peninsula of Setubal, in Portugal. They identified environmental, social and technical dimensions and integrated these dimensions using MACBETH approach (Measuring Attractiveness by a Categorical Based Evaluation Technique). They also used cost-benefit analysis like Brouwer and van Ek (2004). They concluded that MCA is a better approach since conversion of the environmental, socio-cultural and health effects to monetary terms are very difficult. Similarly, Penning-Rowsell et al. (2003) studied MCA evaluation of flood protection measures in the official manual for damage evaluation in the UK. They used multi attribute utility theory instead of MACBETH approach.

Akter and Simonovic (2005) developed a methodology to treat uncertainties which play a major role in decision-making problems with multiple objectives and multiple stakeholders. They aggregated individual stakeholders' input using fuzzy expected value. The methodology is applied to flood management in the Red River Basin, Canada. They concluded that utilization of fuzzy expected value methodology makes the decision-making process more acceptable from technical and social points of view because it allows inclusion of a large number of stakeholders into the analysis and effectively treats uncertainties.

In 2009, Meyer et al. used a GIS based multicriteria analysis for flood risk mapping in the federal state of Saxony, Germany. Two different MCA approaches were used: a disjunctive approach and an additive weighting approach (basic form of MAUT approach). The results showed that both approaches were appropriate to produce multicriteria risk mapping. In same year, Kubal et al. (2009) adapted Meyer's approach to Leipzig, Germany. They as well used an additive weighting approach.

Musungu et al. (2012) used multi-criteria evaluation in GIS environment for flood risk analysis in Cape Town. They used questionnaire to collect community-based information. Pairwise comparison method was selected as MCA method because of its simplicity.

Saini and Kaushik (2012) assessed the risk and vulnerability using multi-criteria assessment for Guhla block, Kaithal, Haryana, India. They used Rank Sum method to calculate the weights of factors that contribute to the flood hazard.

Pornasdoro et al. (2014) investigated flood prone areas within Metro Manila to reveal their degrees of disaster risk using MCA in the GIS environment. The population density, the gender and age population, structural materials and the recorded depths of floods were considered variables in the study.

Raji et al. (2014) developed flood hazard map and flood risk map within the Lower Ogun Basin of southwestern Nigeria. Flood hazard map was produced using environmental variables such as slope, digital elevation map, geological formation etc. Population data was combined with these data to produce flood risk map. WEIGHT-AHP (Analytical Hierarchy Process) was selected as the MCA method.

Ouma and Tateishi (2014) developed an integrated approach for creating flood hazard map for Eldoret Municipality in Kenya by using AHP as the MCA method. They stated that this methodology can aid decision makers in rapid assessment and evaluation of flood. The results showed that GIS based AHP was effective in flood risk zonation due to the fact that it allows integration of different parameters in the decision-making process.

Yalcin and Akyurek (n.d.) aimed to analyze flood vulnerable areas with multicriteria evaluation in Bartın Basin in the West of Black Sea Region. Ranking method was used to rank every criterion based on decision maker’s preferences. The weights from input preferences were calculated using the pairwise comparison method. At the end of the application, Boolean approach, ranking method, pairwise comparison method and ordered weighting averaging methods were compared. The results showed that the Boolean approach was not suitable. Ranking method and pairwise comparison method produced better results than the Boolean approach. Ordered weighting averaging method also produced realistic results and taking into account uncertainty was its main advantage.

As can be seen from previous studies, MCA techniques were more successful than cost-benefit analysis because non-monetary terms can be considered in MCA techniques. Techniques used in literature showed that most of them produced successful results in flood risk mapping. Meyer et al. (2009) and Kubal et al. (2009) both stated that MAUT produced appropriate results despite the fact that basic form of MAUT which is simple additive weighting was used in their studies. In addition to its simplicity, Velasquez and Hester (2013) stated that the main advantage of MAUT is its ability to treat uncertainty. Papadopoulos and Konidari (2011) stated that MAUT helps decision makers to understand the problem and gain further knowledge. In the same study, they compared some of the MCA techniques and they stated the advantages as follows:

- It produces good outcomes.
- Its utilization is very easy.
- Its time and money requirements are low.
- There are many relevant softwares to conduct MAUT

In this study, basic form of Multi Attribute Utility Theory (MAUT) which is simple additive weighting approach is used to create flood risk maps due to above mentioned reasons. The procedure of this approach is summarized in Figure 2.6.

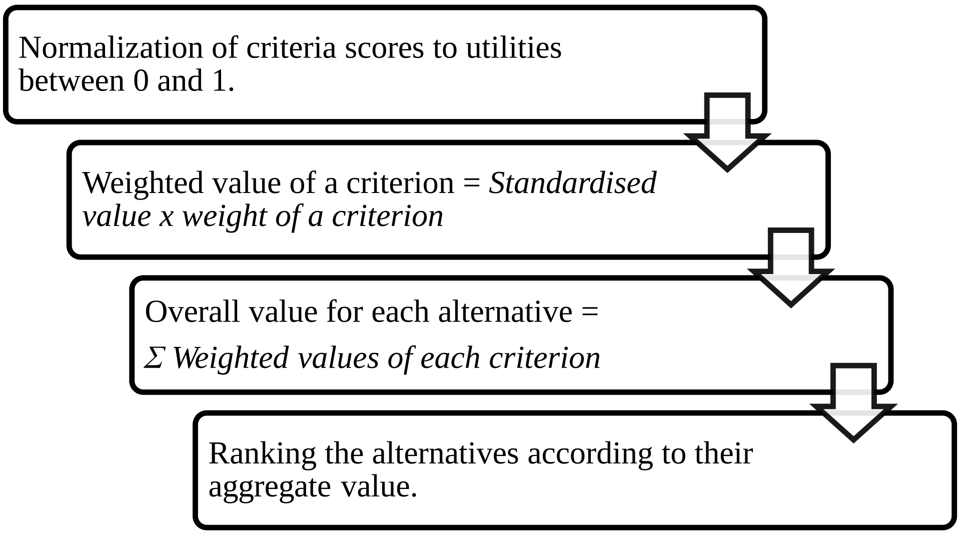

Figure 2.6: The Procedure of Multi Attribute Utility Theory Approach (Adapted from Meyer et al, 2009)

2.6 Vulnerability and Resilience

In the past years, vulnerability concept has been widely used in different areas in the literature. Thus, vulnerability has different definitions in different areas of research. In this study flood vulnerability is included into the flood risk analysis. Two dimensions of vulnerability is commonly identified: biophysical vulnerability, which is broadly equivalent to the natural hazards concept of risk (Brooks, 2003) and social vulnerability which is related to coping responses of communities, including societal resistance and resilience to hazards (Messner and Meyer, 2006). In this study, we focus on the social vulnerability. The social dimension of the risk is assumed to increase with increasing social vulnerability. Resilience is included into this study as a factor which will affect economic dimension of the risk.

Balica (2012) describes the resilience as the ability of a system to preserve its basic roles and structures in a time of distress and disturbance. The most detailed definition of resilience is given by The United Nations Office for Disaster Risk Reduction in 2004. It defines the resilience as capacity of a system, community or society potentially exposed to hazards to adapt by resisting or changing in order to reach and maintain an acceptable level of functioning and structure. In this study, resilience is used in the economic dimension of risk. It is assumed that the higher the resilience of structures that are at risk the lower the economic risk. To summarize, in this study vulnerability of community is included in the social risk dimension while resilience of infrastructures (i.e. houses, roads, buildings, etc.) is included in the economic risk dimension. This is a simple approach to include vulnerability and resilience into the risk analysis. Proper treatment of vulnerability and resilience is dependent on availability of data. This is a preliminary approach to integrate vulnerability and resilience concepts into risk analysis, the approach may be improved and used especially when necessary data is available.

CHAPTER 3

CASE STUDY

In this study, the part of Salkım Stream passing through Yukarıakören Village is selected as the case study. Salkım Stream is located in the Euphrates - Tigris Basin in the southern part of Turkey (Figure 3.1). According to Turkish State Meteorolojical Services, the flood density is not high in the Euphrates- Tigris Basin (Turkish State Meteorological Services, 2011) (Figure 3.2). However, many floods occurred in Şanlıurfa in recent years. The floods occurred in Şanlıurfa Merkez, Ceylanpınar and Siverek in 2006, Bozova Yaylak, Şanlıurfa Merkez Karaköprü and Birecik Ayran in 2011 and Hilvan Kepirce, Şanlıurfa Merkez Karaköprü-Sırrın River in 2012 (Sepetçioğlu, 2013). A map showing areas where flood events have been observed is provided in Figure 3.3. It can be seen from Figure 3.3 that the majority of settlements in Şanlıurfa are exposed to floods. These floods resulted in various damages. Due to increasing flood events, 15th Regional Directorate of DSI prepared flood protection master plan reports. Additionally, availability of flood hydrographs and detailed maps of the area are other reasons for the selection of this site as the case study. Location of the project site on the map of Şanlıurfa is given in Figure 3.4 while a more detailed map of the project site is provided in Figure 3.5.

Figure 3.1: Basins in Turkey (Terrain Monitoring System, 2011)

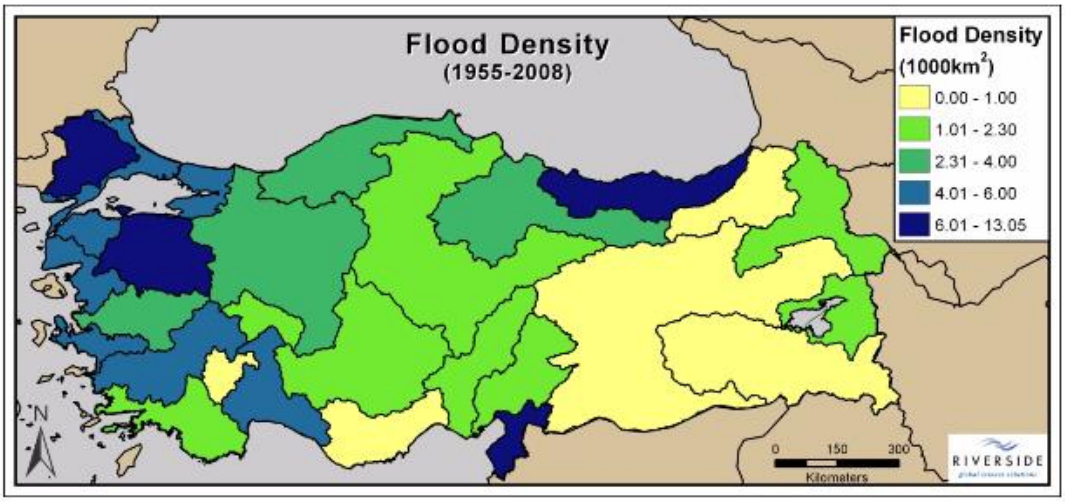

Figure 3.2: Flood Density of Turkey based on number of events per basin (Turkish State Meteorological Services, 2011)

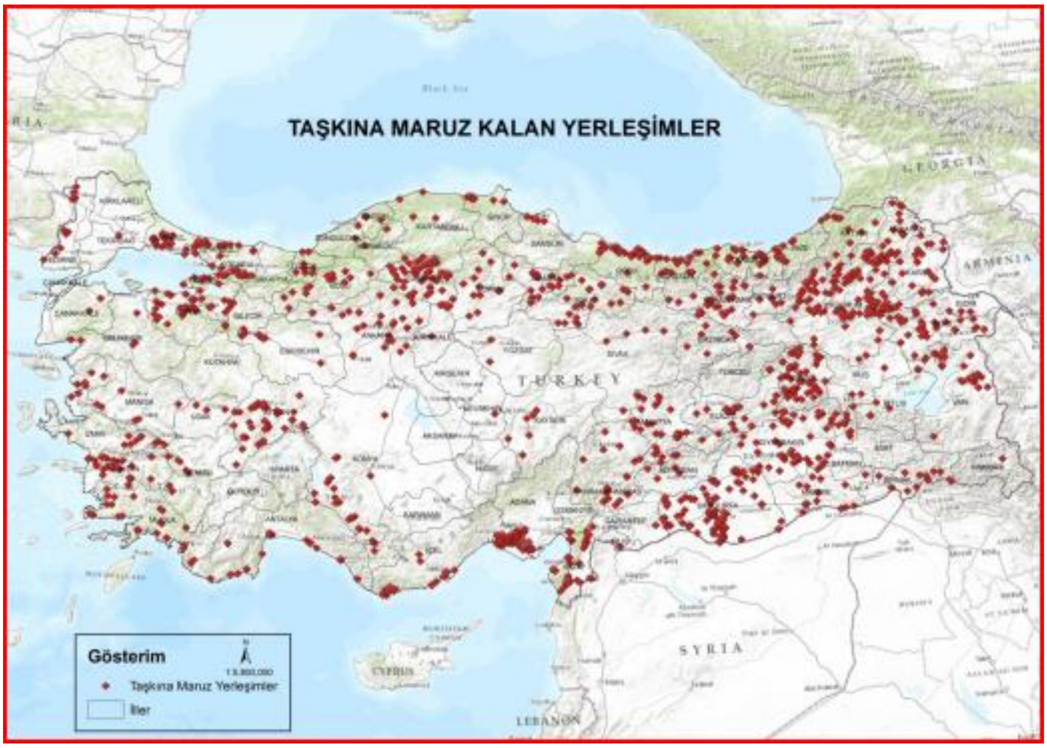

Figure 3.3: Settlements Exposed to Flood (Selek and Darama, 2013)

Figure 3.4: Location of the Project Site on Google Earth

Figure 3.5: Detailed View of the Project Site on Google Earth

The 1/1000 scaled map of the project site created in the AutoCAD environment can be seen in Figure 3.6 (Eser Project & Engineering Co. Inc., 2013). In this map, the contours, the elevations, the coordinates and important structures are marked. The point data of elevation values is provided in Figure 3.7. This data is used to generate digital elevation model in ArcGIS. Area of the sub-basin is approximately 25.39 km^2 and the flood discharges are provided in Table 3.1 (Eser Project & Engineering Co. Inc., 2012). The calculation of these values are given in Appendix A. The calculated values are slightly different from the values in the mentioned report. The reason may be the usage of different software and calculation techniques. However, the values in the report are used in the remaining part of this study because the differences are too small. Furthermore digital elevation map (DEM) of the study area generated in ArcGIS is given in Figure 3.8.

Table 3.1: Flood Discharges for different return periods (m^3/s) (Eser Project & Engineering Co. Inc., 2013)

Q_2	Q_5	Q_{10}	Q_{25}	Q_{50}	Q_{100}	Q_{500}	Q_{1000}
1.61	6.85	12.77	22.97	32.38	43.19	64.23	73.30

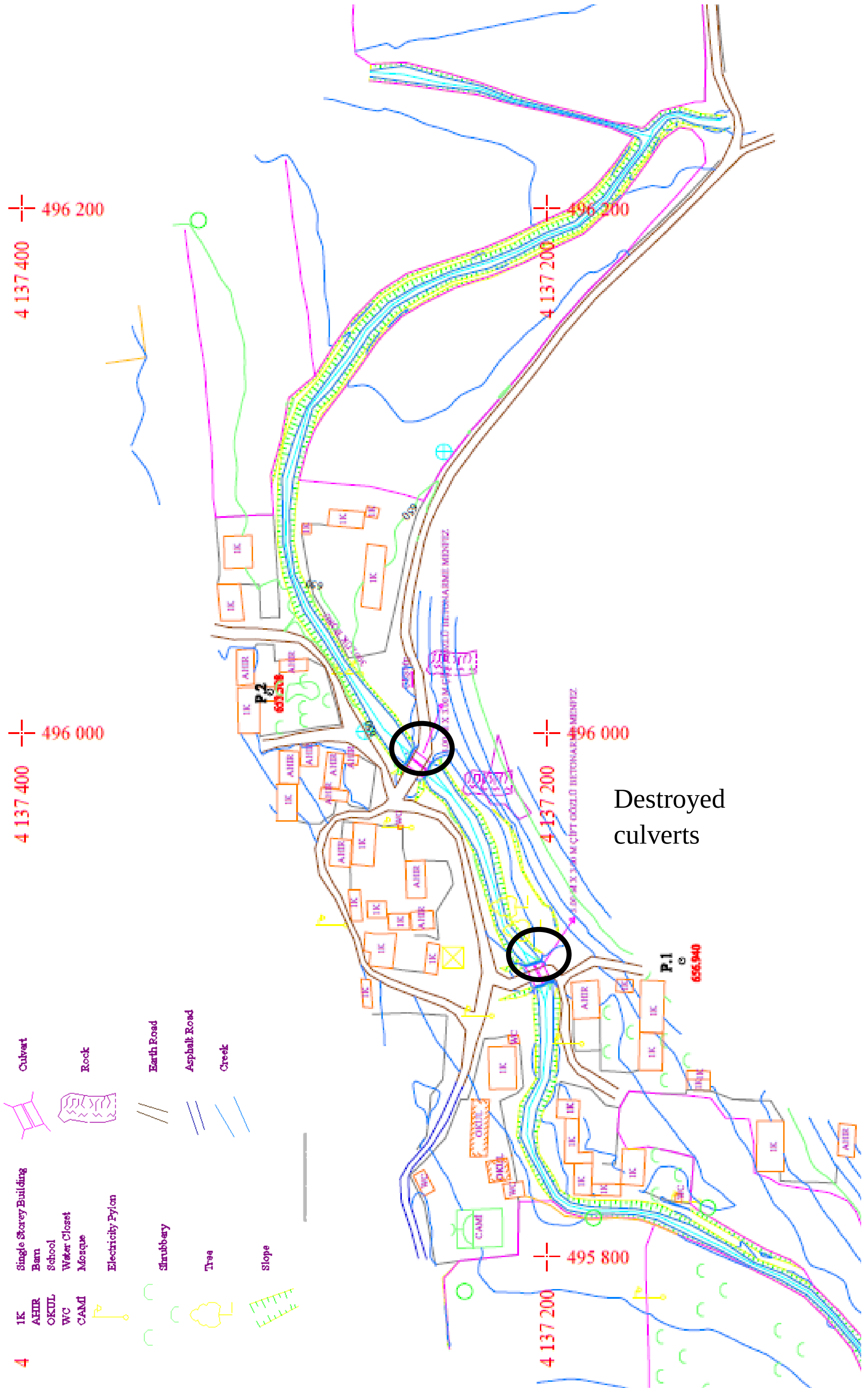

Figure 3.6: 1/1000 Scaled Map of the Project Site in AutoCAD Environment (Eser Project & Engineering Co. Inc., 2013)

Figure 3.7: The Point Data with Elevation Values (Eser Project & Engineering Co. Inc., 2013)

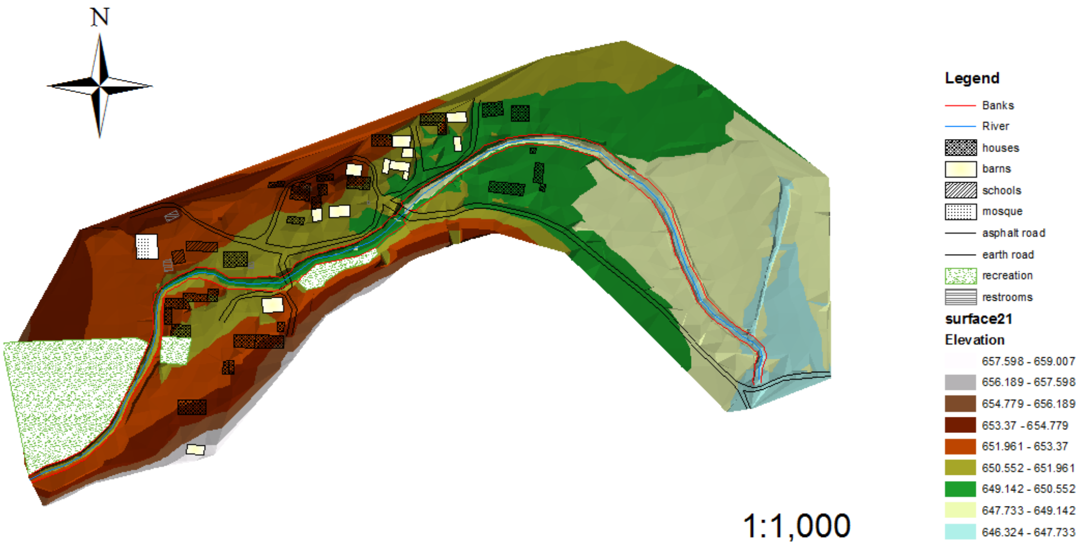

Figure 3.8: Digital Elevation Model of Study Area in ArcGIS Environment

According to 2009 Population Census, Yukarıakören's population is 699 (Kutluay, 2010). There are approximately 50 buildings in the village and these buildings are single-storey buildings. In addition to this, majority of these buildings are reinforced concrete structures. These buildings are shown in Figure 3.5 as "1K". There is a school and a mosque which are shown as "OKUL" and "CAMİ" respectively. Agriculture and animal breeding are essential sources of living in Yukarıakören. Cereal types are the most planted crops in Yukarıakören. Furthermore, there are approximately 20 barns in the village. They are marked as "AHIR" in Figure 3.6. Cattle farming, sheep, goat farming and poultry raising are common in the village.

The elements at risk are summarized in Tables 5.1, 5.2 and 5.3 of "Discussion and Results" Chapter. The study conducted by Meyer et al. (2009) is an excellent guide for this case study because that study covers the most basic and important forms of elements at risk. In that study, three dimensions are mentioned: economic, social and environmental. The elements at risk mentioned in that study can be seen in Figure 3.9.

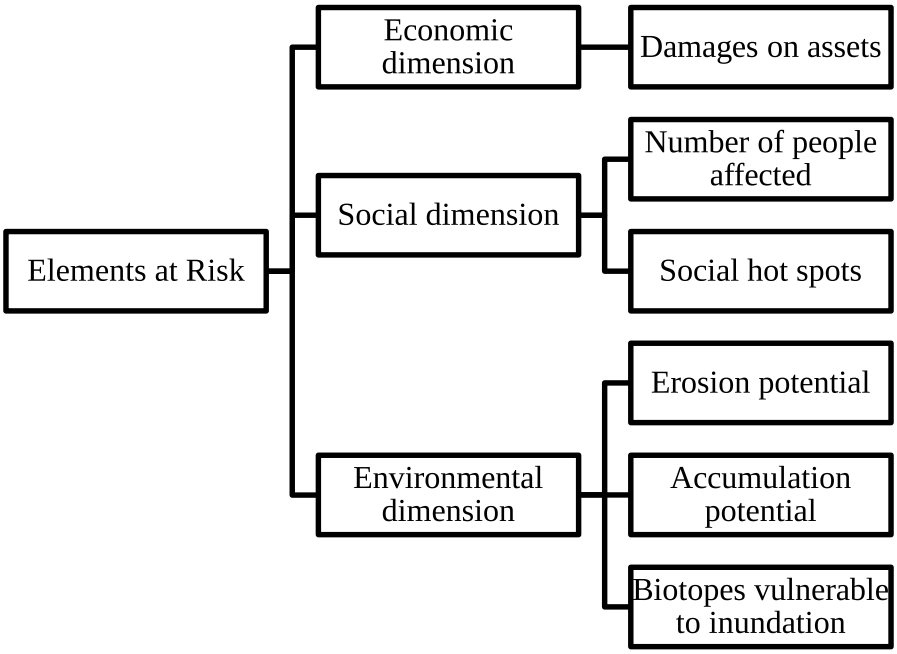

Figure 3.9: Elements at risk (Meyer et al., (2009)

Floods may be destructive in the village because of some reasons. Firstly, the geometry of the stream is very irregular and disturbed – mostly narrowed - by public settlement. This may increase the inundated area even if floods with small return periods occur. Inundated areas caused by floods with different return periods will be given in following chapters. Secondly, majority of the structures and arable lands are very close to stream bed which endangers people and animals around and this can be considered under “number of people affected” element. This element can be also divided into sub-groups with respect to age. This is an important element because floods can cause very dramatic results for people. Furthermore, inundation of arable lands and barns may interrupt the economic activities of the public because the essential sources of living are agriculture and animal breeding. This term can be considered as a risk element because the shortage of economic activities may create indirect damages (Merz et al. 2010). This will be included in the economic dimension. The structures which will be inundated can be considered under the economic dimension as well as the social dimension. The inundation of structures create economic damage. This economic damage can be classified as economic damage on buildings, economic damage on roads, economic damage on land value etc. On the other hand, the inundation of structures as school, mosque etc. can be considered as social hot spots causing social damage. These structures are important for public because of their roles. Finally, floods may cause health problems. The most encountered health problem after floods is diarrhea originating from polluted water and nutrition. Furthermore, it may increase the number of rodents and mosquito that may cause health problems on people. Floods may also damage water and sewerage systems which cause biological and chemical contamination (Ünüvar, n.d.). These health problems may be included under the social dimension as a separate risk element or under "number of people affected" risk element. Erosion potential and potential pollution will be investigated as elements at risk under environmental dimension. If they pose a threat, they will be included in risk analysis by using simple Boolean yes/no damage function (Meyer et al.2009).

.

CHAPTER 4

METHODOLOGY

The procedure of obtaining risk maps is given in Figure 4.1. Each step is explained in detail in the following sections.

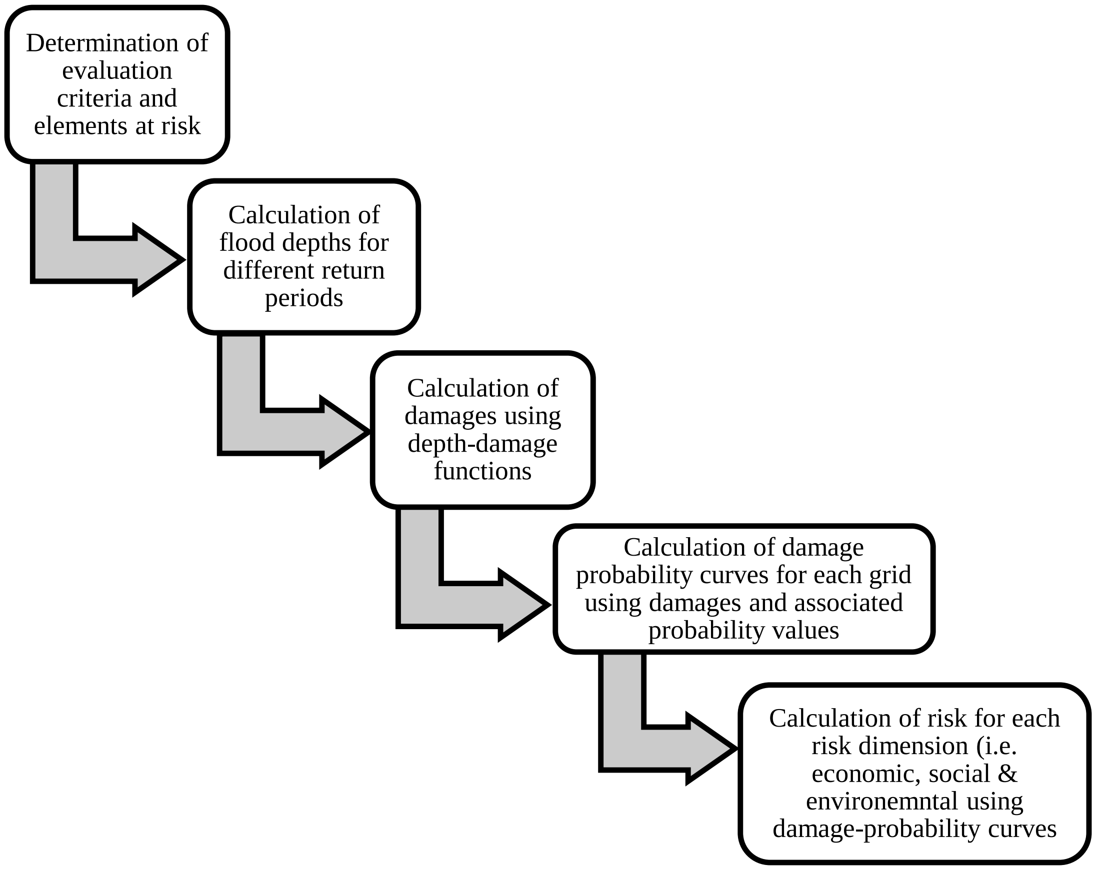

Figure 4.1: Flood Risk Map Generation Procedure

4.1 Determining Evaluation Criteria & Elements at Risk

Considering site specific characteristics and availability of data, evaluation criteria for each dimension of risk should be decided. Elements at risk are generally classified under three risk dimension: economic, social and environmental. For example, residential buildings, roads, administrative buildings, industrial buildings etc. may be categorized under economic elements at risk. Social risk dimension may include population, social hot spots, animals, cultural heritage sites etc. Furthermore, erosion potential, accumulation potential, pollution, forests may be included under the environmental elements at risk.

4.2 Calculation of Water Depths

Water depths for different return periods are calculated in ArcGIS environment by using HEC-GeoRAS tool. The procedure of calculation of water depths are summarized step by step below:

- Creation of river centerline: It is used to establish river reach network for HEC-RAS.
- Creation of river banks: They are used to differentiate main channel from the overbank floodplain areas.
- Creation of flowpaths: There are three types of flowpaths: centerline, left overbank and right overbank. They are used to determine the downstream reach lengths between cross-sections in the main channel and over bank areas.
- Creation of cross-sections: They are used to create a ground profile by extracting the elevation data from the surface.

After above-mentioned steps, the geometry data created in ArcGIS environment is exported to HEC-RAS to carry out hydraulic calculations such as water depth, water velocity, shear stress etc. Step-wise procedure to make necessary calculations in HEC-RAS is summarized below:

- The geometry data exported from ArcGIS is imported to HEC-RAS.
- According to Cowan (1956) the Manning roughness coefficient depends on surface irregularities, variation in shape and size of the cross section, obstructions, vegetations, flow conditions and meandering of the channel. Since the goal of this study is to perform a complete risk analysis, detailed investigations and experiments are not conducted to estimate Manning roughness coefficient, but uniform values for the main channel and river banks are adapted. Hence, the Manning's Roughness coefficient of cross-sections are entered as 0.035 for main channel and 0.040 for river banks by considering natural river channels (US Army Corps of Engineers Hydraulic Engineering Center, 2010) for the sake of simplicity and due to limited information.
- After editing geometric data, the steady flow data is entered to HEC-RAS. The water depth calculations are carried out for a selected set of return periods. The boundary condition is entered as a normal depth value for both upstream and downstream (US Army Corps of Engineers Hydraulic Engineering Center, 2010).
- After entering steady flow data, water depth calculations are carried out.
- After carrying out hydraulic calculations in HEC-RAS, the necessary files are exported to ArcGIS. In ArcGIS, for each return period water surfaces are generated and floodplains are delineated. After delineation of floodplain, for every return period, water depths are calculated.

4.3 Calculation of Damages

Calculation of damages is an important part of the risk mapping studies. There are different methods to calculate damages. For example, economic damages are calculated using depth-damage functions while social and environmental damages are calculated using the binary approach (Kubal et al., 2009; Meyer et al., 2009). The damage calculation methods of the associated risk dimensions are explained in detail in the following sections.

4.3.1 Economic Damage Calculations

The most important part of the economic damage calculations is to determine economic elements at risk. For calculating damage, the study area is gridded into a large number of cells. Cell dimensions should be selected according to the details of the map of the study area. The selected elements at risk are digitized in ArcGIS. These elements at risk and water depths are used in damage and risk calculations.

In this study, the method proposed by Kubal et al. (2009) is used to calculate economic damage. Kubal et al. (2009) used a damage function (Equation 4-1) taken from HOWAS-database which is the biggest database on flood damages in Germany. Although this damage function was derived for residential buildings it used for all economic elements at risk because of its simplicity.

$$D_i^j = 0.27 \times \sqrt{h_i^j} \qquad \forall\, i, j \qquad (4\text{-}1)$$

where D_i^j is the damage at cell j for the flood with return period TR_i, h_i^j is the water depth at cell j for the flood with return period TR_i. Using Equation (4-1) the damage is calculated separately for all economic elements at risk for all flood with selected return periods. For example, $i = 1,2, \dots,$ T may correspond to flood events with 2, 5,…, 1000 year return periods (i.e., $TR_1 = 2\, years,\ TR_2 = 5\, years, \dots, TR_T =$

$1000\ years$). The risk analysis need to be carried out for a selected number of return periods which will result in a representative damage exceedance probability curve which is explained in detail in Section 4.4.

Resilience is a new concept used in damage estimation (Aerts et al., 2013; Velasco, 2014). Resilience is the capacity of an element to withstand loss or damage or to recover from the impact of an emergency or disaster (Thywissen, 2006). If the resilience is higher, the damage tends to be less and the recovery tends to be faster. In this study, a damage function with the resilience term is proposed:

$$D_i^j = \frac{1}{R} \times \frac{27 \times \sqrt{h_i^j}}{100} \qquad R \in (0,1] \qquad \forall\, i, j \qquad (4\text{-}2)$$

where R is the resilience factor which ranges between 0 and 1, 0 is representing the worst resilience and 1 is representing the best resilience.

4.3.2 Social Damage Calculations

The most important part of the social damage calculations and social risk mapping is to determine social elements at risk such as population, social hot spots or in other words attributes which represent social dimension of risk. The selected elements at risk are digitized in ArcGIS. These elements at risk and water depths are used in damage and risk calculations.

In the social damage calculations, the damage is calculated using a binary approach. If a grid cell is flooded and a social element at risk exists in that cell, the social damage is taken as 1, if it is not flooded, the social damage is taken as 0 (Kubal et al., 2009; Meyer et al., 2009). Calculation of social damage is difficult because it is very hard to assign depth – damage functions for social elements at risk. Hence, the binary approach is plausible to represent the social damage (Kubal et al., 2009). By using the binary approach, the social damage is calculated separately for all social elements at risk for all return periods using Equation 4-3:

$$D_i^j = fh_i^j \cap fs^j \qquad \forall\, i,j \qquad (4\text{-}3)$$

$$fh_i^j = \begin{cases} 1, if\ h_i^j > 0 \\ 0, if\ h_i^j = 0 \end{cases} \qquad \forall\, i,j \qquad (4\text{-}4)$$

$$fs^j = \begin{cases} 1, if\ cell\ j\ has\ a\ social\ element\ at\ risk \\ 0, if\ cell\ j\ does\ not\ have\ a\ social\ element\ at\ risk \end{cases} \qquad \forall\, j \qquad (4\text{-}5)$$

where fh_i^j is the flag to determine if cell j is flooded for the flood with return period TR_i and fs^j is the flag to determine if a social element at risk exists at cell j.

To include vulnerability term into the social risk analysis, Equation 4-6 is proposed. Vulnerability is defined by The United Nations Office for Disaster Risk Reduction as the characteristics and circumstances of a community, system or asset that make it susceptible to the damaging effects of a hazard (European Environment Agency, 2010).

$$D_i^j = V \times \left(fh_i^j \cap fs^j\right) \qquad V \in [1, L] \qquad \forall\, i,j \qquad (4\text{-}6)$$

where V is vulnerability which ranges between 1 and L, 1 representing no vulnerability and L (a large number such as 10) representing high vulnerability. L should be selected based on the specific characteristics of the case study and fs^j is the flag to determine if a social element at risk exists at cell j.

4.3.3 Environmental Damage Calculations

First environmental elements at risk need to be identified considering site-specific characteristics. The selected elements at risk are digitized in ArcGIS. These elements at risk and water depths are used in damage and risk calculations. Two environmental elements at risk used in this study are pollution and erosion. Damage calculations for these two elements are explained below.

In the environmental damage calculations for pollution, the damage is calculated using a binary approach. If a grid cell is flooded and an environmental element at risk exists, the damage is taken as 1, if it is not flooded, the damage is taken as 0 (Kubal et al., 2009; Meyer et al., 2009).

$$D_i^j = fh_i^j \cap fe^j \qquad \forall\, i, j \qquad (4\text{-}7)$$

$$fe^j = \begin{cases} 1, \text{if there is a pollution source at cell j} \\ 0, \text{if there is no pollution source at cell j} \end{cases} \qquad \forall\, j \qquad (4\text{-}8)$$

where fe^j is the flag to determine if a pollution source exists at cell j.

Calculation of environmental damage is very difficult because environmental damage cannot be directly quantified. There are no depth-damage functions for environmental elements at risk. Hence, the binary approach is plausible to represent the environmental damage (Kubal et al., 2009).

As the environmental damage function for erosion, Equation 4-9 is proposed. The damage is represented with one of the four values: If there is no vegetation cover or the surface is pervious and the slope is bigger than 18°, the damage is 1; if there is no vegetation cover or the surface is pervious and the slope is between 8° and 18°, the damage is 0.67; if there is no vegetation cover or the surface is pervious and the slope is between 3° and 8°, the damage is 0.33 and if the slope is smaller than 3°, the damage is 0. If there is vegetation cover or the surface is impervious, it is assumed that there is no erosion risk. Erosion potential with respect to slope is explained in Section 5.1.3.

$$D_i^j = (fh_i^j \cap fsl^j) \cap fv^j \qquad \forall\, i, j \qquad (4\text{-}9)$$

$$fsl^j = \begin{cases} 1, & \text{if slope} > 18° \\ 0.67, & \text{if } 18° > \text{slope} > 8° \\ 0.33, & \text{if } 8° > \text{slope} > 3° \\ 0, & \text{if } 3° > \text{slope} \end{cases} \qquad \forall\, j \qquad (4\text{-}10)$$

$$fv^j = \begin{cases} 1, \text{if there is no vegetation cover or the surface is pervious at cell j} \\ 0, \text{if there is vegetation cover or the surface is impervious at cell j} \end{cases} \qquad \forall\, j \qquad (4\text{-}11)$$

where fsl^j is the flag to determine which range the slope is at cell j and fv^j is the flag to determine if vegetation cover or impervious surface exist at cell j.

The damage is calculated separately for all environmental elements at risk for all return periods using Equation 4-7 and Equation 4-9, for pollution and erosion respectively.

4.4 Calculation of Damage – Exceedance Probability Curves

A damage-exceedance probability curve needs to be derived for each element at risk and for each cell within the study area. To do this, first a set of return periods are selected to carry out risk estimations. Corresponding exceedance probabilities are calculated by taking the inverse of the selected return periods. Economic, environmental and social damages are calculated using the procedures explained in the previous sections for all selected return periods. Then damage- exceedance probability curves are derived for each cell and each element at risk. Since risk is the multiplication of the consequence and the associated probability, the area under the damage - exceedance probability curve gives an overall estimate of the risk.

4.5 Calculation of Risk

Calculation of risk is the final step of risk mapping studies. The risk is calculated using damage-exceedance probability curves. The risk is the area under the damage-exceedance probability curves. The calculation of risk for each dimension is given detailed in the following chapters.

4.5.1 Economic Risk Calculations

After completing economic damage mapping, economic risk at each cell is calculated using Equation 4-12:

$$ER^j = \sum_{i=1}^{k} |P_i - P_{i-1}| \times (D_i^j + D_{i-1}^j) \times \frac{1}{2}, \qquad \forall j \qquad (4\text{-}12)$$

where ER^j is the economic risk at cell j (j = 1, 2, 3…N) where N is total number of cells in the study area, i is index for the return period (for example i=1,2,.. may correspond to TR_1 = 2 years, TR_2 = 5 years etc.), P_i is the exceedance probability of the flood event which has a return period of TR_i, D_i^j is the damage of the TR_i – year flood at cell j.

As can be seen from Equation 4-12, the risk is the area under the damage - exceedance probability curve. Damage - exceedance probability curves are different for each cell because the damage function depends on the water depth. Since same damage equation (Equation 4-1) is used for all economic elements at risk, the damage – exceedance probability curves are same for all elements at risk. If different damage equations are generated for different elements at risk then the damage – exceedance probability curves will be different. To calculate overall economic risk, risks for all economic elements needs to be summed up:

$$OER^j = \sum_{\substack{for\ all\ economic \\ elements\ at\ risk}} ER^j \qquad \forall j \quad (4\text{-}13)$$

After calculating overall economic risk for each cell, economic risk maps are created and these maps are normalized to range [0,1] so that economic risk maps will be comparable to social and environmental risk maps. The normalization of the risk values are carried out using:

$$NOER^j = \frac{OER^j}{Max\{OER^1, OER^2 \ldots OER^N\}} \qquad \forall j \quad (4\text{-}14)$$

where $NOER^j$ is normalized overall economic risk at cell j and OER^j is overall economic risk at cell j.

4.5.2 Social Risk Calculations

For each social element at risk social risk at each cell is created using Equation 4-15:

$$SR^j = \sum_{i=1}^{k} |P_i - P_{i-1}| \times (D_i^j + D_{i-1}^j) \times \frac{1}{2}, \qquad \forall j \quad (4\text{-}15)$$

where SR_j is social risk at cell j.

To calculate overall social risk, risks for all social elements needs to be summed up:

$$OSR^j = \sum_{\substack{for\ all\ social \\ elements\ at\ risk}} SR^j \qquad \forall j \quad (4\text{-}16)$$

Overall social risks calculated for each cell are used to generate social risk maps. These maps are normalized to range [0,1] as well to compare them with the other risk maps (environmental and economic) easily. The normalization of the social risk values are carried out by using Equation 4-17:

$$NOSR^j = \frac{OSR^j}{Max\{OSR^1,\ OSR^2 \dots OSR^N\}} \qquad \forall j \quad (4\text{-}17)$$

where $NOSR^j$ is normalized overall social risk at cell j and OSR^j is overall social risk at cell j.

4.5.3 Environmental Risk Calculations

For each environmental element at risk environmental risk at each cell is created using Equation 4-18:

$$ENR^j = \sum_{i=1}^{k} |P_i - P_{i-1}| \times (D_i^j + D_{i-1}^j) \times \frac{1}{2}, \qquad \forall j \quad (4\text{-}18)$$

where ENR^j is environmental risk at cell j.

To calculate overall environmental risk, risks for all environmental elements needs to be summed up:

$$OENR^j = \sum_{\substack{for\ all\ environmental \\ elements\ at\ risk}} ENR^j \qquad \forall j \quad (4\text{-}19)$$

Environmental risk maps are normalized to range [0,1] as well using:

$$NOENR^j = \frac{OENR^j}{Max\{OENR^1, OENR^2 \dots OENR^N\}} \qquad \forall j \quad (4\text{-}20)$$

where $NOENR^j$ is normalized overall environmental risk at cell j and $OENR^j$ is overall environmental risk at cell j.

4.6 Aggregation of Economic, Environmental and Social Risk Maps

After calculating risk maps separately, these maps are aggregated using simple additive weighting approach (Equation 4-21). In the aggregation process, normalised risk maps are used. In each cell, risk values are multiplied by its weight. After that, the weighted risk values are added to obtain a final total risk value.

$$TRisk^j = \sum_{m=1}^{n} w_m \times NOR_m^j \qquad \forall j \qquad (4\text{-}21)$$

where $TRisk^j$ is the total risk at cell j, m is the index for the risk dimension (economic, social and environmental risk dimensions), w_m is the weight of the risk dimension m, n is the total number of the risk dimensions, NOR_m^j is the normalized risk value of related risk dimension at cell j. In this study $m = 3$ and $NOR_1^j = NOER^j, NOR_2^j = NOSR^j, NOR_3^j = NOENR^j$.

4.7 Economic Risk Mapping using Different Depth-Damage Functions

4.7.1 Netherlands Later Curves

In economic damage calculations, the depth-damage function used in Kubal et al. (2009) is used in this study for all economic elements at risk as explained in Section 4.3.1. However, different depth-damage curves have been proposed in the literature for different elements at risk. Some example depth-damage curves are explained in the Literature Review Chapter.

In this study, as an additional analysis, the Netherlands Later Curves (De Moel and Aerts, 2011) as the depth damage functions. The Netherlands Later Curves are given in Figure 4.2. Approximate economic damage functions are derived from this figure and given in Equations 4-22, 4-23 and 4-24. Equation 4-22 is for residential buildings, barns, restrooms and roads. Equation 4-23 is for recreation area. Equation 4-24 is for schools and mosques.

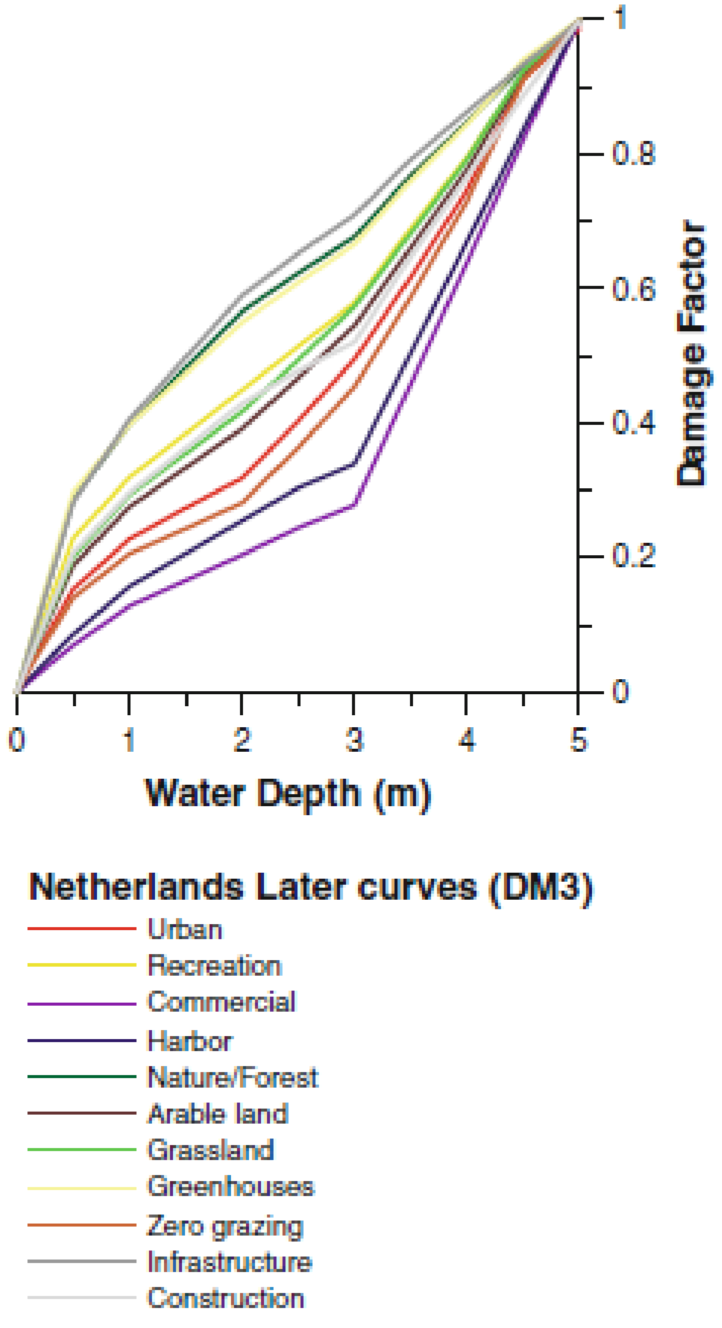

Figure 4.2: Netherlands Later Curves (De Moel and Aerts, 2011)

$$D_i^j = \begin{cases} 0.92 - \frac{0.42 \times (4.50 - h_i^j)}{1.50}, \text{if } 4.50 \text{ m} > h_i^j > 3.00 \text{ m} \\ 0.50 - 0.18 \times (3.00 - h_i^j), \text{if } 3.00 \text{ m} > h_i^j > 2.00 \text{ m} \\ 0.32 - 0.07 \times (2.00 - h_i^j), \text{if } 2.00 \text{ m} > h_i^j > 1.00 \text{ m} \\ 0.25 - \frac{0.07 \times (1.00 - h_i^j)}{0.50}, \text{if } 1.00 \text{ m} > h_i^j > 0.50 \text{ m} \\ 0.18 - \frac{0.18 \times (0.50 - h_i^j)}{0.50}, \text{if } 0.50 \text{ m} > h_i^j > 0.00\, m \end{cases} \quad \forall\, i, j \qquad (4\text{-}22)$$

$$D_i^j = \begin{cases} 0.92 - 0.32 \times (4.20 - h_i^j), \text{if } 4.20 \text{ m} > h_i^j > 3.20 \text{ m} \\ 0.60 - \frac{0.22 \times (3.20 - h_i^j)}{2.20}, \text{if } 3.20 \text{ m} > h_i^j > 1.00 \text{ m} \\ 0.38 - \frac{0.08 \times (1.00 - h_i^j)}{0.50}, \text{if } 1.00 \text{ m} > h_i^j > 0.50 \text{ m} \\ 0.30 - \frac{0.30 \times (0.50 - h_i^j)}{0.50}, \text{if } 0.50 \text{ m} > h_i^j > 0.00 \text{ m} \end{cases} \quad \forall i, j \qquad (4\text{-}23)$$

$$D_i^j = \begin{cases} 1.00 - \frac{0.28 \times (5.00 - h_i^j)}{2.00}, \text{if } 5.00\, m > h_i^j > 3.00 \text{ m} \\ 0.72 - 0.12 \times (3.00 - h_i^j), \text{if } 3.00 \text{ m} > h_i^j > 2.00 \text{ m} \\ 0.60 - 0.15 \times (2.00 - h_i^j), \text{if } 2.00 \text{ m} > h_i^j > 1.00 \text{ m} \\ 0.45 - \frac{0.13 \times (1.00 - h_i^j)}{0.50}, \text{if } 1.00 \text{ m} > h_i^j > 0.50 \text{ m} \\ 0.32 - \frac{0.32 \times (0.50 - h_i^j)}{0.50}, \text{if } 0.50 \text{ m} > h_i^j > 0.00 \text{ m} \end{cases} \quad \forall\, i, j \qquad (4\text{-}24)$$

4.7.2 Monetary Damage Calculations using Netherlands Depth-Damage Functions

In the literature, there are depth-damage functions which represent damages in monetary unit such as dollars, euros etc. Frequently used depth-damage functions with monetary terms in the Netherlands are used to generate economic risk map in this study as well. The depth damage curves are given in Figure 4.3. These curves are approximately from the Figure 4.3 and Equations 4.25, 4.26, 4.27 and 4.28 are derived. Equation 4.25 is used for earth roads and asphalt roads, Equation 4.26 is used for barns and rest rooms, Equation 4.27 is used for residential buildings, mosques, schools and finally Equation 4.28 is used for recreation areas.

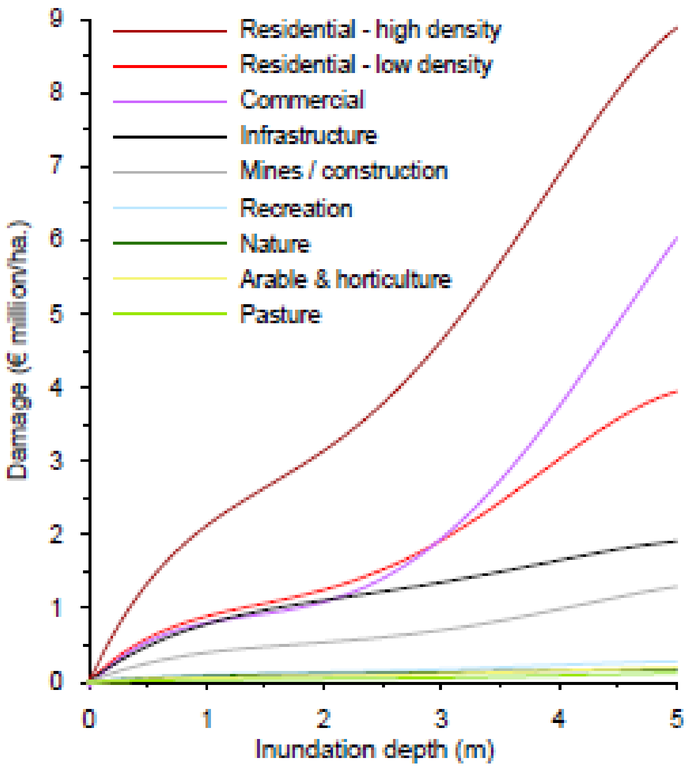

Figure 4.3: The Depth-Damage Curve (Ward et al. 2011)

$$D_i^j = \begin{cases} 1.50 - \frac{0.50 \times \left(5.00 - h_i^j\right)}{4.20}, \text{if } 5.00\ m > \ h_i^j \ > \ 0.80 \text{ m} \\ 1.00 - \frac{\left(0.80 - h_i^j\right)}{0.80}, \text{if } 0.80 \text{ m} > \ h_i^j \ > 0.00 \text{ m} \end{cases} \qquad \forall\ i, j \quad (4\text{-}25)$$

$$D_i^j = \begin{cases} 4.00 - \frac{0.50 \times \left(5.00 - h_i^j\right)}{3.00}, \text{if } 5.00\ m > \ h_i^j \ > \ 2.00 \text{ m} \\ 2.50 \times h_i^j - 1.50, \text{if } 2.00 \text{ m} > h_i^j \ > \ 1.00 \text{ m} \\ h_i^j, \text{if } 1.00\ m > h_i^j \ > \ 0.00 \text{ m} \end{cases} \qquad \forall\ i, j \quad (4\text{-}26)$$

$$D_i^j = \begin{cases} 1.00 + h_i^j, \text{if } 5.00\ m > \ h_i^j \ > \ 1.00 \text{ m} \\ 2.00 \times h_i^j, \text{if } 1.00\ m > h_i^j \ > \ 0.00 \text{ m} \end{cases} \qquad \forall\ i, j \quad (4\text{-}27)$$

$$D_i^j = 0.25 - 0.25 \times \frac{5.00 - h_i^j}{5.00}, \ 5.00\ m > \ h_i^j \ > \ 0.00 \text{ m} \qquad \forall\ i, j \quad (4\text{-}28)$$

CHAPTER 5

DISCUSSIONS AND RESULTS

In this section, the results of damage and risk analysis are given. Damage and risk maps for all three dimensions, economic, environmental and social, and associated discussions are provided in the following sections.

5.1 Selection of the Evaluation Criteria & Elements at Risk

Elements at risk for economic, environmental and social dimensions of the risk are selected based on the characteristics of the study area. Each risk dimension is explained separately in the following sections.

5.1.1 Economic Elements at Risk

The economic elements at risk used in this study are given in Table 5.1. Based on case specific characteristics of the study area under investigation, elements at risk can be populated. For example, administrative buildings, commercial buildings, industrial buildings, death of animals, agricultural losses can also be added to the list. Since the study area is located at a rural region such economic elements are not included in this study. Roads, residential buildings, recreation area, critical infrastructure, barns and rest rooms are chosen as economic elements at risk for this case study. There is no detailed information about the study area but it is known that green area exists and it is used as a recreation area. The exact location is not known so the recreation area is marked as in Figure 5.1

The study area is gridded into 10 m x 10 m cells. The cell size is selected in accordance with the scale of the map. Bigger cell sizes can be accomodated for smaller scaled maps. After a number of trial and error runs, it is decided that 10 m x 10 m cells are good enough to represent elements at risk. There are a total 1914 grid cells in the study area. The economic elements at risk in Table 5.1 are digitized in Arc-GIS by the help of 1/1000 scaled AutoCAD file of the study area and the elements at risk and water depths are used in economic damage and economic risk calcuations. This AutoCAD file can be seen in the Case Study Chapter. The gridded study area and economic elements at risk is given in Figure 5.1, on which, four cells are highlighted and marked as Cell 1, Cell 2, Cell 3 and Cell 4. These cells are used for demonstration of the results throughout this chapter.

Table 5.1: Economic Elements at Risk

Flood Risk Dimension	**Evaluation Criteria**	**Elements at Risk**	**Spatial Unit**
Economic Risk Dimension	Transport	Asphalt roads Earth roads	Line
	Housing	Residential buildings	Area
	Recreation	Parks, lakeside, picnic area	Area
	Critical Infrastructure	Hospitals, schools, mosques, nursing homes	Area
	Barns	Barns	Area
	Rest rooms	Restrooms	Area

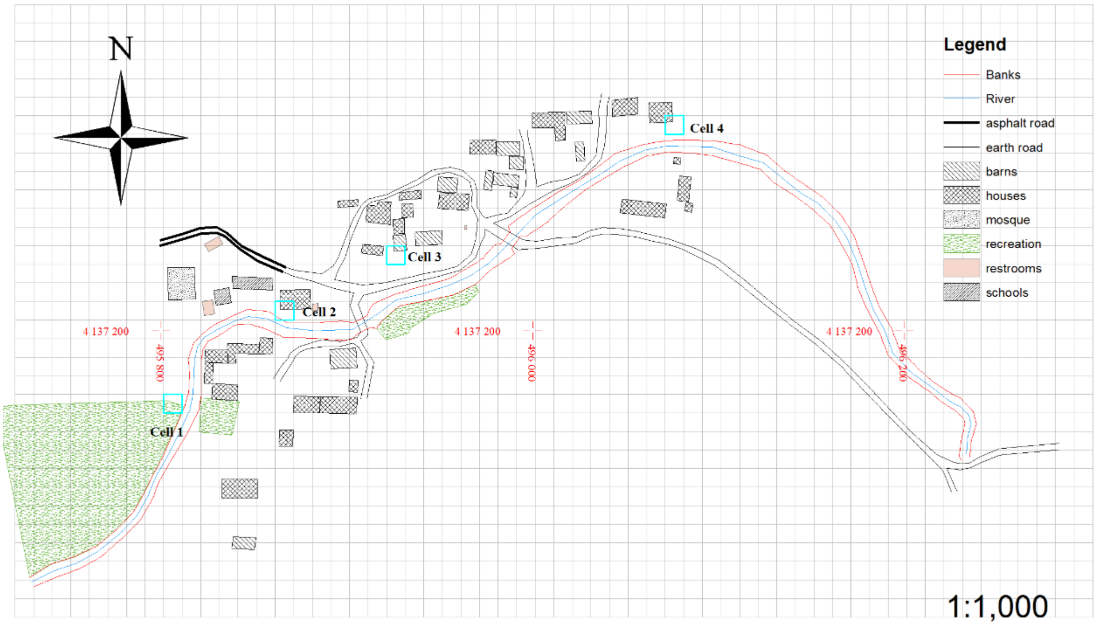

Figure 5.1: Gridded Study Area and Economic Elements at Risk

5.1.2 Social Elements at Risk

The social elements at risk used in this study can be seen in Table 5.2. These elements can be increased. For example, population can be divided into classes such as children younger than 12, elderly people older than 60 and people with ages between 12 and 60. The children and the elderly people are more vulnerable than people with ages between 12 and 60. However, there is no information about the age distribution for the residential buildings. Hence, in this study, population is used as a social risk element. It is assumed that there are people in each residential building. Another important social criterion is the cultural heritage sites such as monuments, museums etc. However, there is no such place in the study area. Hence, they are not included in the social elements at risk. Schools and mosques are identified as social hot spots within the study area and marked as social elements at risk. Finally, animals are included in the list. It is assumed that there are animals in each barn and flood water may harm or kill these animals. The elements at risk in Table 5.2 are digitized in Arc-GIS by help of 1/1000 scaled AutoCAD file to calculate social damage and social risk. The social elements at risk can be seen in Figure 5.2.

Table 5.2: Social Elements at Risk

Flood Risk Dimension	**Evaluation Criteria**	**Elements at Risk**	**Spatial Unit**
Social Risk Dimension	Population	Population	Area
	Social hot spots	Critical infrastructure such as schools, mosques, hospitals	Area
	Animals harmed or died	Dead or injured animals	Area

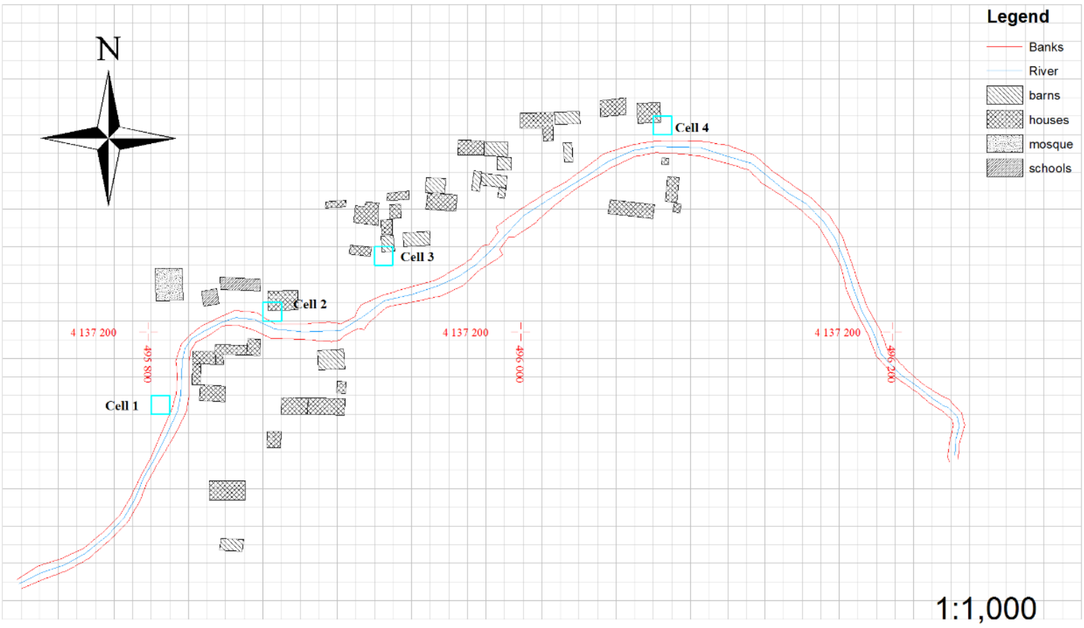

Figure 5.2: Gridded Study Area and Social Elements at Risk

5.1.3 Environmental Elements at Risk

The environmental elements at risk used in this study are given in Table 5.3. These elements can be populated. For example, endemic species living in water or land may be affected from floods. If there exist such elements, they should be included in the list. Furthermore, the tree species sensitive to inundation should be included in the list. In the study area, there are not any tree species sensitive to inundation so they are not included in the list.

Potential pollution is an important environmental risk element. It is assumed that if there is a barn or rest room and if it is flooded, it will cause pollution. The other risk element is the erodibility of the surface. In this study, the erodibility potential of the surface is used as an environmental damage indicator as well. The slope of the surface is calculated by the help of the ArcGIS program. Then this raster map is converted to point data. If the slope of the terrain is bigger than 18° and there is no vegetation cover or impervious surface, erosion might be a severe environmental problem. If the slope of the terrain is smaller than 18° and bigger than 8° and there is no vegetation cover or impervious surface, this might be referred to as moderate erosion. If the slope of the terrain is between 3° and 8°, erosion risk is considered to be slight. If the slope of the terrain is less than 3° or the vegetation cover exists or the surface is impervious, it might be evaluated as no erosion risk. (Niog, 1998). This information is used to generate damage functions given in Section 4.3.3 (see Equation 4.9). When site specific data such as slope of the terrain, cover of the surface, type of the soil, rainfall, runoff etc. is available erosion calculations should be based on these data. Due to data limitations erosion risk is simply evaluated as a funciton of slope and exitance of vegetation cover in this study. The elements at risk in Table 5.3 are digitized in ArcGIS by help of 1/1000 scaled AutoCAD file and it is used to calculate damage and risk. The elements at risk and the slope of the surface in degrees can be seen in Figure 5.3.

Table 5.3: Environmental Elements at Risk

Flood Risk Dimension	**Evaluation Criteria**	**Elements at Risk**	**Spatial Unit**
Environmental Risk Dimension	Potential pollution	Animal barns, rest rooms	Area
	Erodibility	The slope of the surface	Point

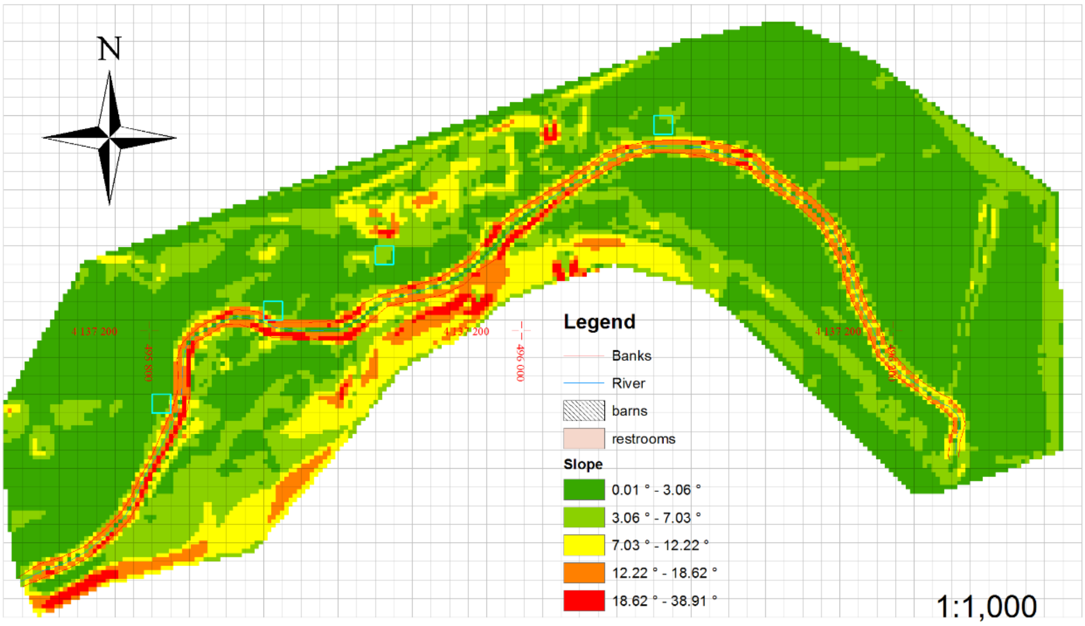

Figure 5.3: Environmental Elements at Risk and Slope of the Terrain in Degrees

5.2 Water Depths in the Study Area

The generated digital elevation model using 1/25000 scaled map of the project area is given in Figure 5.4-a. The digital elevation model in Figure 5.4-b is created using 1/1000 scaled map (see Figure 3.6). The width of the cross-sections depends on the digital elevation model and the distance between two cross-sections vary. When the distance between cross-sections is short (i.e. 10 m, 20 m etc.), the cross-sections intersect with each other in the meandering sections of the river. Hence, shorter cross sections are used in the meandering parts of the river. However, shortened cross-sections could not enclose the floodplain. For this reason, the number of cross-sections are decreased in the meandering sections of the river. Although HEC-RAS is frequently used in flood risk studies in the literature, in our experience it is not successful in the meandering sections of the river. A total of 23 cross-sections are generated to calculate water depths along the modeled section of Salkım Stream which is approximately 711 meters long. Four cross-sections named as cross-section 1, 2, 3 and 4 are identified and marked on Figure 5.4-b. These cross-sections are used to demonstrate results throughout this section.

In this study, seven return periods (i.e. 5, 10, 25, 50, 100, 500 and 1000 years) are used to generate damage-exceedance probability curves. The normal depth value is calculated as 0.008 which is the average slope of the river bed and it is used as the boundary condition. Discharges for different return period floods and and corresponding HEC-RAS names are given in Table 5.4. The leeves are used in HEC-RAS Model to prevent water flow to irrevelant locations. Calculated water depths at cross-sections 1, 2, 3 and 4 are given in Figure 5.5.

The resolution of map is good enough but in some places there are wrong elevation values because of two destroyed culverts. Destroyed culverts are given in Figure 3.6. The point data in these locations are deleted to generate more accurate digital elevation model.

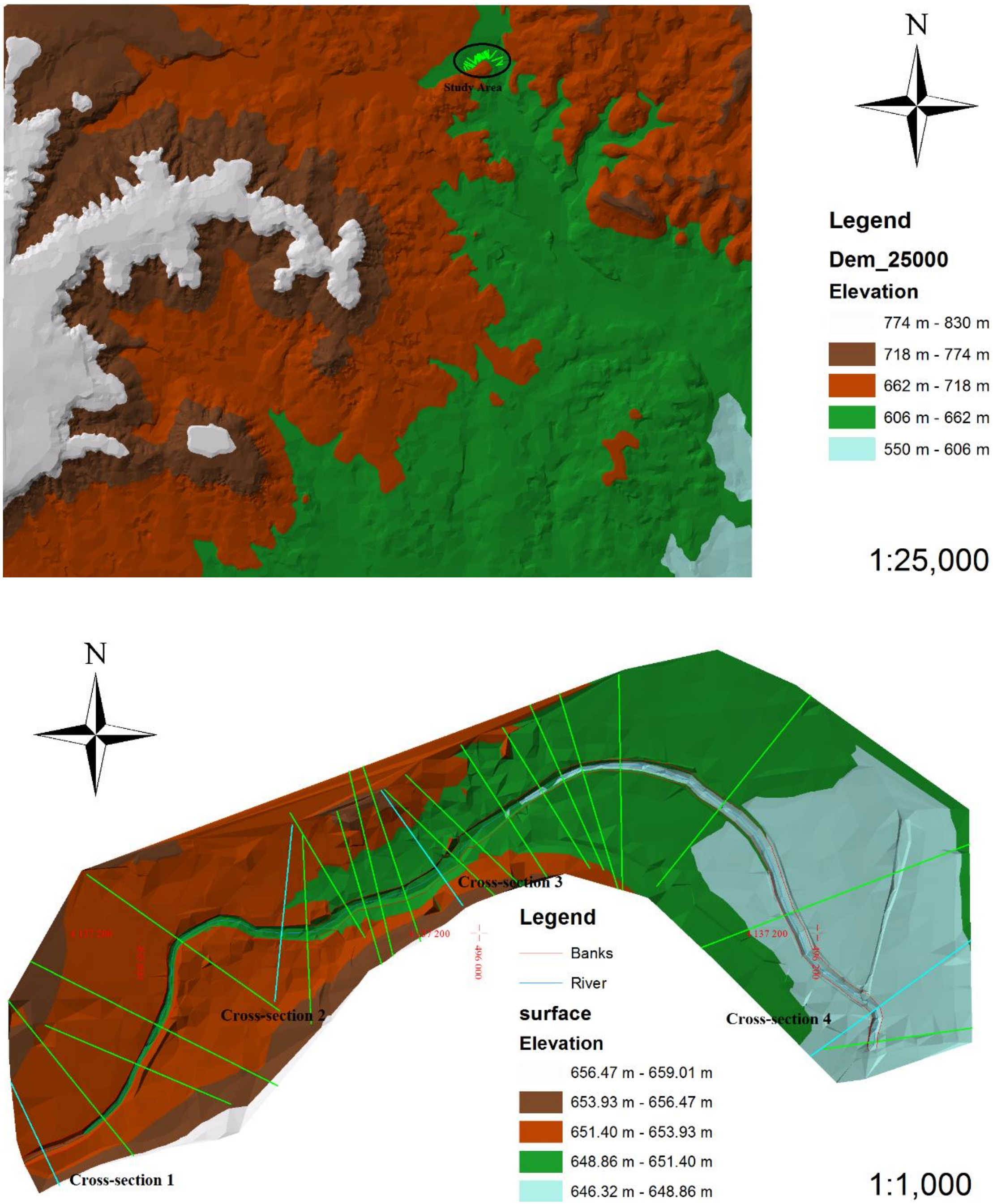

Figure 5.4: The Digital Elevation Model of the Studied Area in ArcGIS Environment (a) 1/25000 Scaled Map (b) 1/1000 Scaled Map

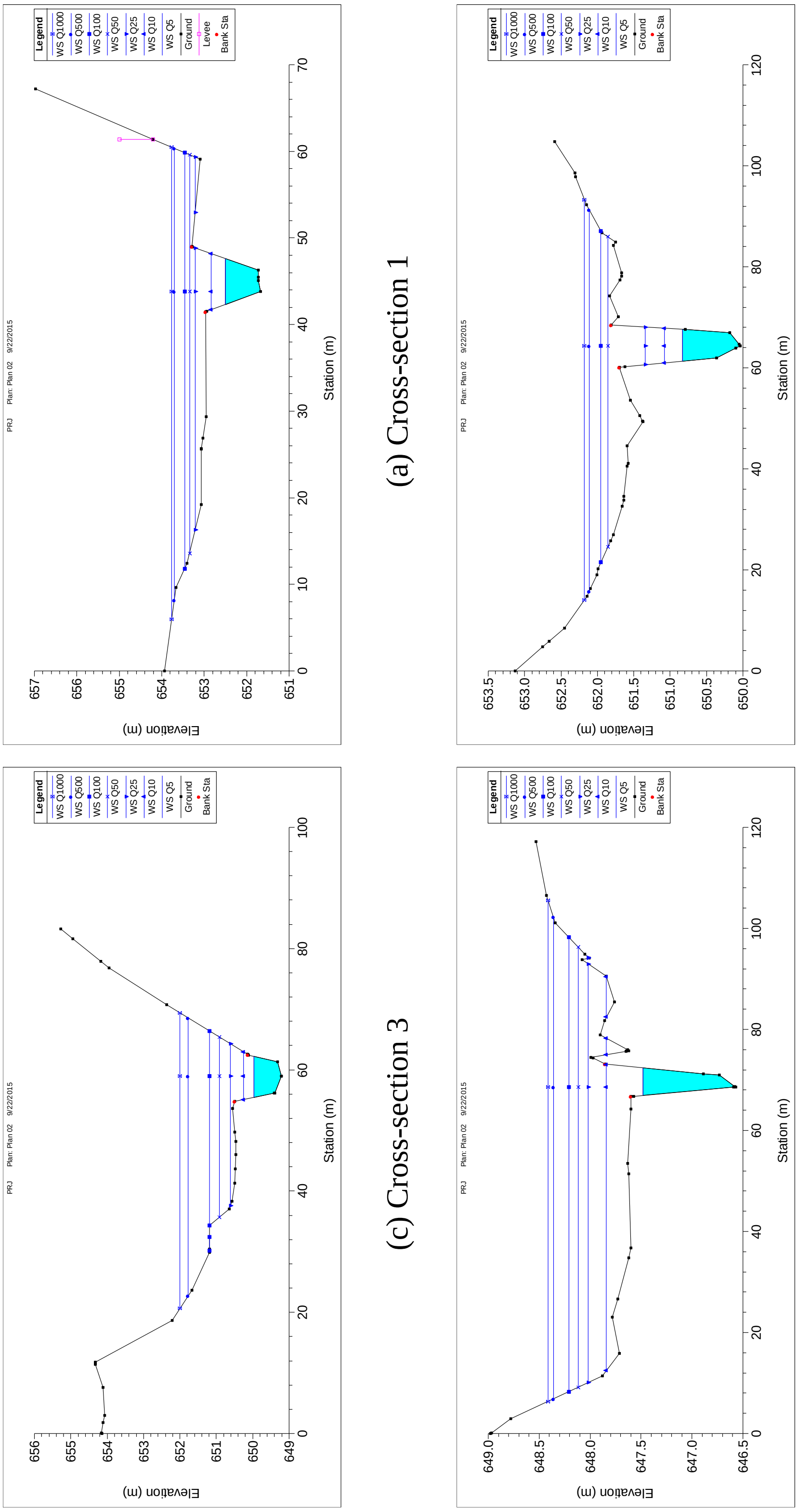

Figure 5.5: Water Depths Calculated using HEC-RAS at (a) Cross section 1 (b) Cross section 2 (c) Cross section 3 (d) Cross section 4

Table 5.4: Discharge Values for Different Return Periods

HEC-RAS name	Return Period, T_r (year)	Discharge (m^3/s)
Q5	5	6.85
Q10	10	12.77
Q25	25	22.97
Q50	50	32.38
Q100	100	43.19
Q500	500	64.23
Q1000	1000	73.30

Water depth maps for different return periods are given in Figure 5.6. As can be seen from Figure 5.6-a, for 5-year flood, maximum water depth is approximately 1.38 m. This value gets bigger with the increasing return period. The maximum water depth for 1000 year return period is approximately 3.01 m which can be seen in Figure 5.6-g.

5.3 Calculated Damages

Damage calculations are carried out using the procedure explained in Section 4.3. For each dimension of risk, economic, social and environmental, damage calculations are carried out separately. Damage maps generated for each dimension of risk are given in the following sections.

5.3.1 Economic Damage Maps

In this study, the same damage function (Equation 4-1) is used for all economic elements at risk because no depth-damage functions are available for Turkey. When depth-damage curves became available for Turkey, damage calculations can easily be repeated using these curves and this will result in more realistic estimates because depth-damage functions are created using data from past flood events.

In this study, resilience factor is considered for residential buildings and roads. For residential buildings, resilience factor may be assigned based on utilization of appropriate building materials, construction in accordance with building codes and existance of insurance (European Investment Bank, 2007; Guildford Borough, 2010). Unfortunately, there is no information about the building materials or if they were built using building codes etc. Hence, a hypotetical situation is created assigning random resilience factors between 0.1 and 1 to the residential buildings found in the study area. Furthermore, the resilience factor is considered as 0.5 for earth roads and 1.0 for asphalt roads. Damage calculations are carried out using Equation 4-2.

The economic damage maps are created for all return periods for each economic element at risk. The economic damage maps for earth road, rest rooms, mosques and asphalt road, schools, barns, recreation area and residential buildings are given in Figures 5.7, 5.8, 5.9, 5.10, 5.11, 5.12, and 5.13, respectively. In Figure 5.9, economic damage maps for only floods with 500 and 1000 year return periods are given since for the smaller return periods no economic damage was observed. As it can be seen, the damage is higher close to the river and it is getting smaller away from the river. In Figure 5.14, the economic damage map in which resilience factors for residential buildings are integrated is given. As can be seen from Figure 5.14, the damage factor in some cells is 10 times bigger than Kubal et al.'s approach (2009) because of the resilience factor. In Figure 5.15, the economic damage map in which resilience factor for earth roads is integrated into the calculations is given. It can be seen that the damage is doubled at all cells where earth road is located and flooded because the resilience factor for earth road is taken as 0.5. Compared to the asphalt road, the earth road is expected to be damaged more and may take longer to be put back in operation.

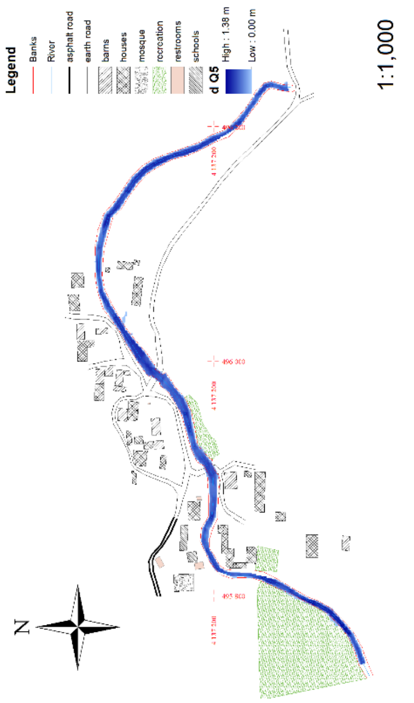

(a) 5-year flood

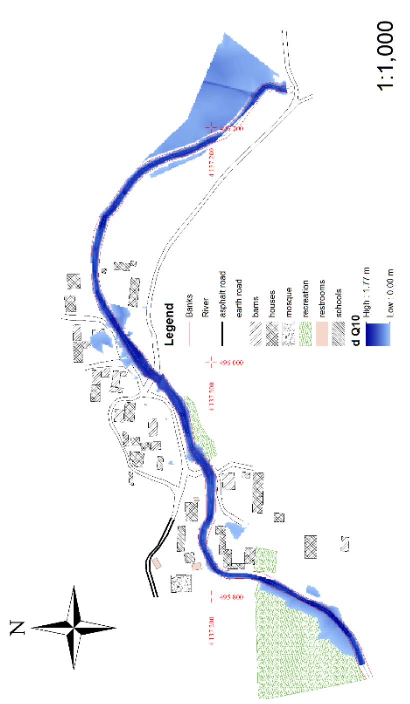

(b) 10-year flood

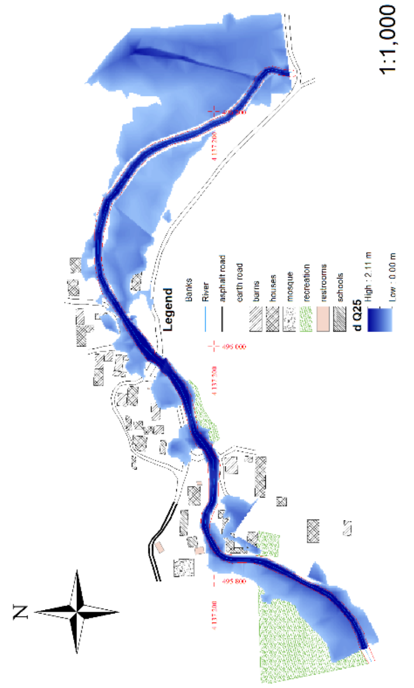

(c) 25-year flood

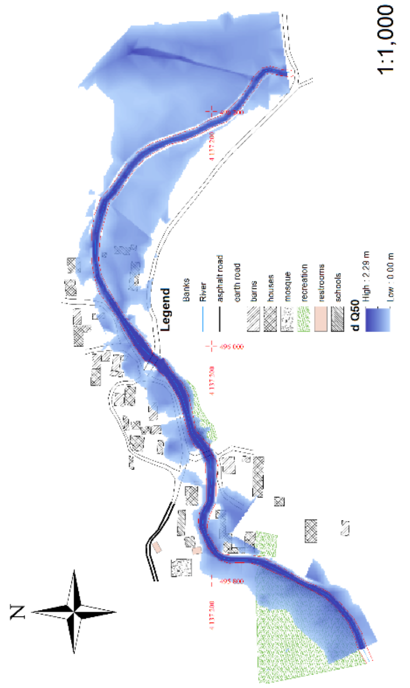

(d) 50-year flood

Figure 5.6: Water Depth Maps for (a) 5-Year Flood (b) 10-Year Flood (c) 25-Year Flood (d) 50-Year Flood (e) 100-Year Flood (f) 500-Year Flood (g) 1000-Year Flood

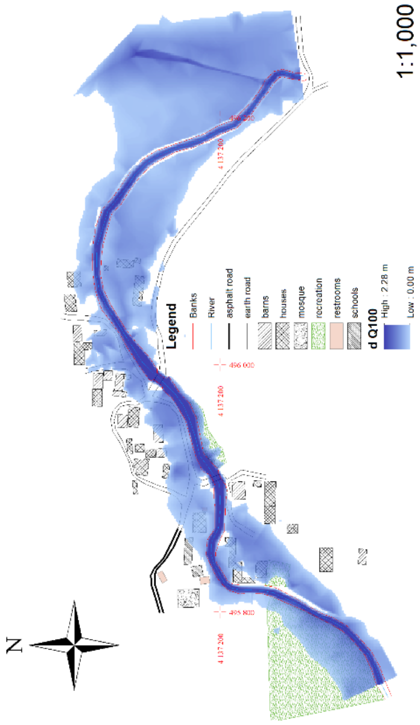

(e) 100-year flood

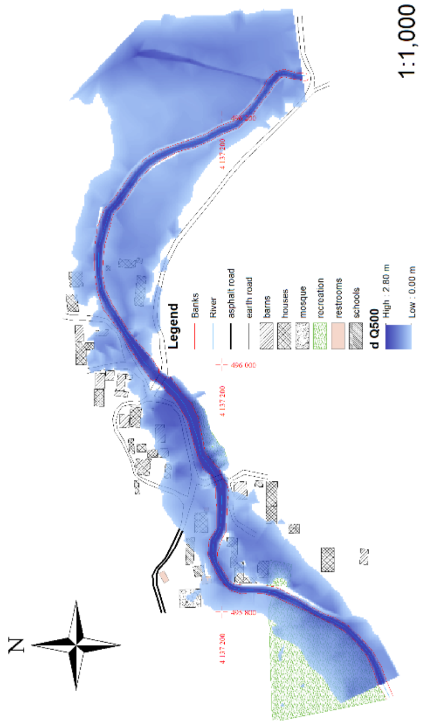

(f) 500-year flood

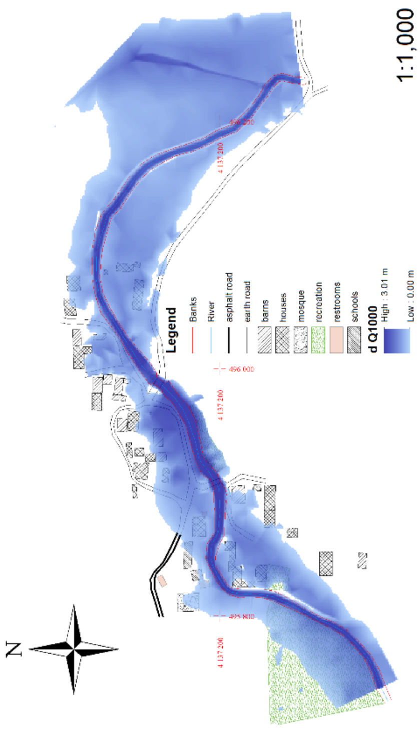

(g) 1000-year flood

Figure 5.6 (cont'd)

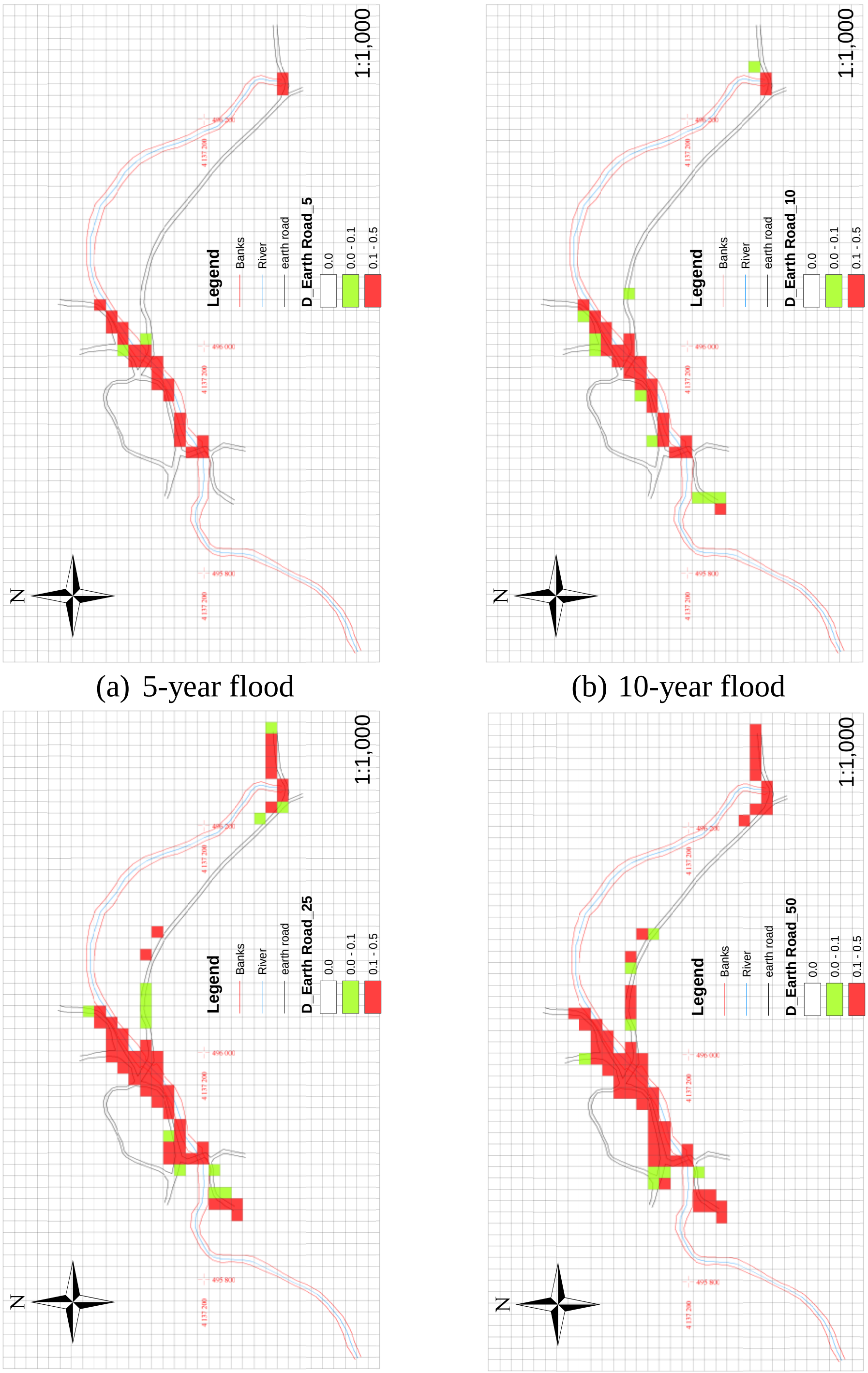

(a) 5-year flood

(b) 10-year flood

(c) 25-year flood

(d) 50-year flood

Figure 5.7: Economic Damage Maps for Earth Road for (a) 5-Year Flood (b) 10-Year Flood (c) 25-Year Flood (d) 50-Year Flood (e) 100-Year Flood (f) 500-Year Flood (g) 1000-Year Flood

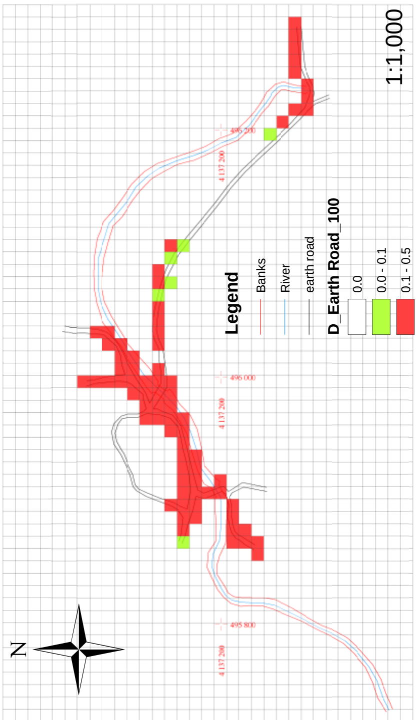

(e) 100-year flood

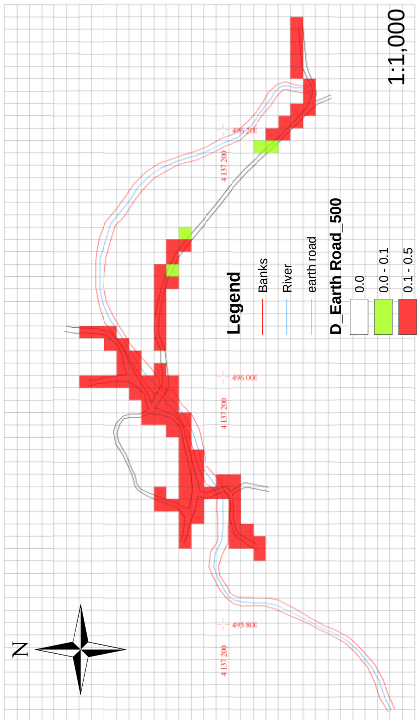

(f) 500-year flood

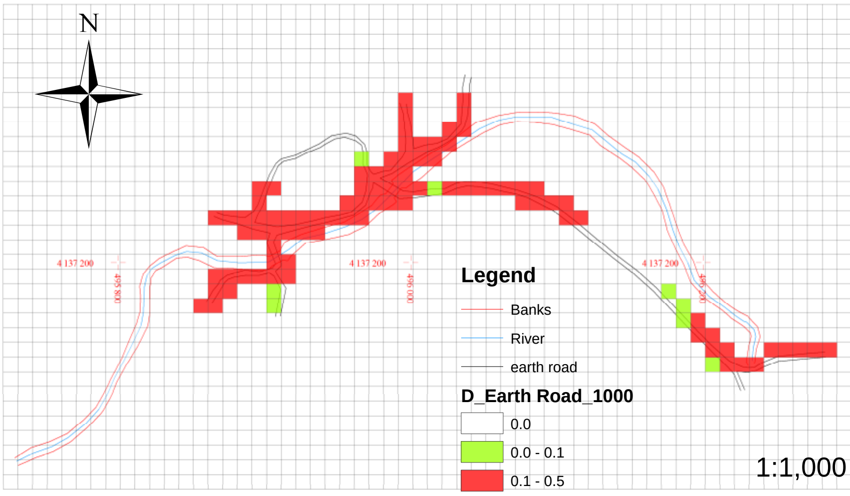

(g) 1000-year flood

Figure 5.7 (cont'd)

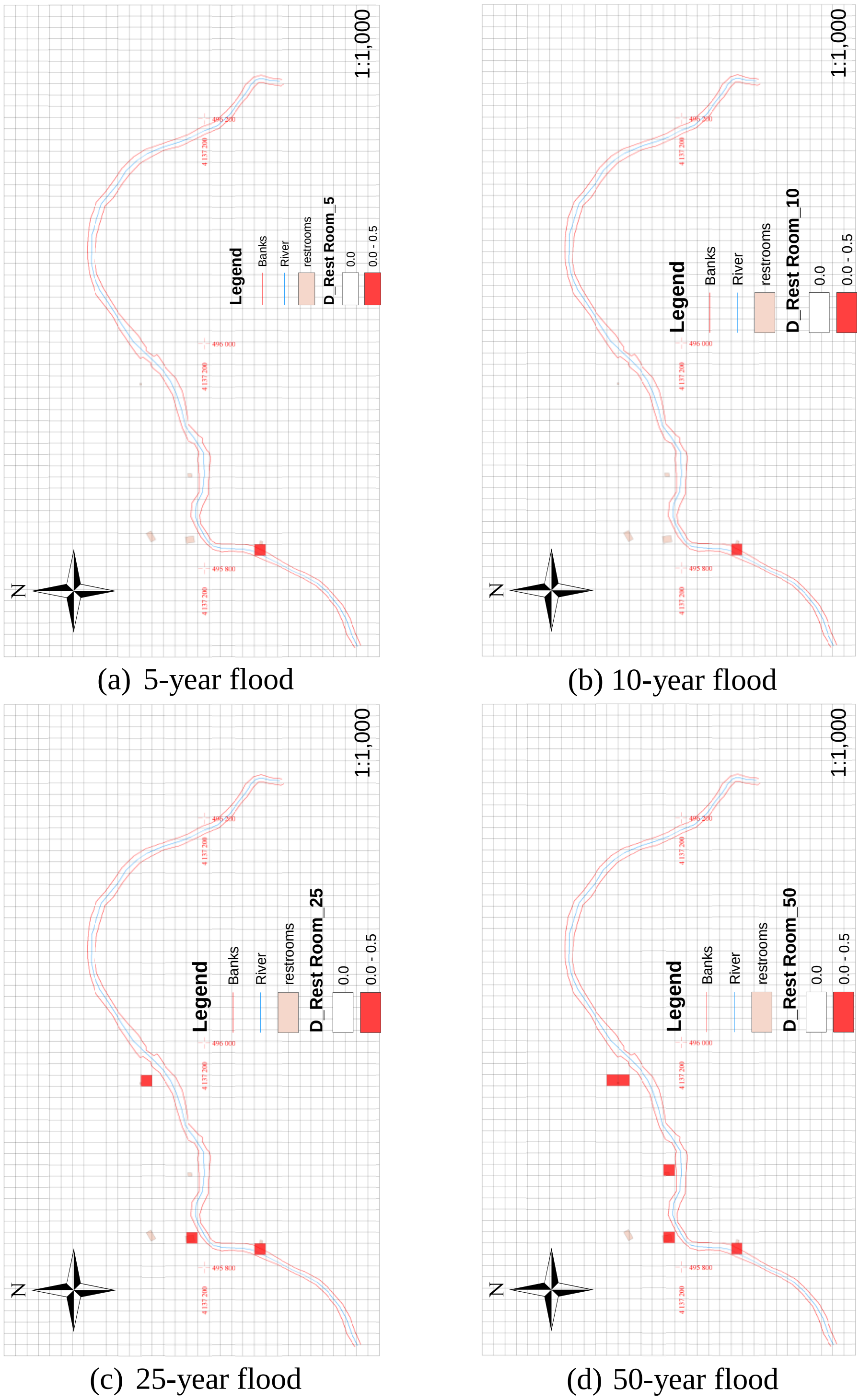

(a) 5-year flood

(b) 10-year flood

(c) 25-year flood

(d) 50-year flood

Figure 5.8: Economic Damage Maps for Rest Room for (a) 5-Year Flood (b) 10-Year Flood (c) 25-Year Flood (d) 50-Year Flood (e) 100-Year Flood (f) 500-Year Flood (g) 1000-Year Flood

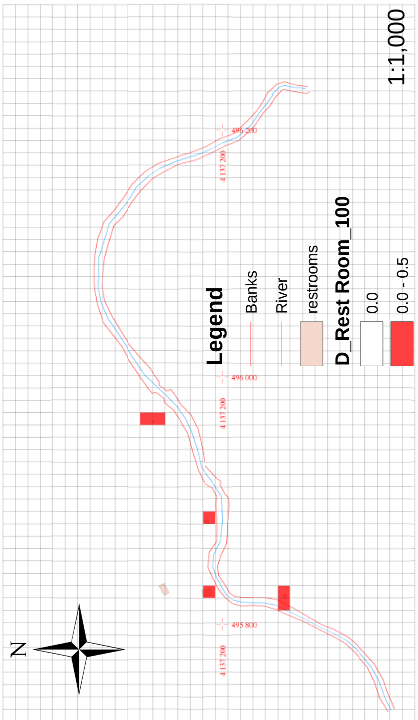

(e) 100-year flood

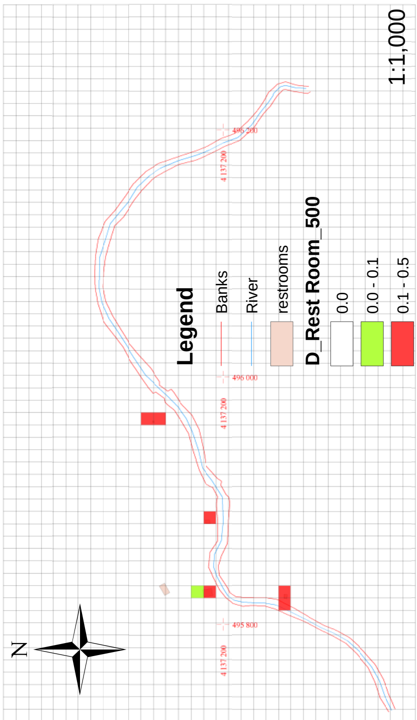

(f) 500-year flood

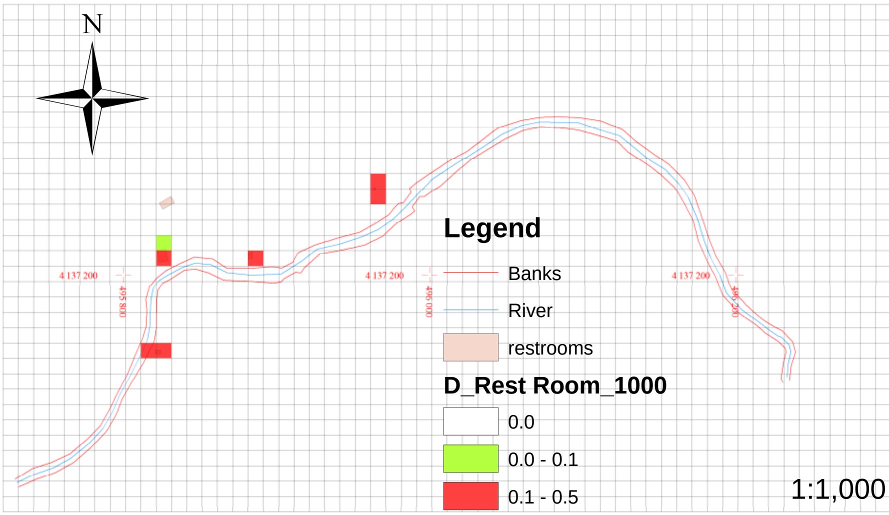

(g) 1000-year flood

Figure 5.8 (cont'd)

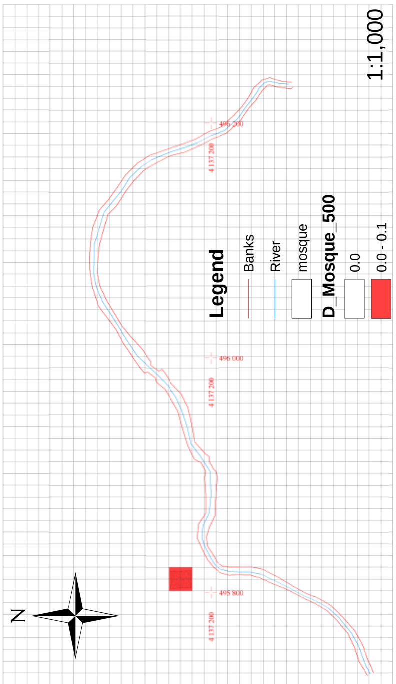

(a) 500-year flood

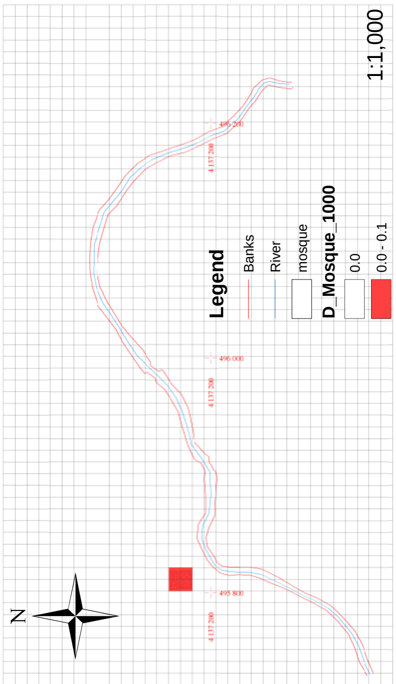

(b) 1000-year flood

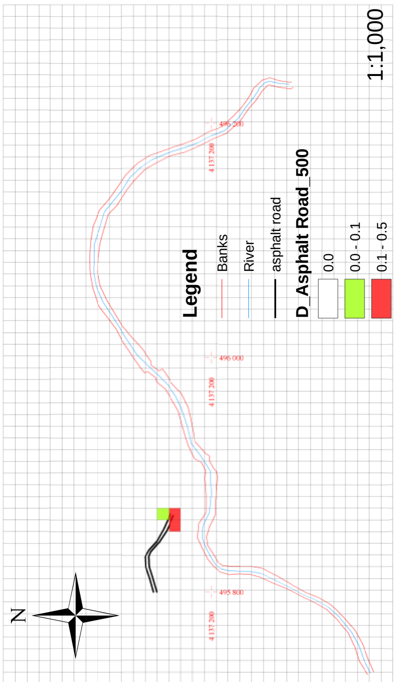

(c) 500-year flood

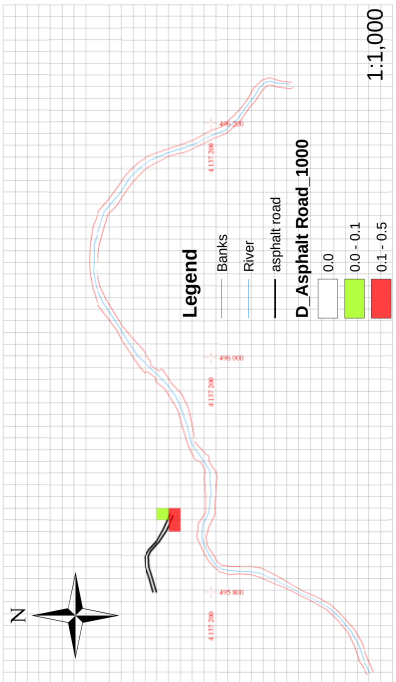

(d) 1000-year flood

Figure 5.9: Economic Damage Maps for Asphalt Roads and Mosques for (a) 500-Year Flood for Mosques (b) 1000-Year Flood for Mosques (c) 500-Year Flood for Asphalt Roads (d) 1000-Year Flood for Asphalt Roads

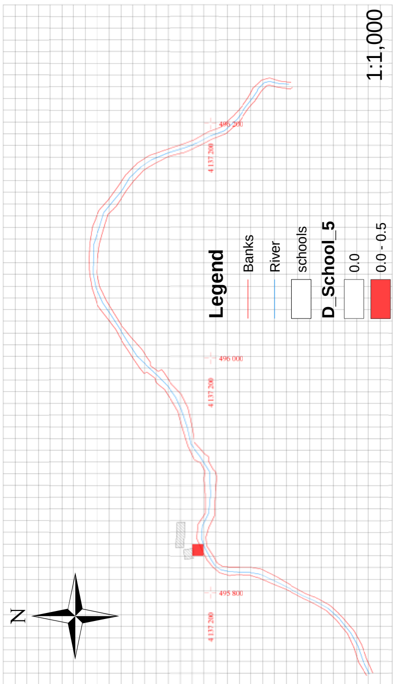

(a) 5-year flood

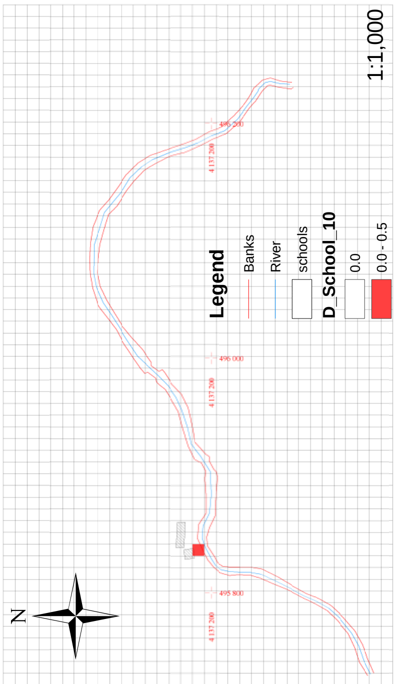

(b) 10-year flood

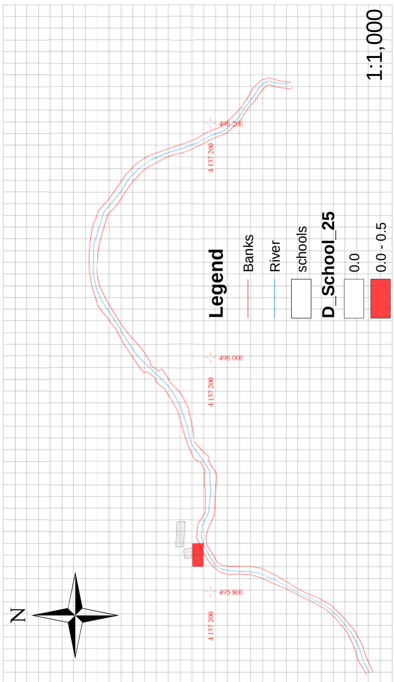

(c) 25-year flood

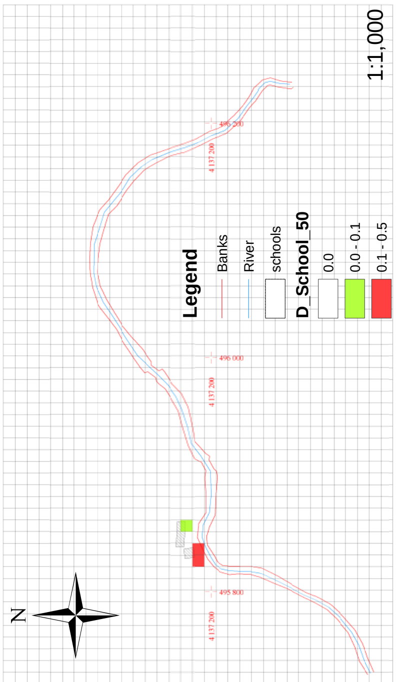

(d) 50-year flood

Figure 5.10: Economic Damage Maps for Schools for (a) 5-Year Flood (b) 10-Year Flood (c) 25-Year Flood (d) 50-Year Flood (e) 100-Year Flood (f) 500-Year Flood (g) 1000-Year Flood

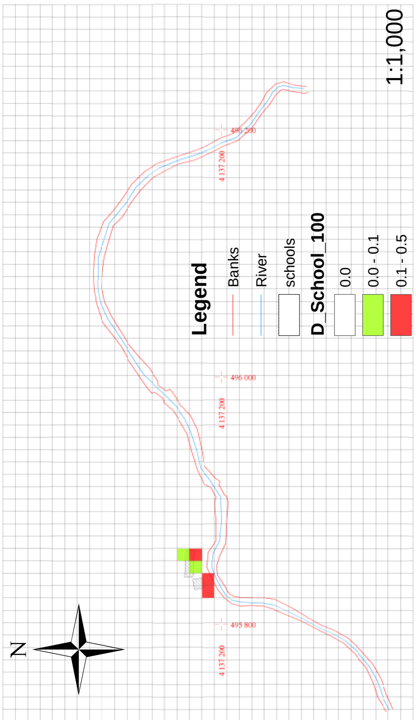

(e) 100-year flood

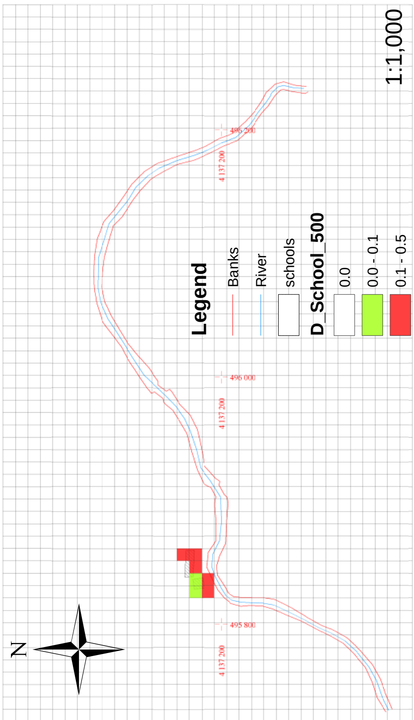

(f) 500-year flood

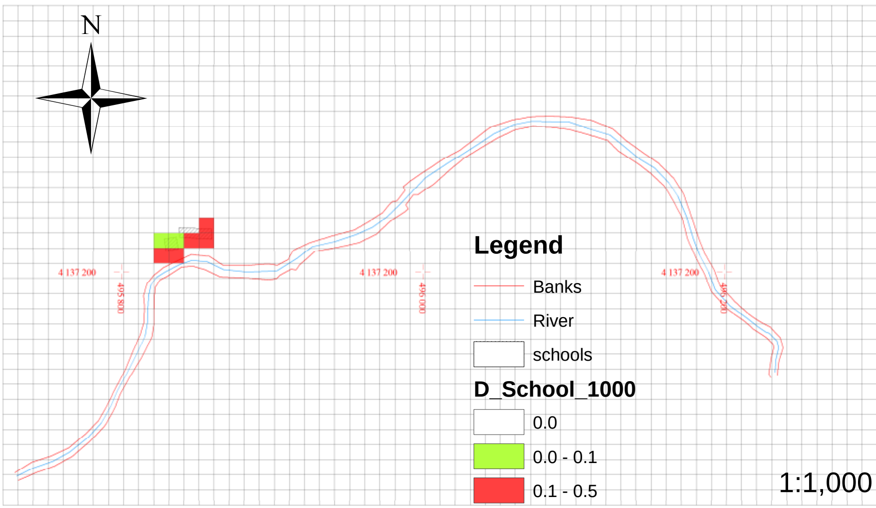

(g) 1000-year flood

Figure 5.10 (cont'd)

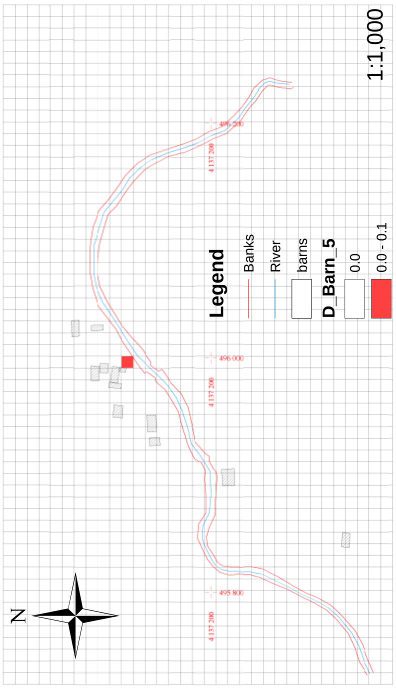

(a) 5-year flood

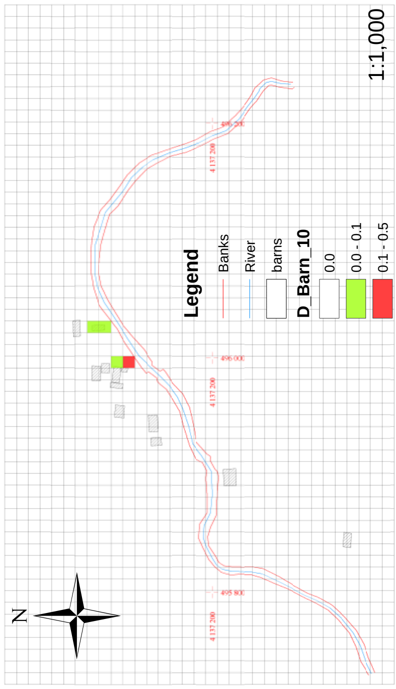

(b) 10-year flood

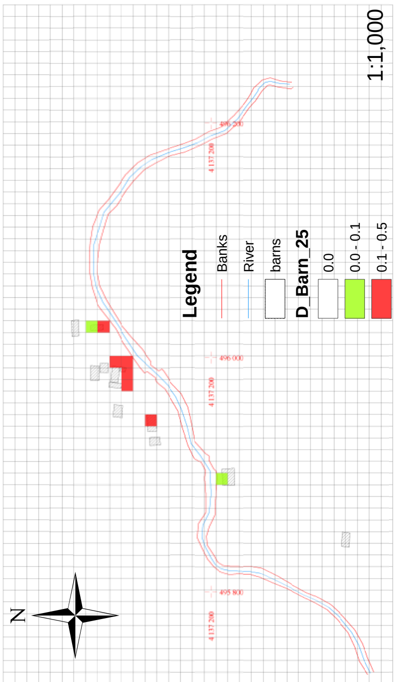

(c) 25-year flood

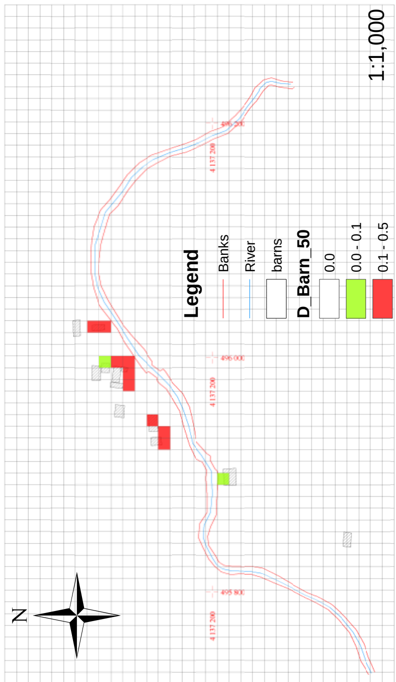

(d) 50-year flood map

Figure 5.11: Economic Damage Maps for Barns for (a) 5-Year Flood (b) 10-Year Flood (c) 25-Year Flood (d) 50-Year Flood (e) 100-Year Flood (f) 500-Year Flood (g) 1000-Year Flood

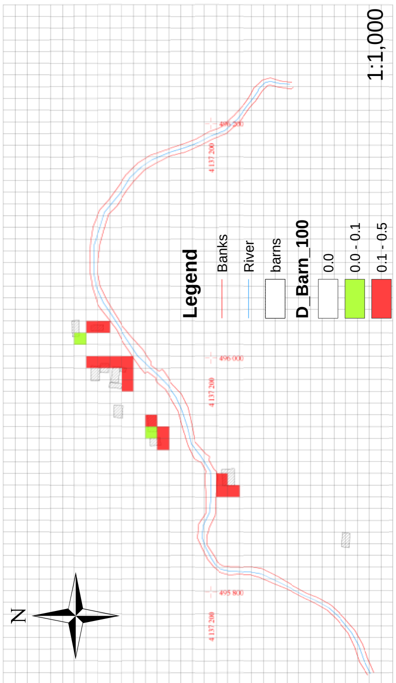

(e) 100-year flood

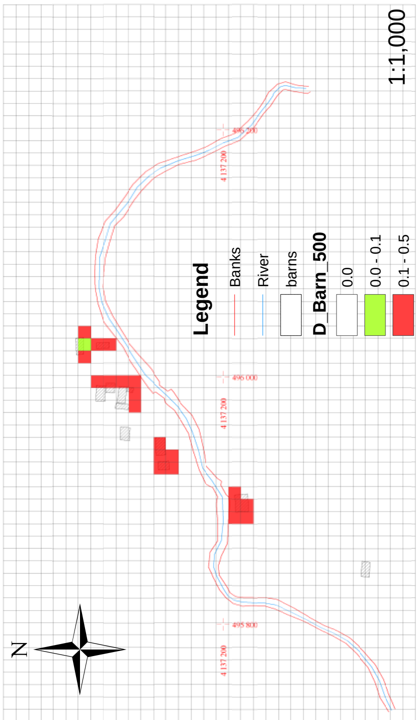

(f) 500-year flood

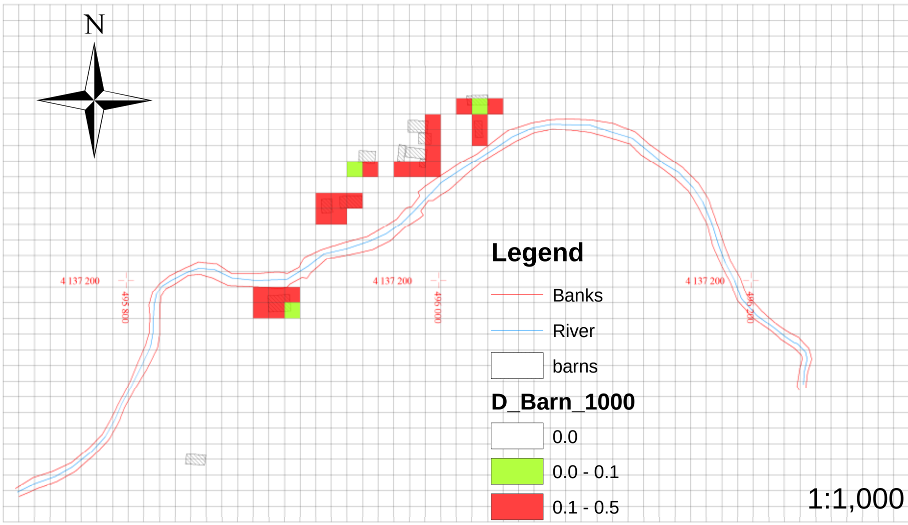

(g) 1000-year flood

Figure 5.11 (cont'd)

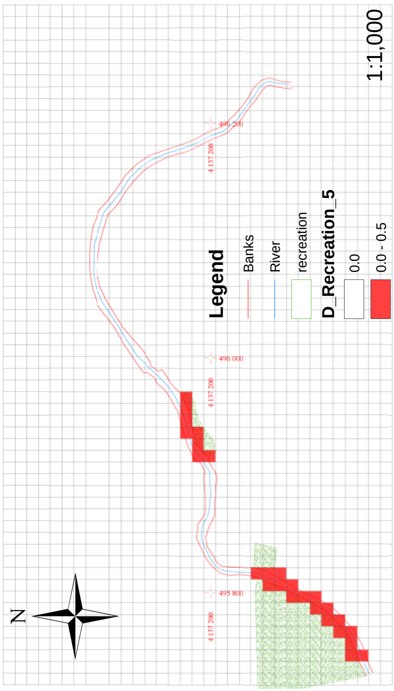

(a) 5-year flood

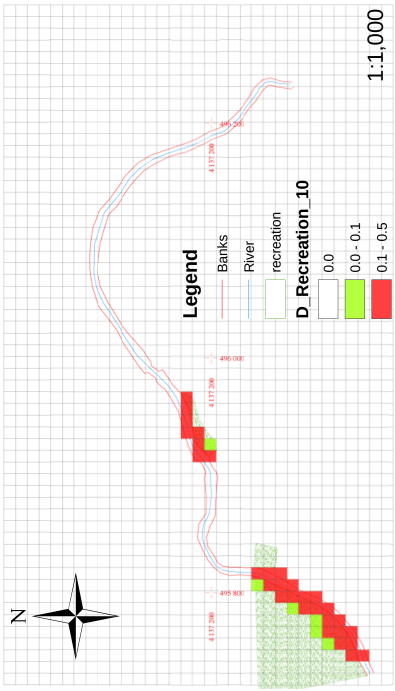

(b) 10-year flood

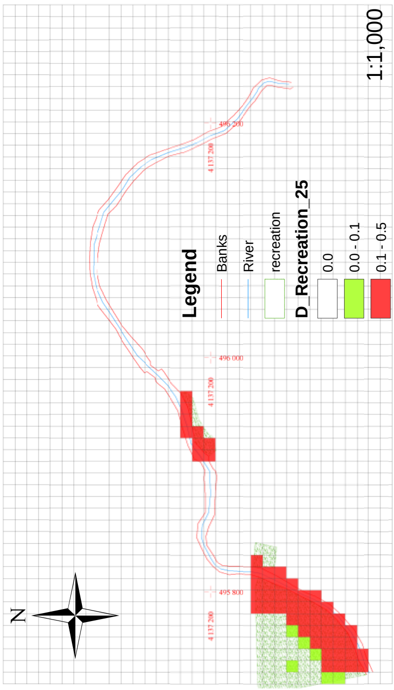

(c) 25-year flood

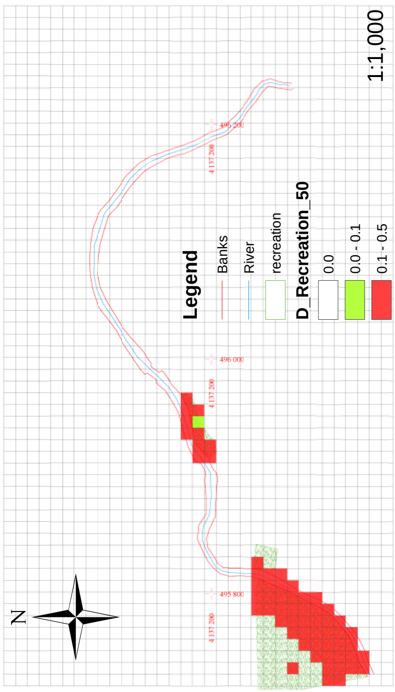

(d) 50-year flood

Figure 5.12: Economic Damage Maps for Recreation Area for (a) 5-Year Flood (b) 10-Year Flood (c) 25-Year Flood (d) 50-Year Flood (e) 100-Year Flood (f) 500-Year Flood (g) 1000-Year Flood

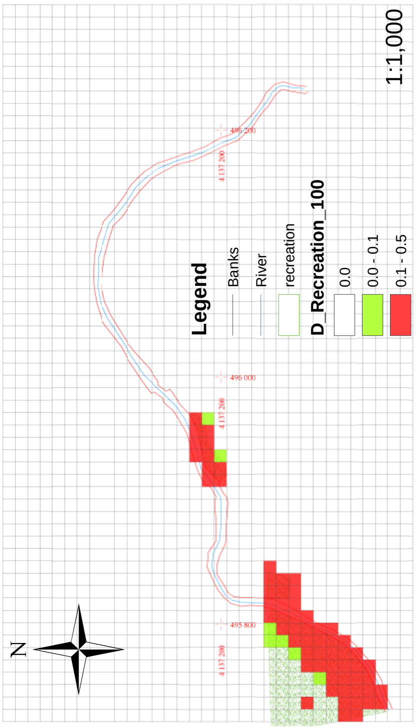

(e) 100-year flood

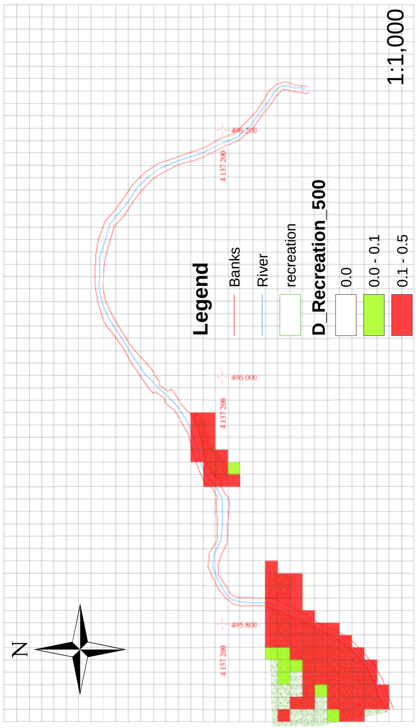

(f) 500-year flood

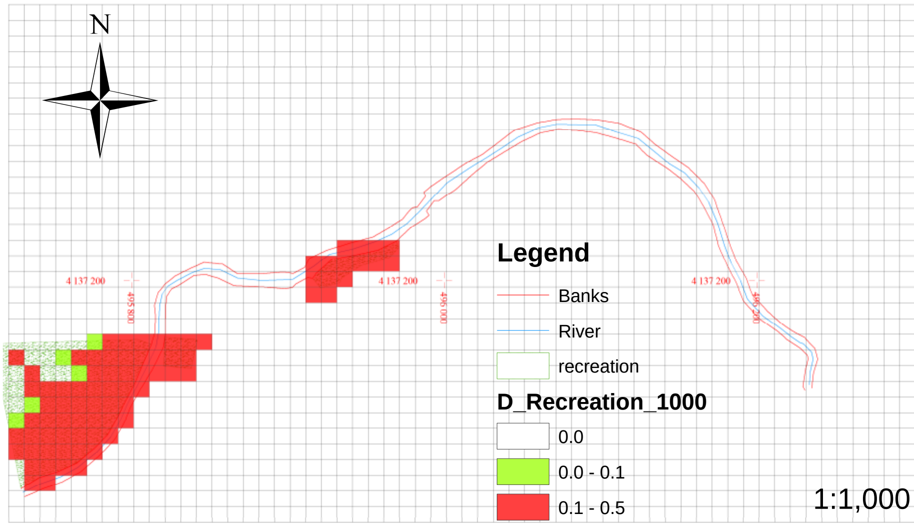

(g) 1000-year flood

Figure 5.12 (cont'd)

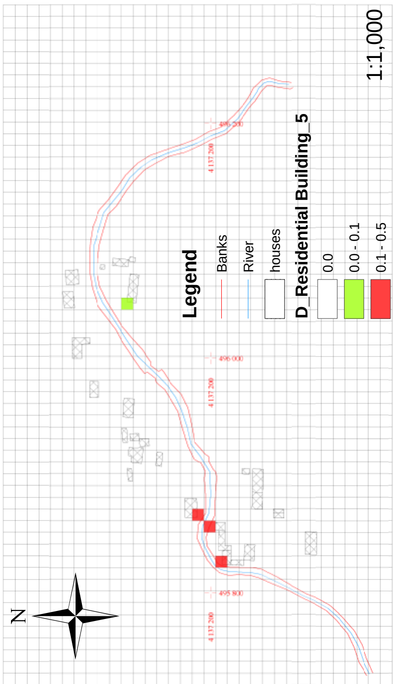

(a) 5-year flood

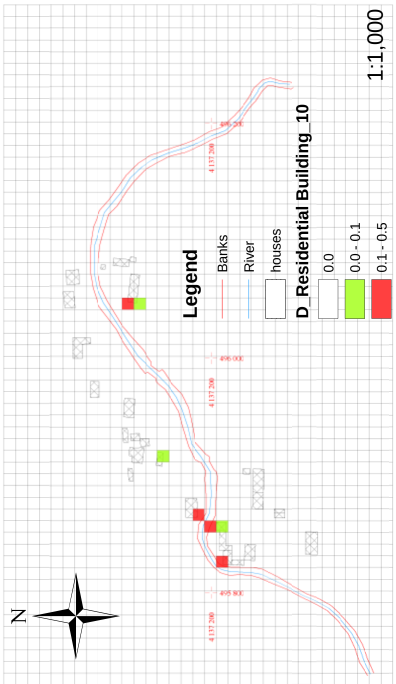

(b) 10-year flood

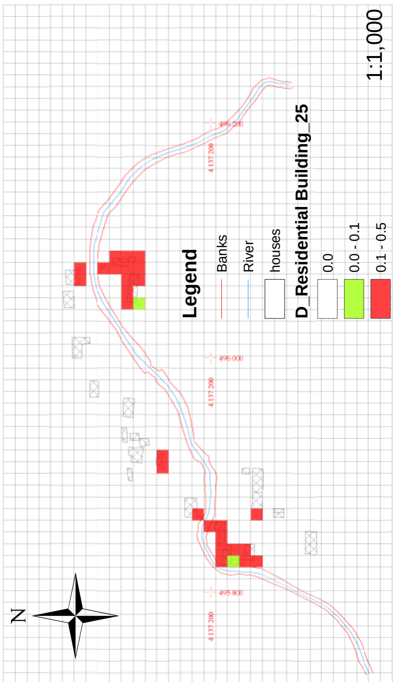

(c) 25-year flood

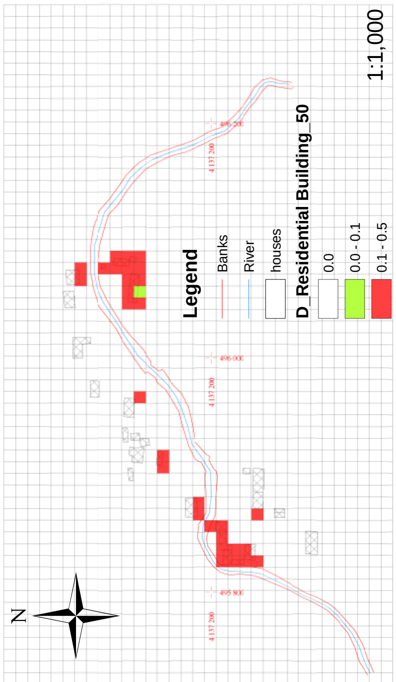

(d) 50-year flood

Figure 5.13: Economic Damage Maps for Residential Buildings for (a) 5-Year Flood (b) 10-Year Flood (c) 25-Year Flood (d) 50-Year Flood (e) 100-Year Flood (f) 500-Year Flood (g) 1000-Year Flood

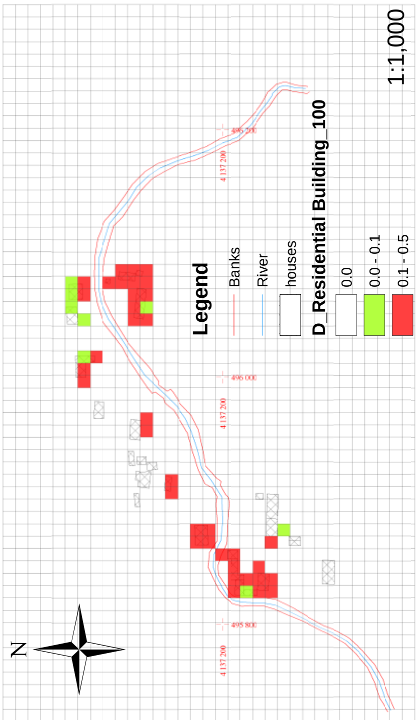

(e) 100-year flood

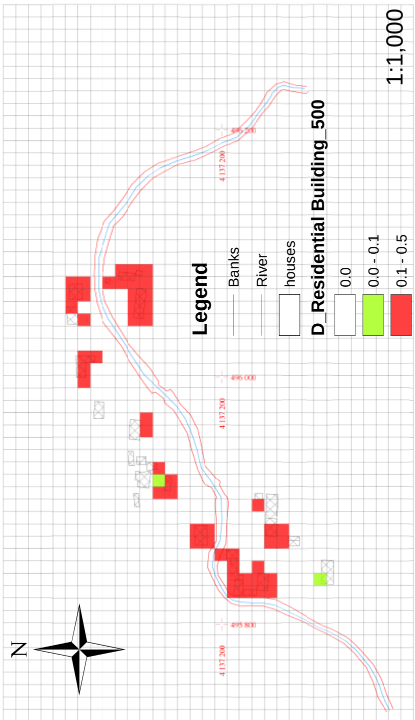

(f) 500-year flood

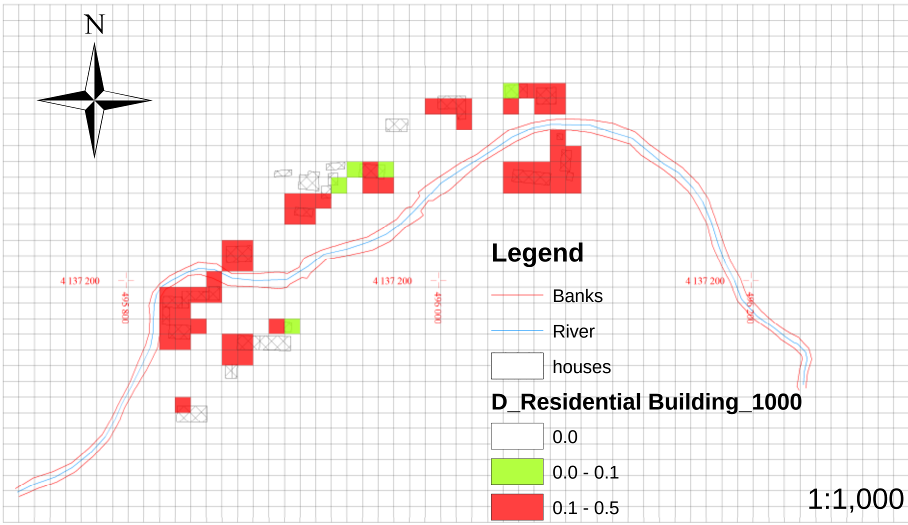

(g) 1000-year flood

Figure 5.13 (cont'd)

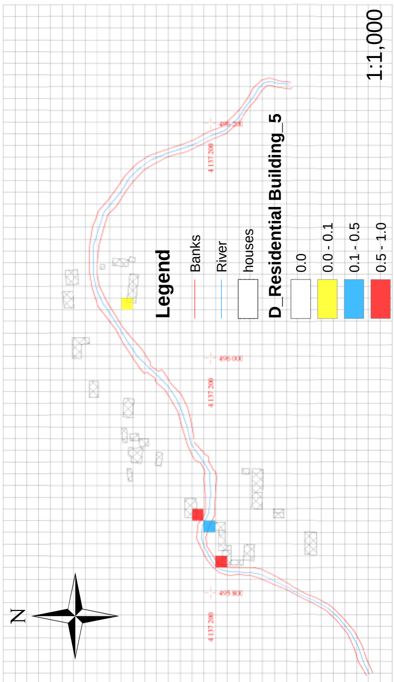

(a) 5-year flood

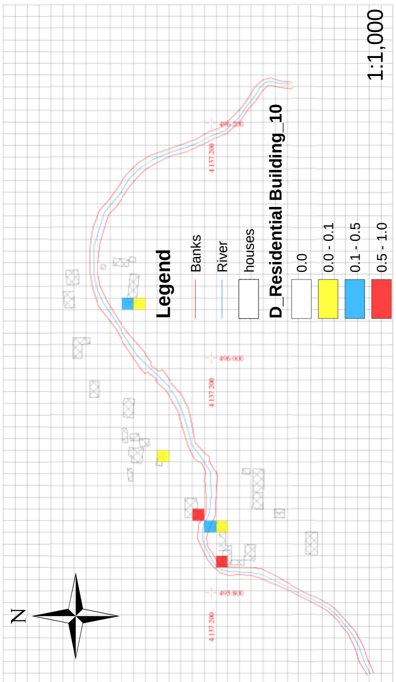

(b) 10-year flood

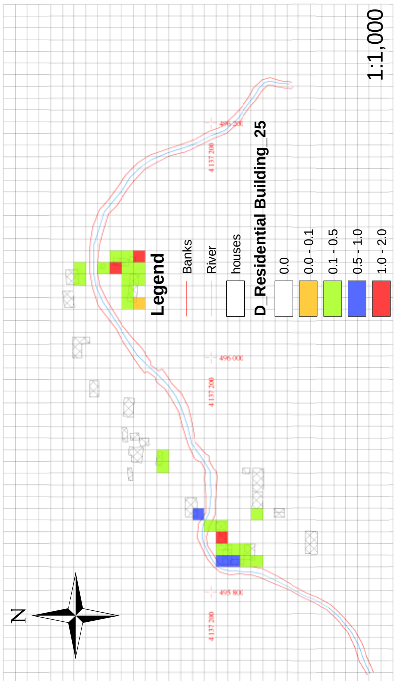

(c) 25-year flood

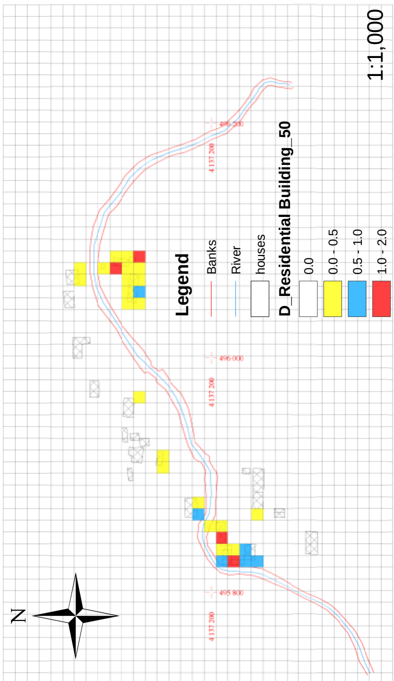

(d) 50-year flood

Figure 5.14: Economic Damage Maps for Residential Buildings using the Resilience Factor for (a) 5-Year Flood (b) 10-Year Flood (c) 25-Year Flood (d) 50-Year Flood (e) 100-Year Flood (f) 500-Year Flood (g) 1000-Year Flood

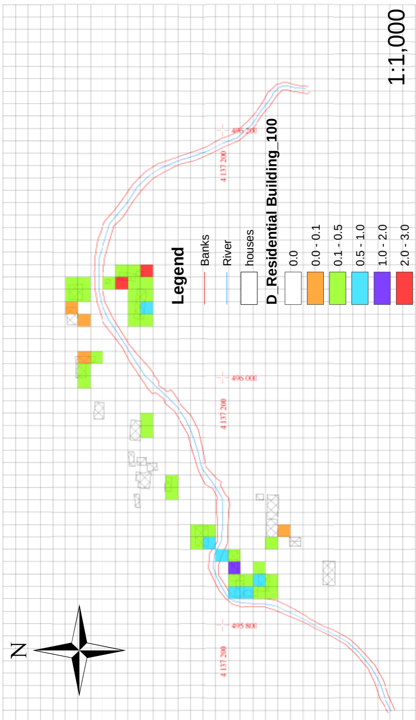

(e) 100-year flood

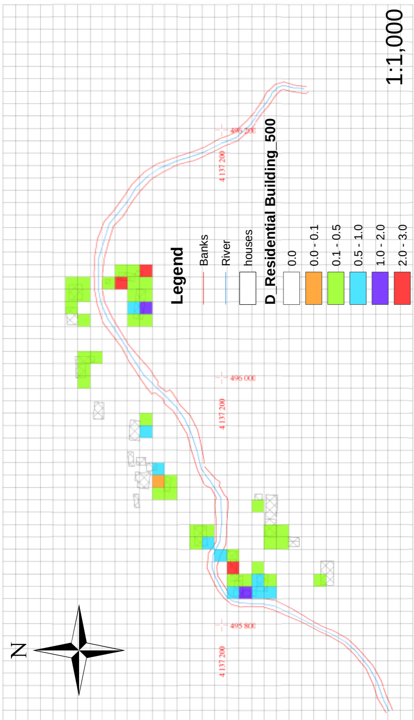

(f) 500-year flood

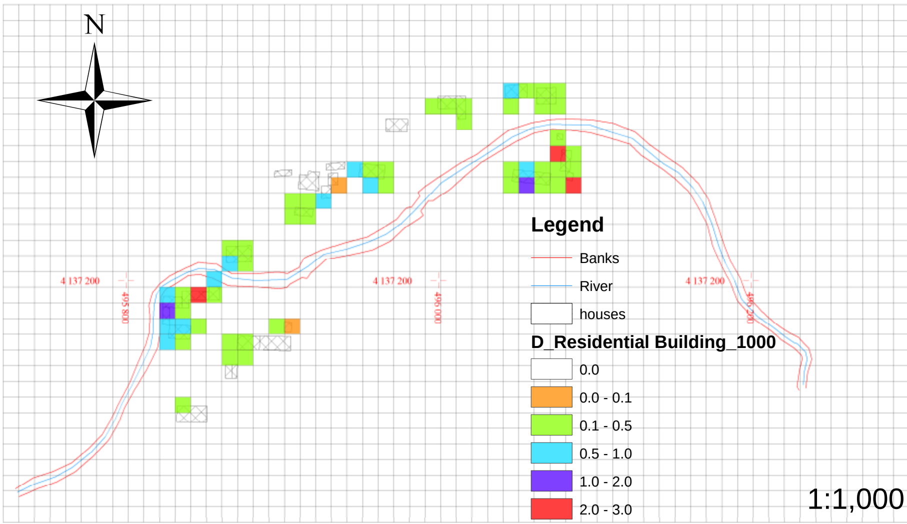

(g) 1000-year flood

Figure 5.14 (cont'd)

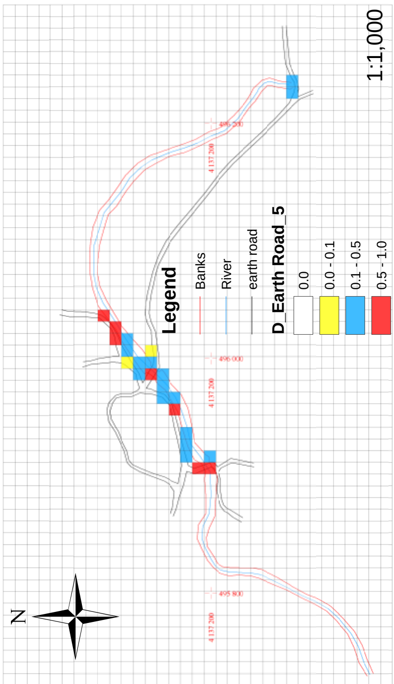

(a) 5-year flood

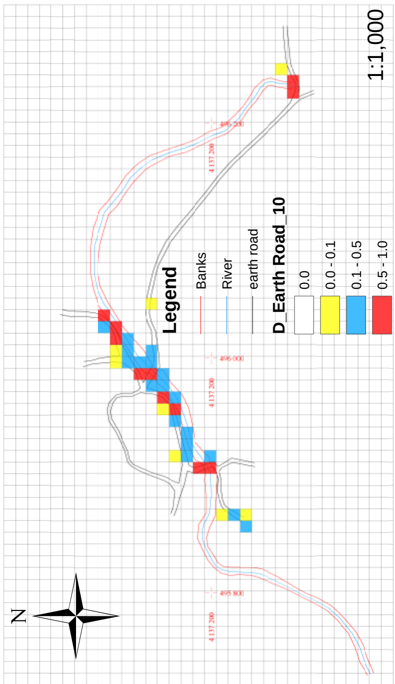

(b) 10-year flood

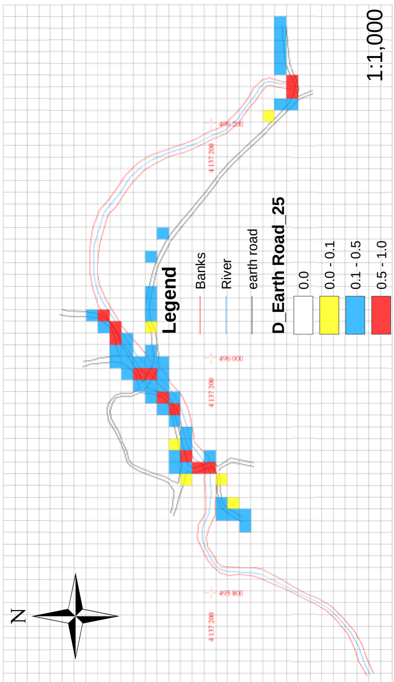

(c) 25-year flood

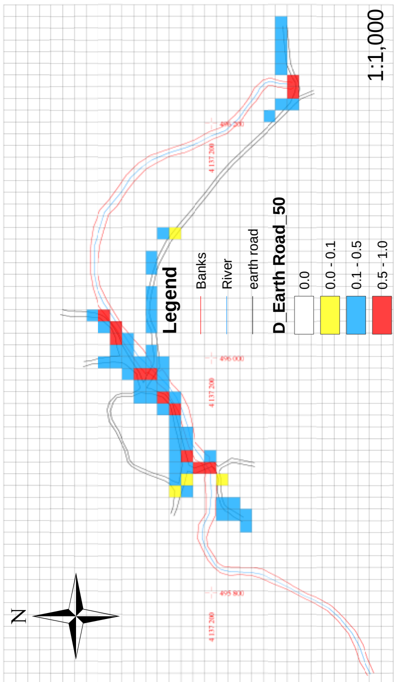

(d) 50-year flood

Figure 5.15: Economic Damage Maps for Earth Roads using the Resilience Factor for (a) 5-Year Flood (b) 10-Year Flood (c) 25-Year Flood (d) 50-Year Flood (e) 100-Year Flood (f) 500-Year Flood (g) 1000-Year Flood

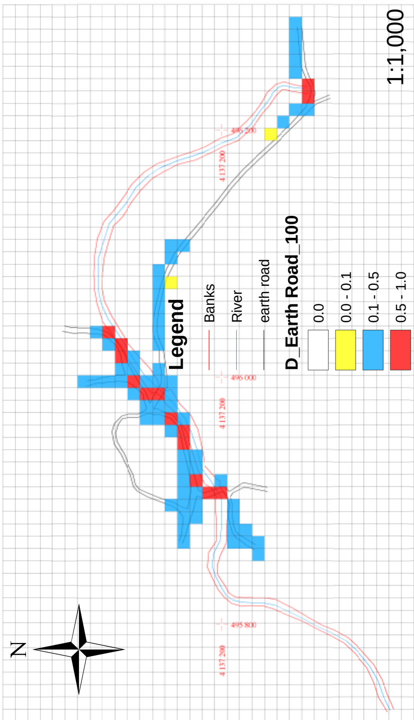

(e) 100-year flood

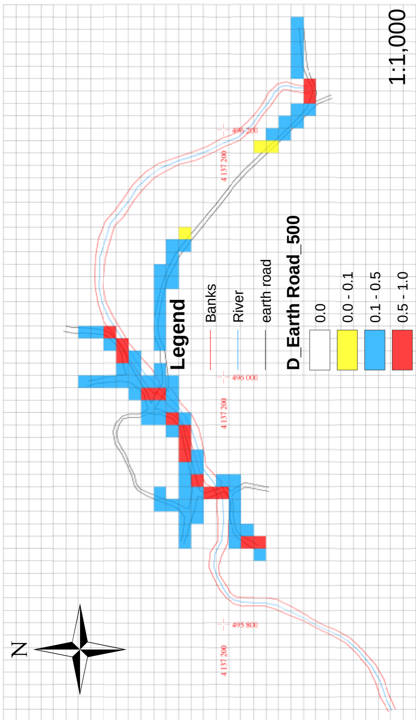

(f) 500-year flood

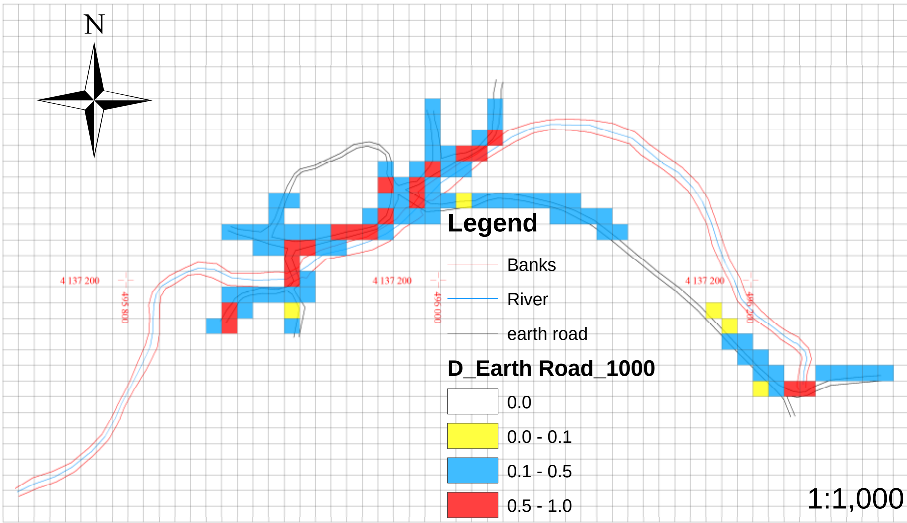

(g) 1000-year flood

Figure 5.15 (cont'd)

5.3.2 Social Damage Maps

In this study, social damage calculations are carried out based on Equation 4-3. To include vulnerability into the social risk analysis Equation 4-6 is used. In this study, vulnerability term is considered just for schools and it is taken as 10 because in the flood situation evacuation of children from the school will be very difficult.

In Figure 5.16 the social damage maps for population, in Figure 5.17 the social damage maps for social hot spots and in Figure 5.18 the social damage maps for animals are given. As can be seen from Figures 5.16, 5.17 and 5.18, social damage can only take two values: 0 or 1 due to the binary approach. In Figure 5-19, the social damage maps for population with the vulnerability factor are given. It can be seen from the Figure 5.19 that damage at a cell can take three values: 0, 1 or 10. In this study, the vulnerability factor of 10 is just used for schools. The cells where a school take a damage value of 10 because schools are more vulnerable due to existance of children.

5.3.3 Environmental Damage Maps

Environmental damage calculations are carried out based on Equation 4-7 and Equation 4-9. Equation 4-7 is used to calculate pollution damage while erosion damage is calculated with Equation 4-9.

In Figure 5.20, environmental damage map for pollution is given. As can be seen from the Figure 5.20, two different damage value exist due to the binary approach: 0 or 1. In Figure 5.21, environmental damage map for erosion is given. Four different damage values are possible: 0, 0.33, 0.67 and 1.00. These values depend on slope of the surface and surface cover. It can be seen from Figure 5.20 and 5.21, the damage is getting smaller away from the river bed.

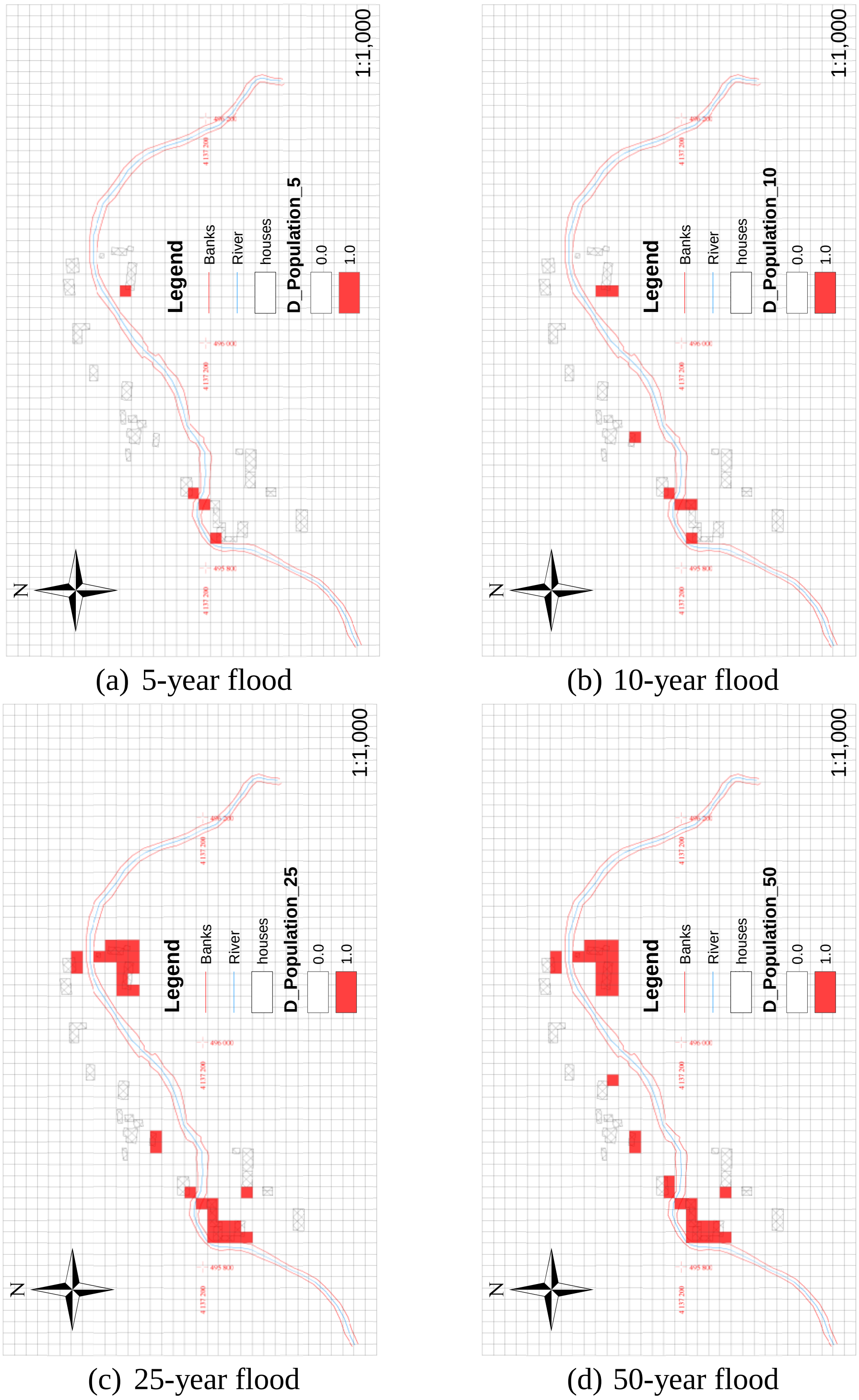

(a) 5-year flood
(b) 10-year flood
(c) 25-year flood
(d) 50-year flood

Figure 5.16: Social Damage Maps for Population for (a) 5-Year Flood (b) 10-Year Flood (c) 25-Year Flood (d) 50-Year Flood (e) 100-Year Flood (f) 500-Year Flood (g) 1000-Year Flood

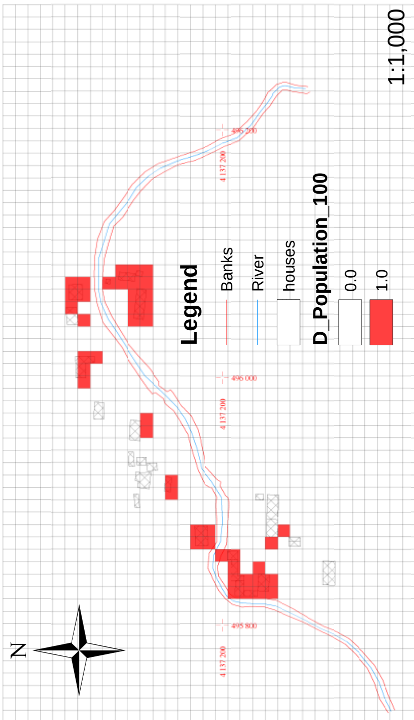

(e) 100-year flood

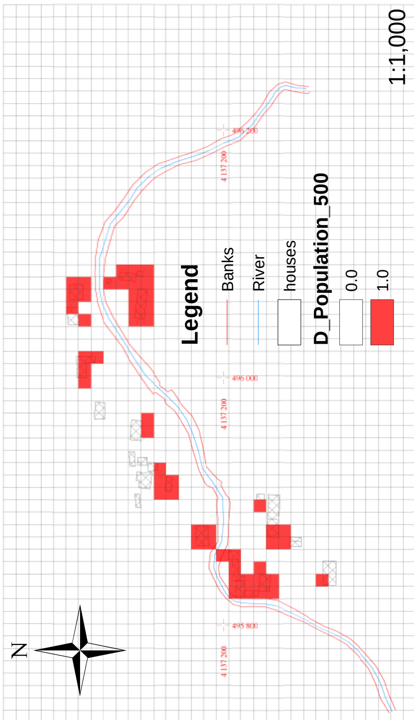

(f) 500-year flood

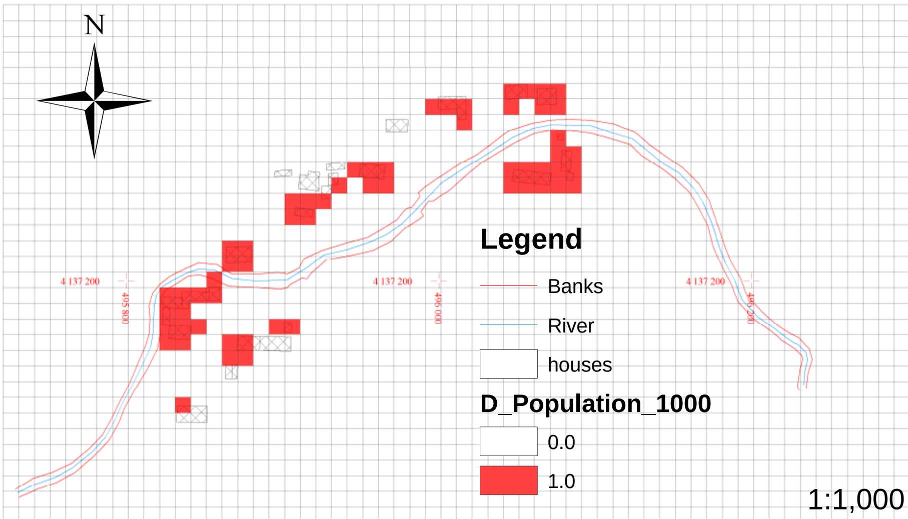

(g) 1000-year flood

Figure 5.16 (cont'd)

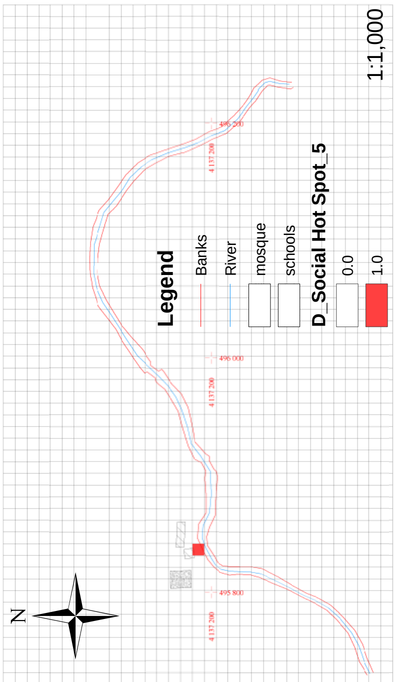

(a) 5-year flood

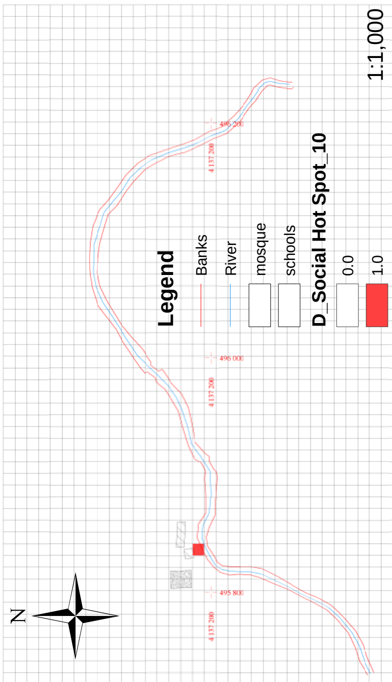

(b) 10-year flood

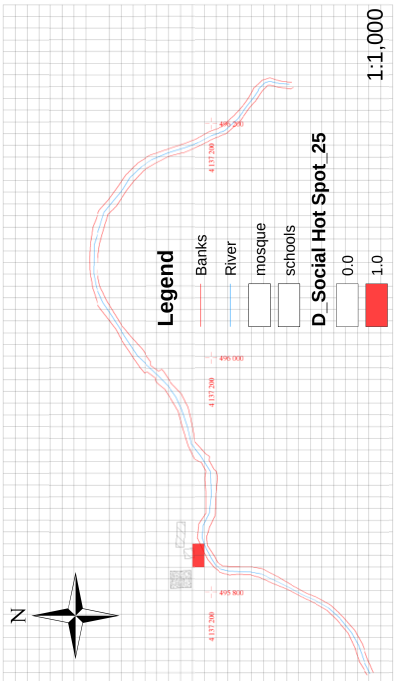

(c) 25-year flood

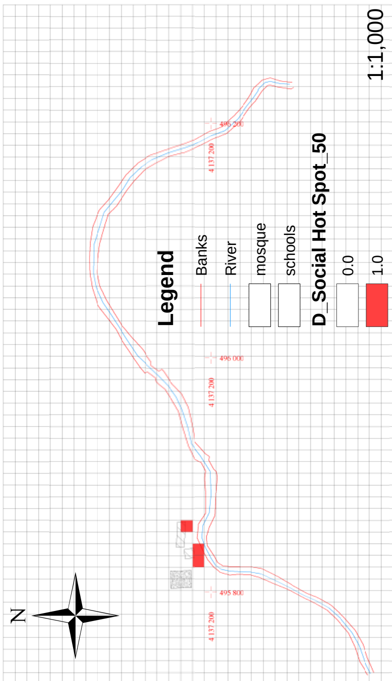

(d) 50-year flood

Figure 5.17: Social Damage Maps for Social Hot Spots for (a) 5-Year Flood (b) 10-Year Flood (c) 25-Year Flood (d) 50-Year Flood (e) 100-Year Flood (f) 500-Year Flood (g) 1000-Year Flood

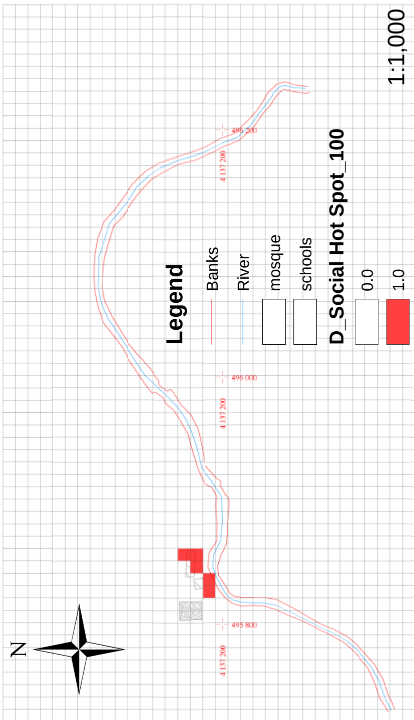

(e) 100-year flood

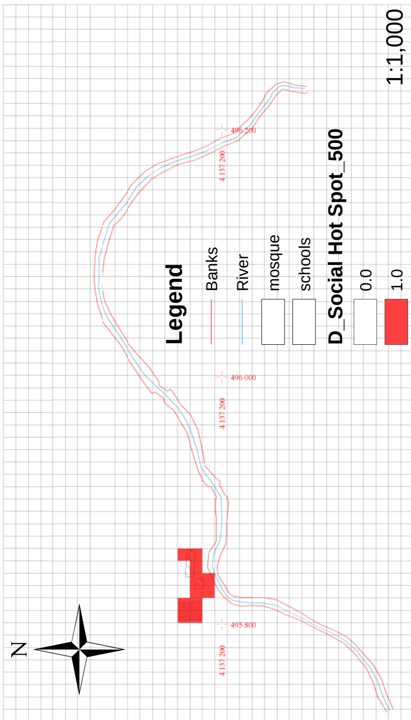

(f) 500-year flood

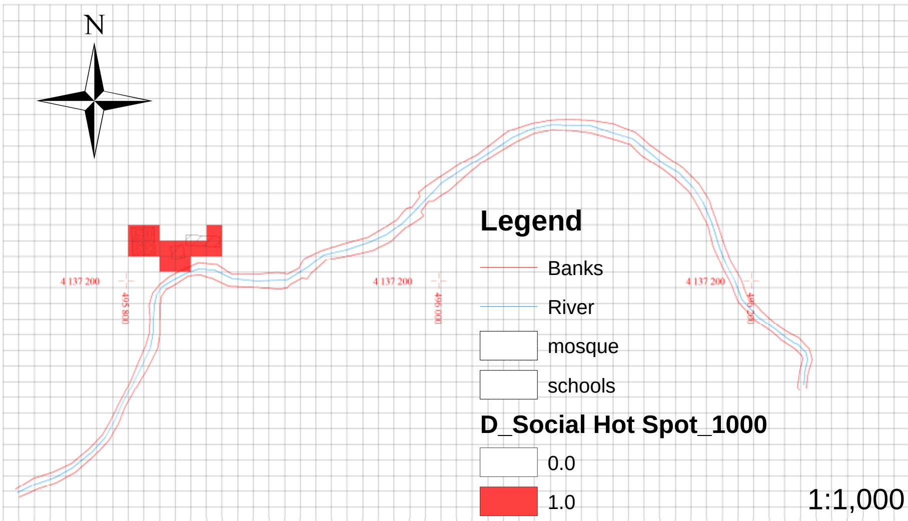

(g) 1000-year flood

Figure 5.17 (cont'd)

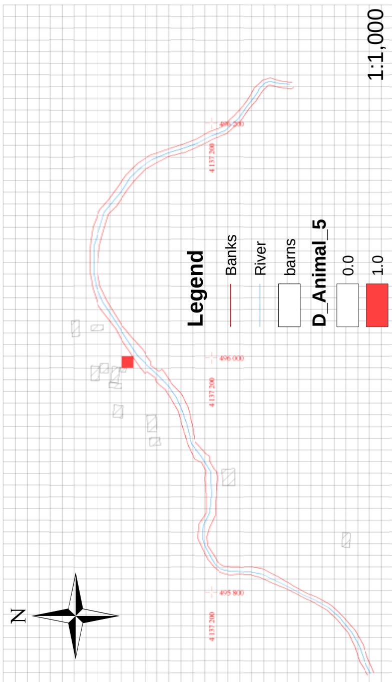

(a) 5-year flood

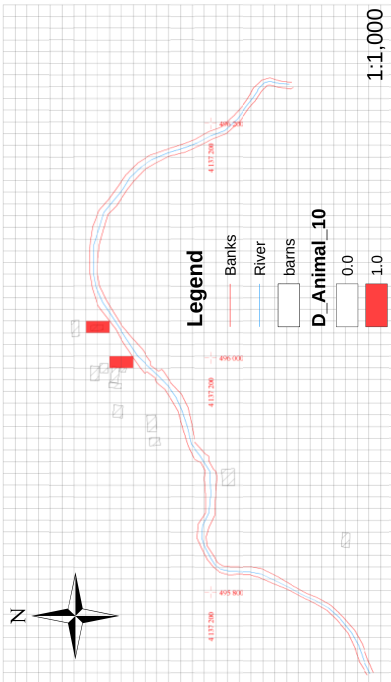

(b) 10-year flood

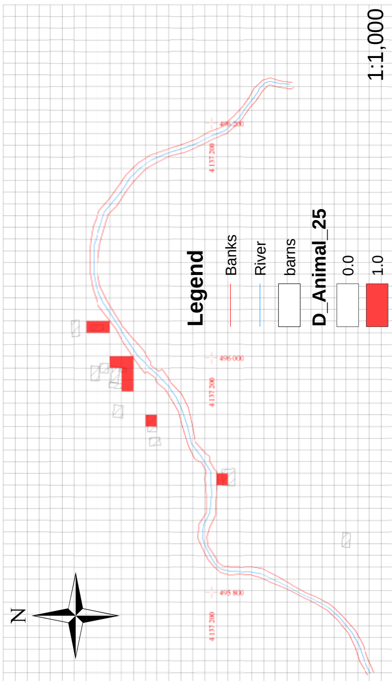

(c) 25-year flood

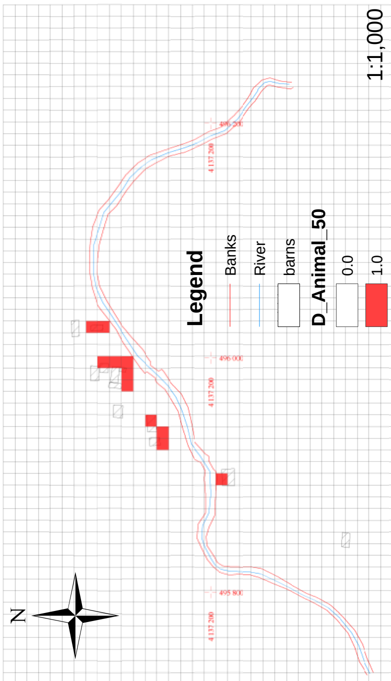

(d) 50-year flood

Figure 5.18: Social Damage Maps for Animals for (a) 5-Year Flood (b) 10-Year Flood (c) 25-Year Flood (d) 50-Year Flood (e) 100-Year Flood (f) 500-Year Flood (g) 1000-Year Flood

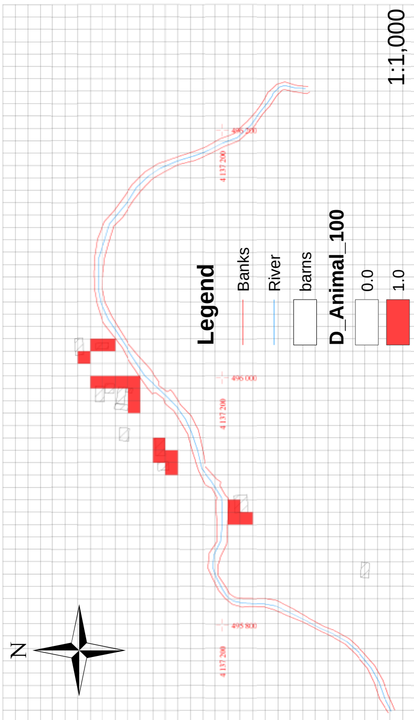

(e) 100 year flood

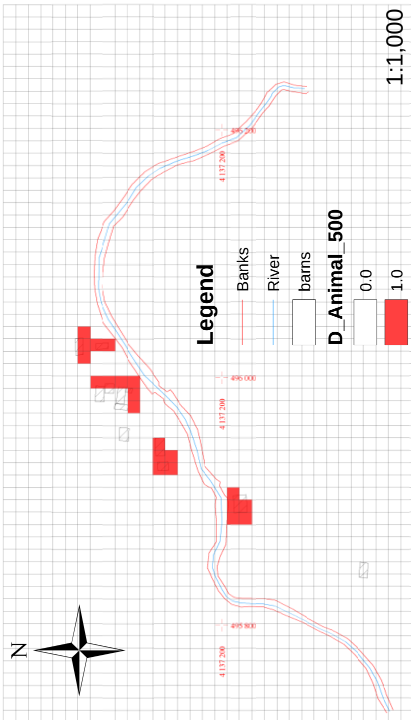

(f) 500-year flood

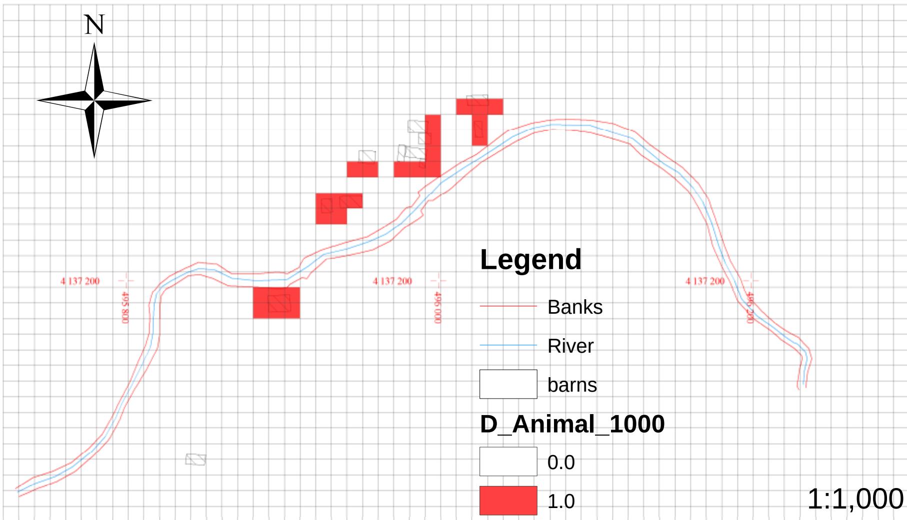

(g) 1000-year flood

Figure 5.18 (cont'd)

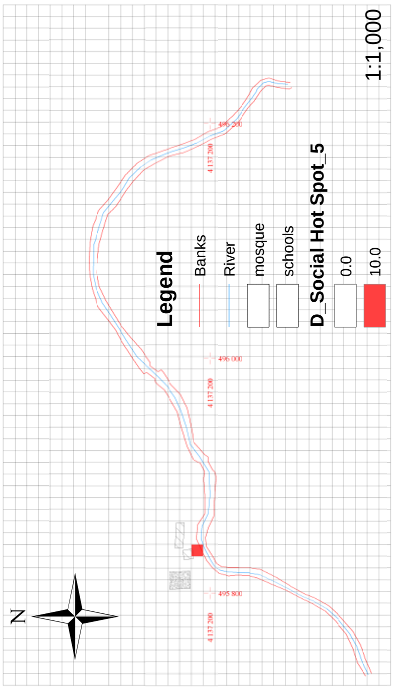

(a) 5-year flood

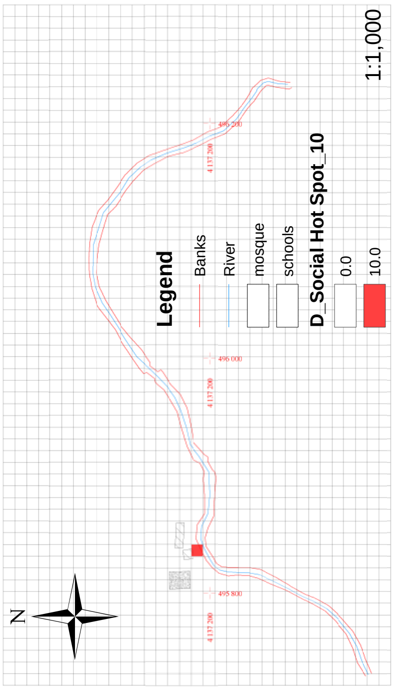

(b) 10-year flood

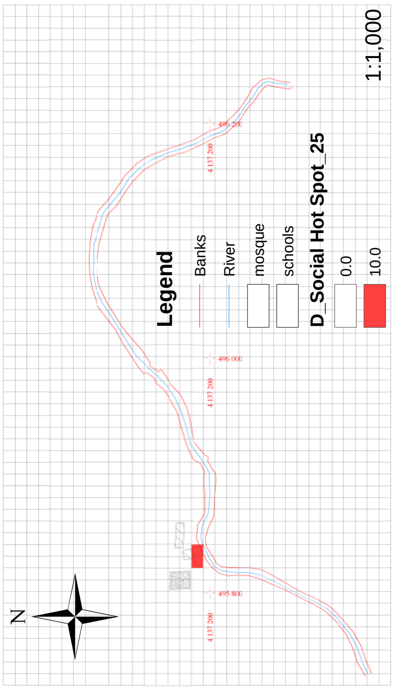

(c) 25-year flood

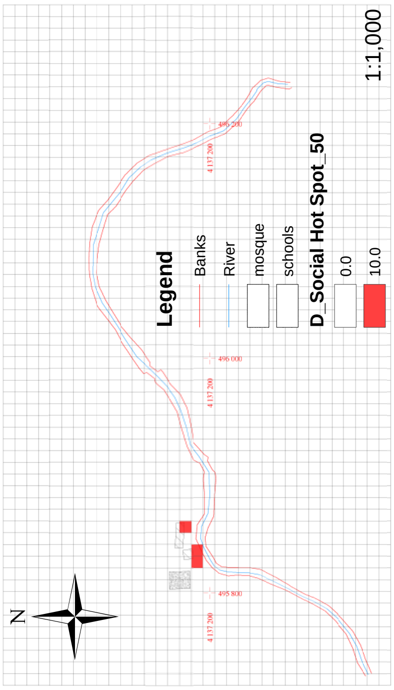

(d) 50-year flood

Figure 5.19: Social Damage Maps for Social Hot Spots including the Vulnerability Factor for (a) 5-Year Flood (b) 10-Year Flood (c) 25-Year Flood (d) 50-Year Flood (e) 100-Year Flood (f) 500-Year Flood (g) 1000-Year Flood

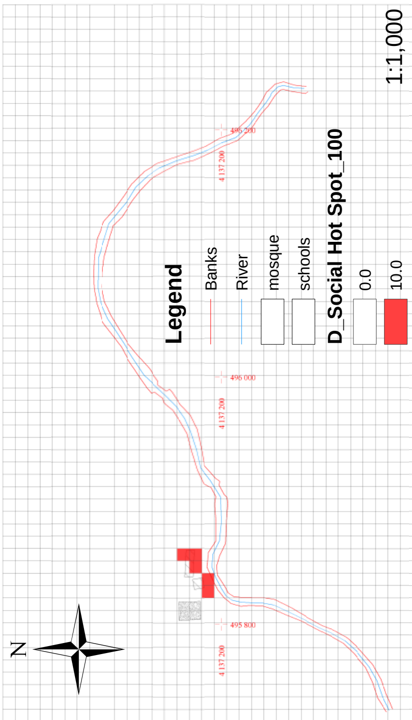

(e) 100-year flood

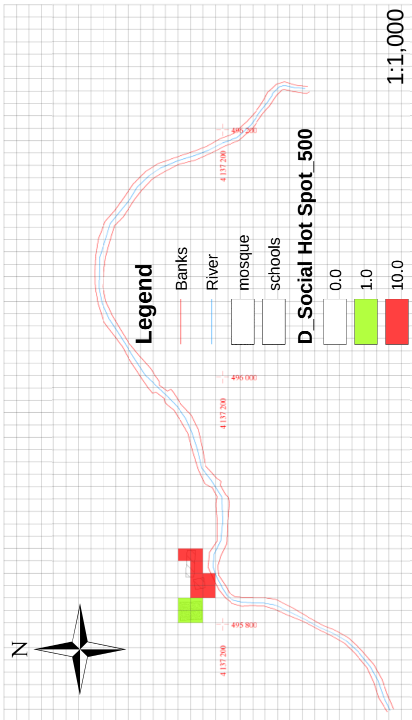

(f) 500-year flood

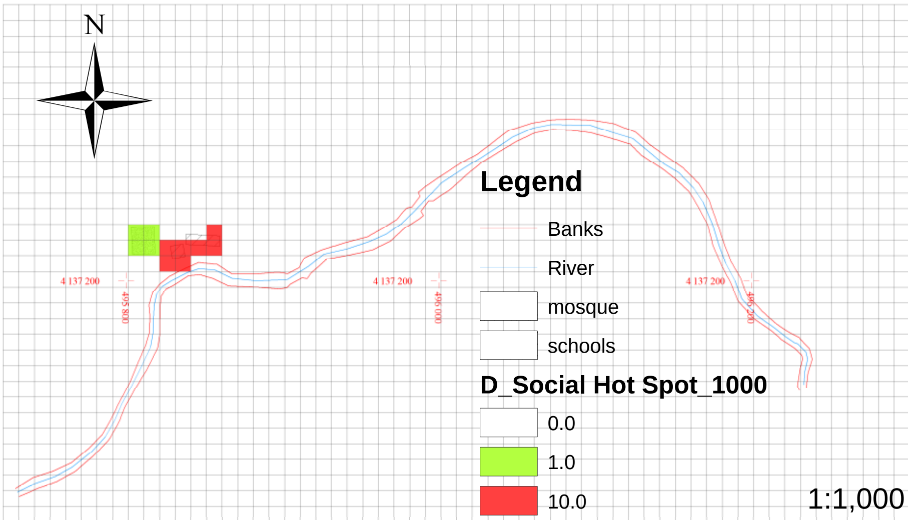

(g) 1000-year flood

Figure 5.19 (cont'd)

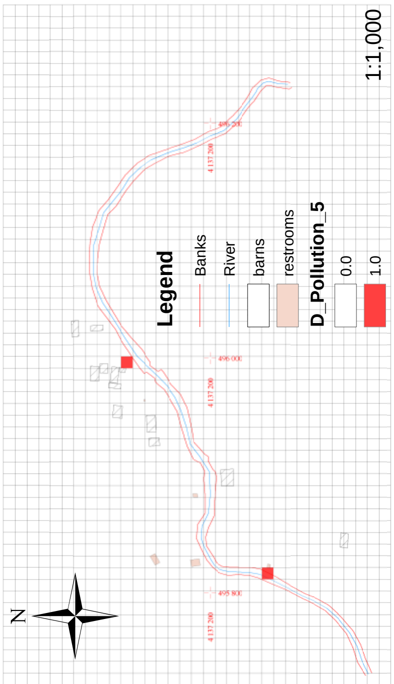

(a) 5-year flood

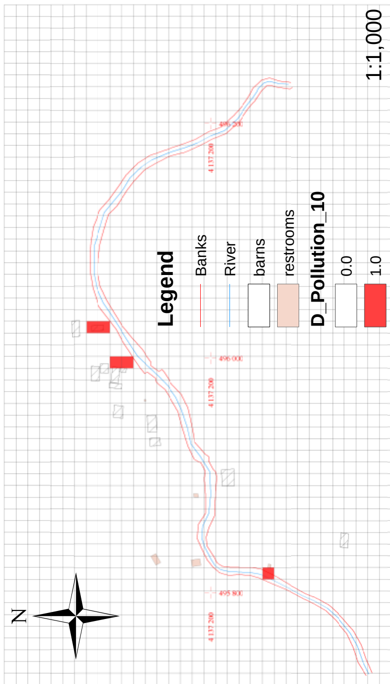

(b) 10-year flood

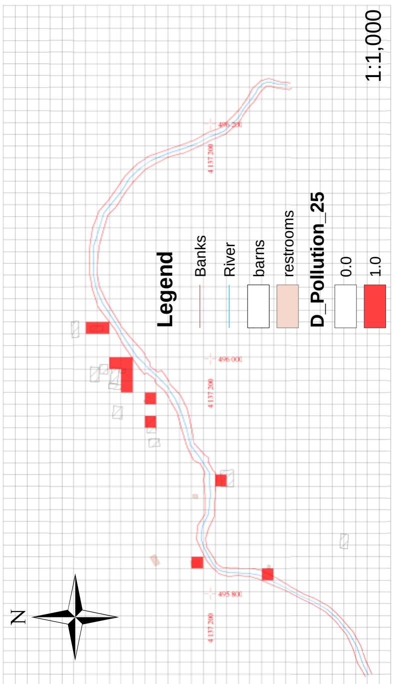

(c) 25-year flood

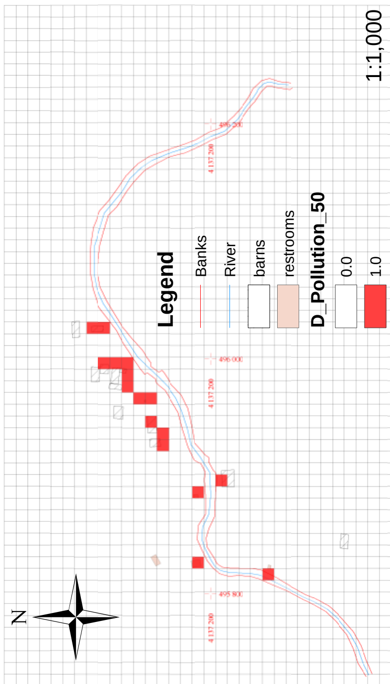

(d) 50-year flood

Figure 5.20: Environmental Damage Maps for Pollution for (a) 5-Year Flood (b) 10-Year Flood (c) 25-Year Flood (d) 50-Year Flood (e) 100-Year Flood (f) 500-Year Flood (g) 1000-Year Flood

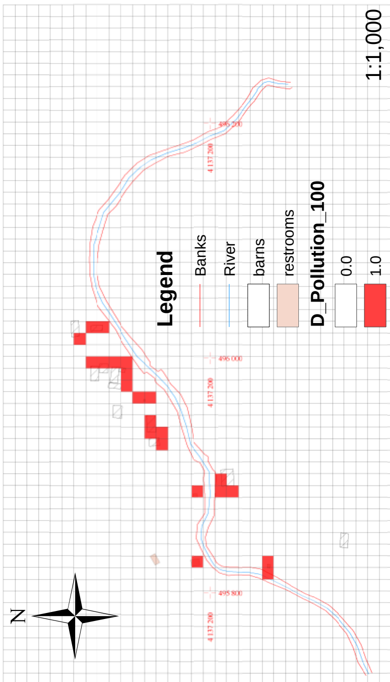

(e) 100-year flood

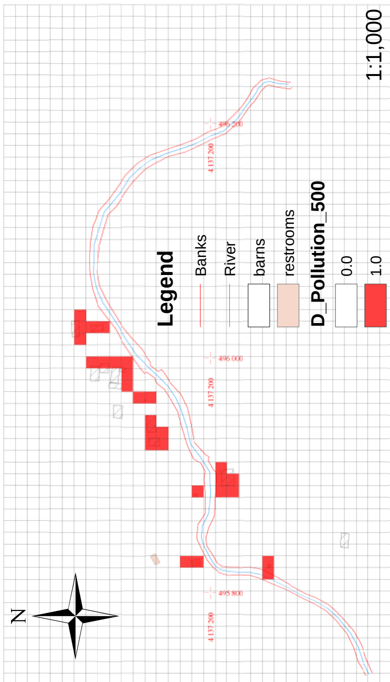

(f) 500-year flood

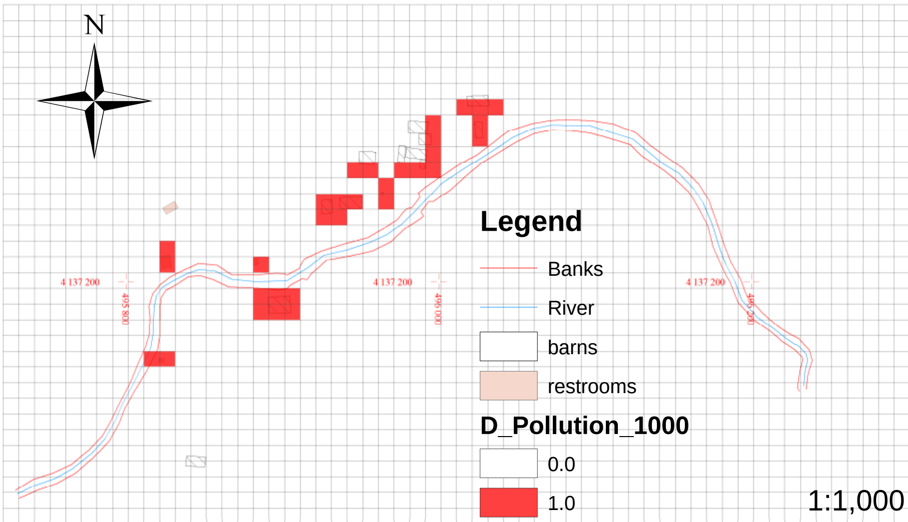

(g) 1000-year flood

Figure 5.20 (cont'd)

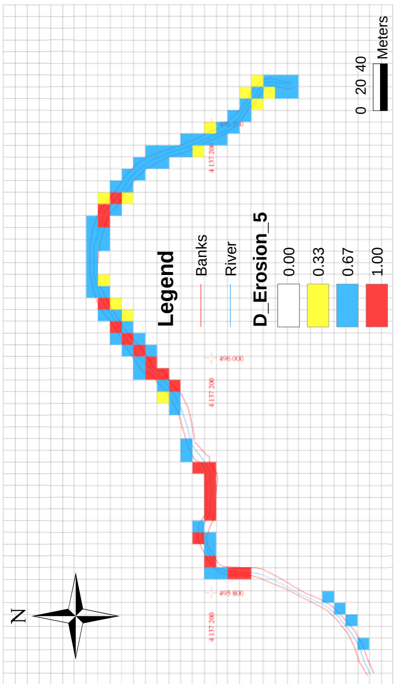

(a) 5-year flood

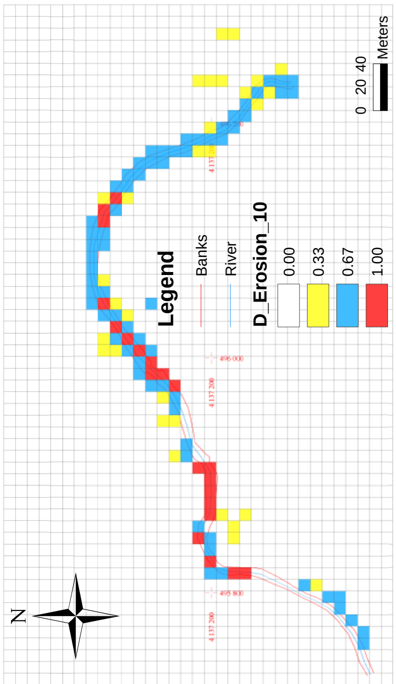

(b) 10-year flood

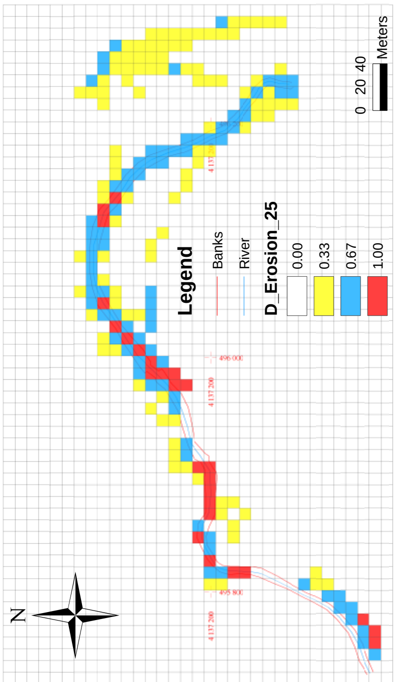

(c) 25-year flood

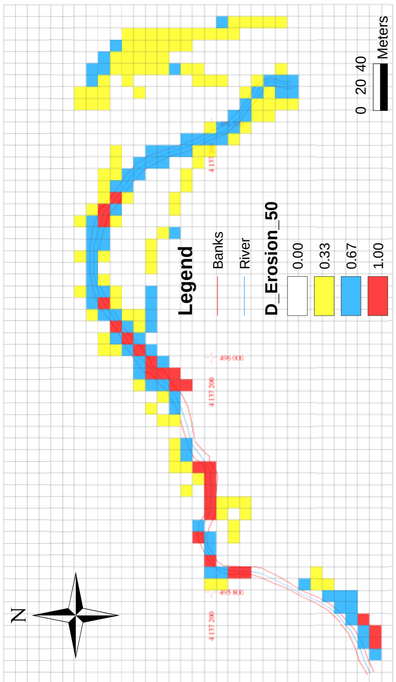

(d) 50-year flood

Figure 5.21: Environmental Damage Maps for Erosion for (a) 5-Year Flood (b) 10-Year Flood (c) 25-Year Flood (d) 50-Year Flood (e) 100-Year Flood (f) 500-Year Flood (g) 1000-Year Flood

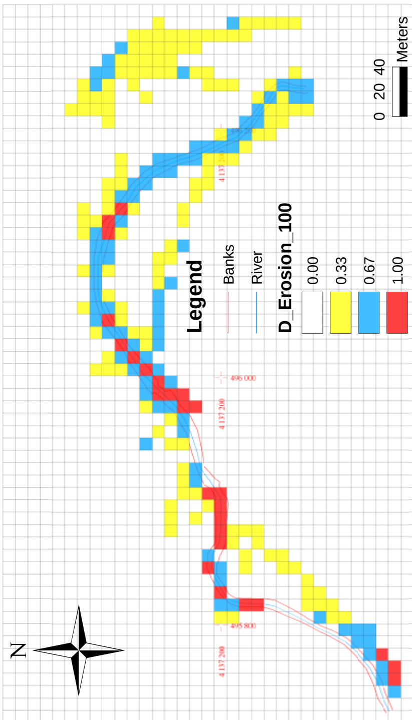

(e) 100-year flood

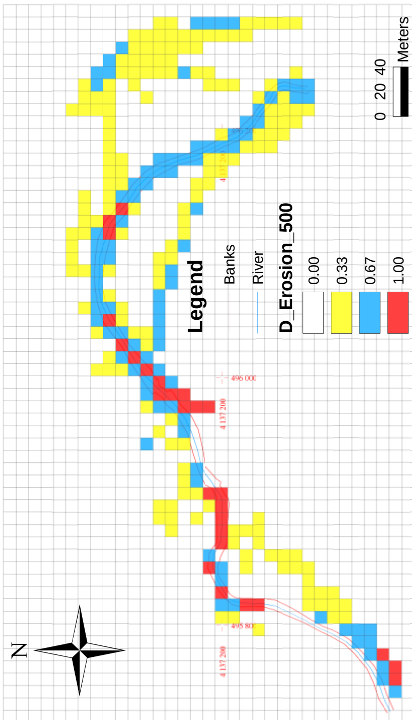

(f) 500-year flood

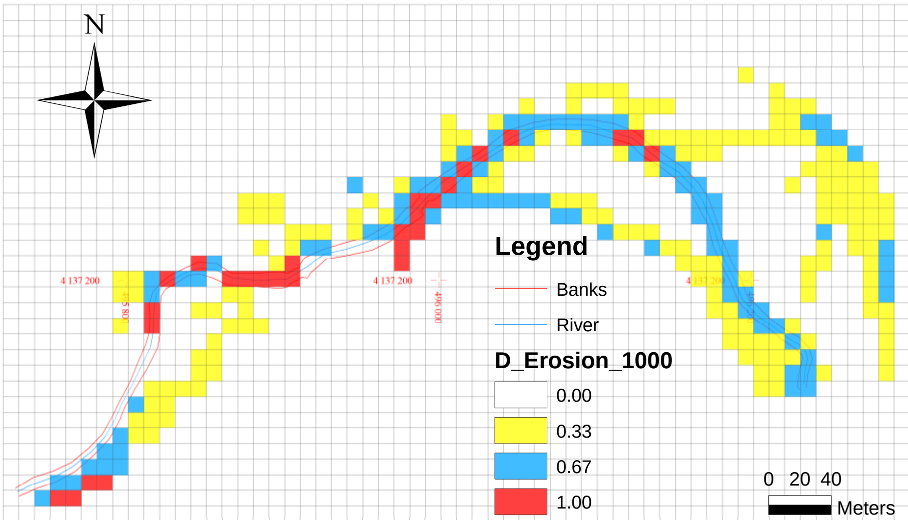

(g) 1000-year flood

Figure 5.21 (cont'd)

5.4 Damage-Exceedance Probability Curves

To calculate risk, damage-exceedance probability curves need to be generated. The areas under these curves are the risks. These curves are calculated for each dimension and for each element at risk. Example damage exceedance probability curves for different elements at risk are provided in the following paragraph. However, it should be noted that one damage exceedance probability curve need to be generated for each cell of the study domain for each element at risk to be able to calculate the overall risk.

The example damage – exceedance probability curves for economic elements at risk for Cell 1, Cell 2, Cell 3 and Cell 4 (see Figure 5.1) are given in Figure 5.22. The damage values depend on the water depth.

The example damage – exceedance probability curves for social elements at risk for Cell 1, Cell 2, Cell 3 and Cell 4 (Figure 5.2) are given in Figure 5.23. The damage can only take two values 0 or 1. For social elements at risk, water depth is not considered. In other words, regardless of the depth of the water, if there is a social element at risk at a cell the social damage is taken as 1.

The example damage – exceedance probability curves environmental elements at risk for for Cell 1, Cell 2, Cell 3 and Cell 4 are given in Figure 5.24. The damage values do not dependent on the water depth for environmental elements at risk similar to those of the social elements at risk. This means if there is an environmental element at risk and even if very small water depth occurs, pollution damage is taken as 1 if there is a pollution source at that cell. In the erosion damage, damage can take 4 values: 0, 0.33, 0.67 or 1 as explained in Section 4.3.3. As can be seen in Figure 5.24, no damage is calculated for cells 1,2 and 4. This is due to the fact that no environmental elements at risk exist in these cells.

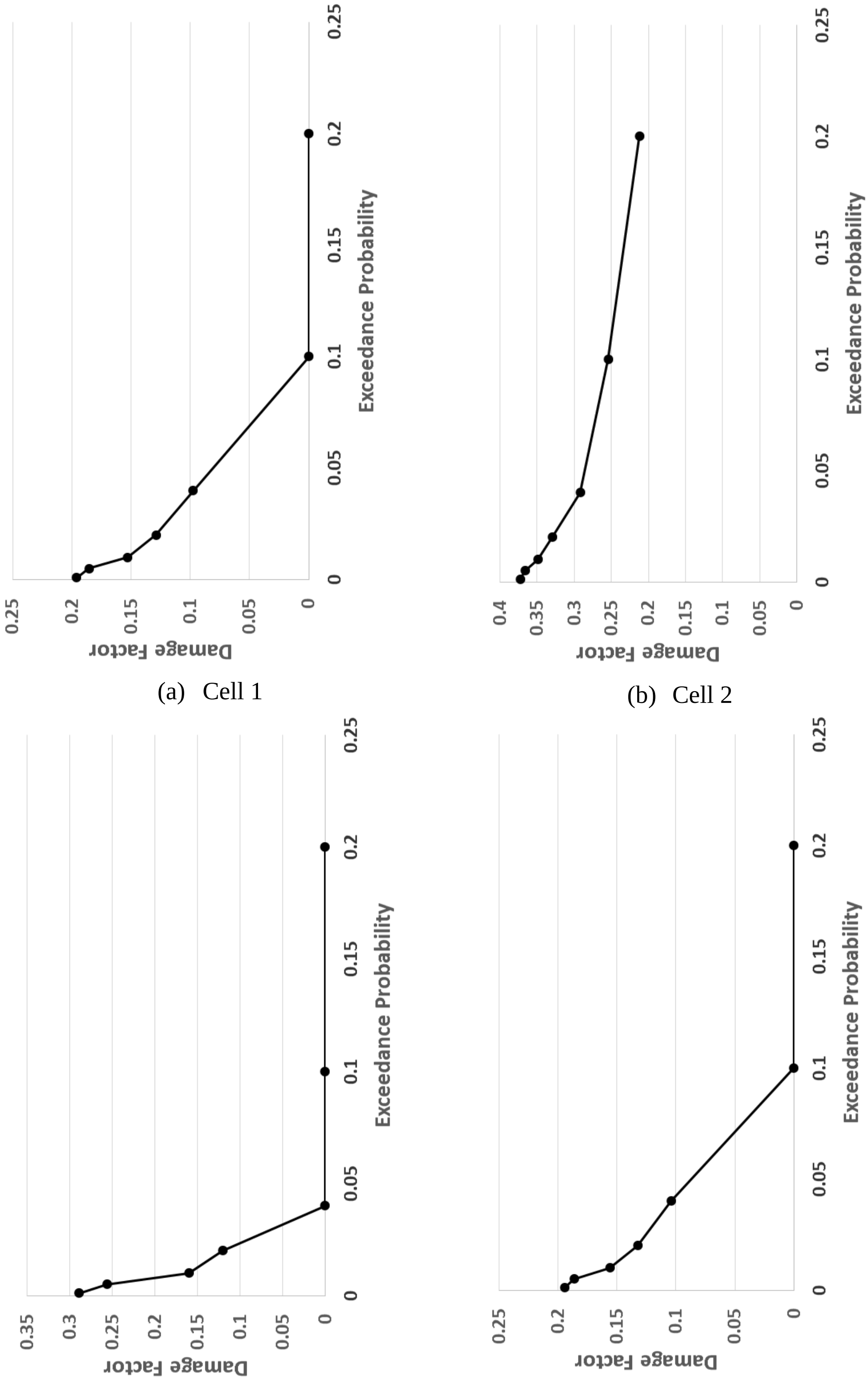

(a) Cell 1 (b) Cell 2

(c) Cell 3 (d) Cell 4

Figure 5.22: Damage-Exceedance Probability Curves for Economic Elements at Risk at (a) Cell 1 (b) Cell 2 (c) Cell 3 (d) Cell

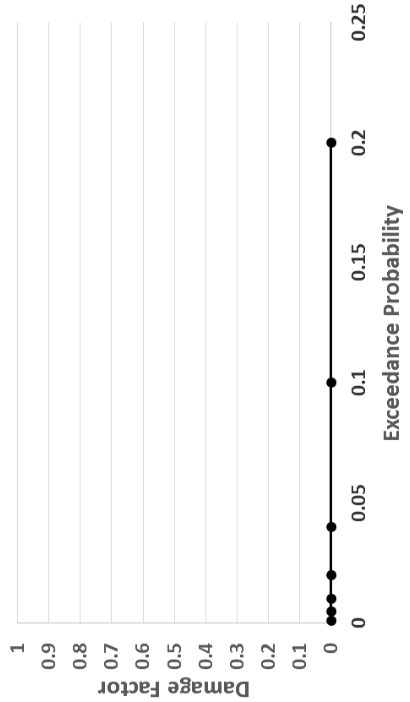

(a) Cell 1

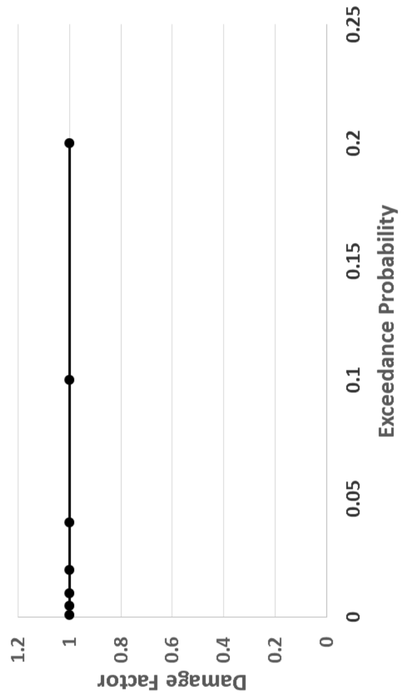

(b) Cell 2

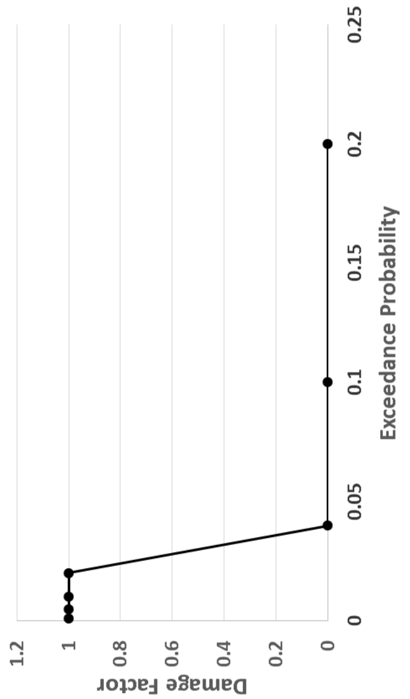

(c) Cell 3

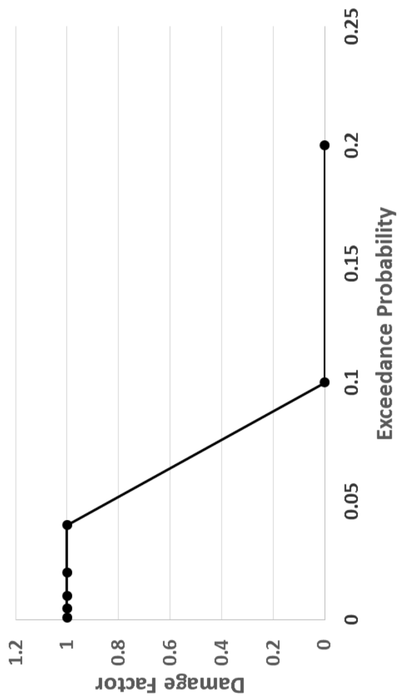

(d) Cell 4

Figure 5.23: Damage-Exceedance Probability Curves for Social Elements at Risk at (a) Cell 1 (b) Cell 2 (c) Cell 3 (d)

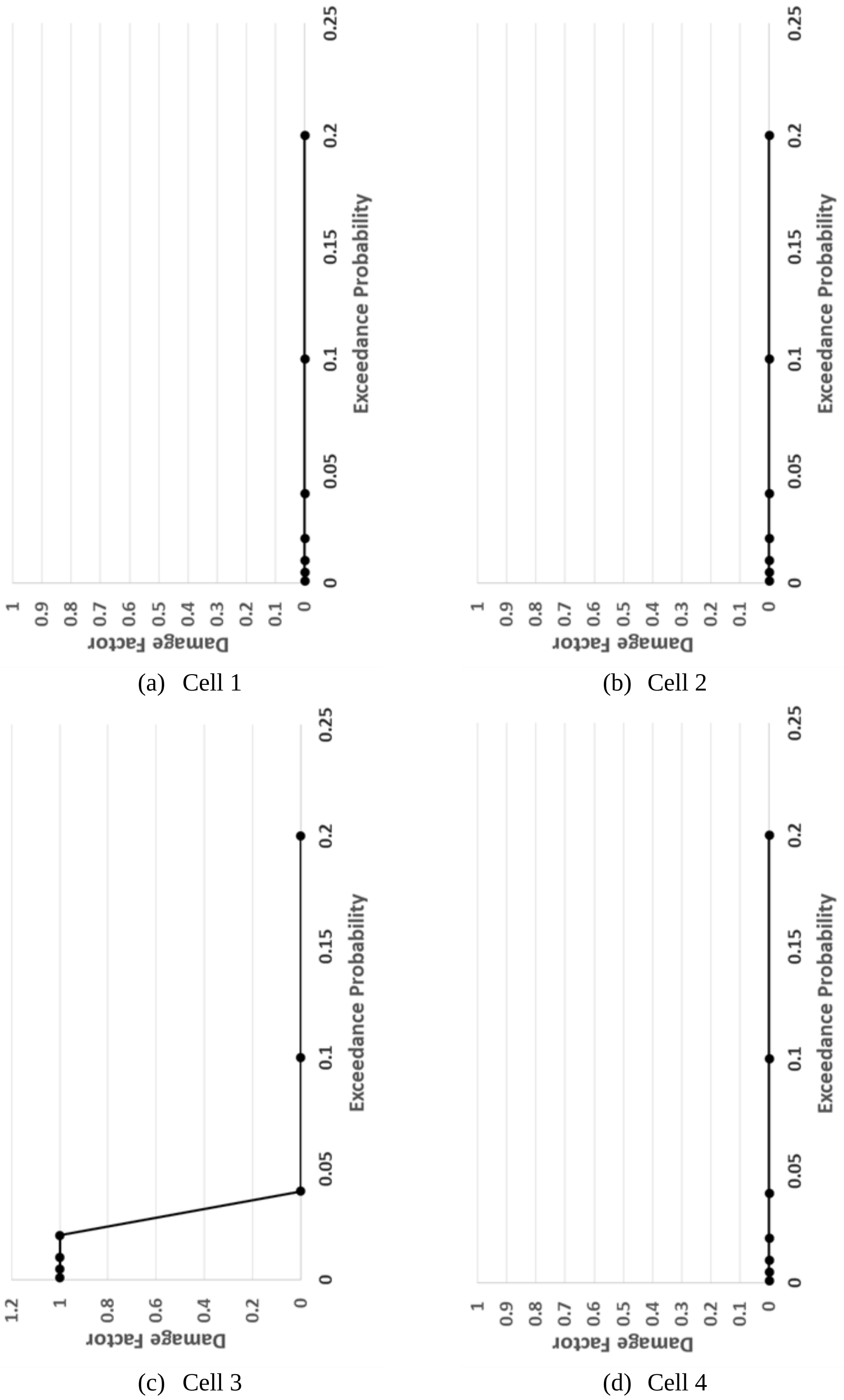

Figure 5.24: Damage-Exceedance Probability Curves for Environmental Elements at Risk at (a) Cell 1 (b) Cell 2 (c) Cell 3 (d) Cell 4

5.5 Risk Calculations

After construction of damage-exceedance probability curves, risks are calculated for each element at risk. Then these risks are aggregated to obtain an overall risk for each dimension. Risk maps are given in the following sections.

5.5.1 Economic Risk Maps

In Figure 5.25, economic risk maps for each element at risk is given and in Figure 5.26, normalized overall economic risk maps with and without resilience factor are given. As can be seen from Figure 5.25 and Figure 5.26, the biggest risk values are calculated in areas where economic elements at risk are populated and close to river bed because in these cells water depths are higher than the other locations. Furthermore, as expected the risky areas in the economic risk map with resilience factor is more than the economic risk map without resilience factor.

5.5.2 Social Risk Maps

In Figure 5.27-a, 5.27-b and 5.27-c, the social risk maps for three social elements at risk namely population, social hot spots and animals are given. In Figure 5.27-d, normalized overall social risk map without the vulnerability factor is given. Social risk does not depend on the water depth because the damage is calculated using the binary approach. In Figure 5.27-e, normalized overall social risk map with the vulnerability factor is given. As can be seen from Figure 5.27, risk value is bigger at cells where school exists because a high vulnerability factor is taken just for schools. Moreover, the risk value is bigger close to the river bed and it is getting smaller away from the river since the extent of the flood gets bigger for only high return period floods. At cells close to the river, water depth for all return periods will be higher than zero and social risks will be calculated if there exists a social element at risk at these cells. However, cells that are away from the river will only be flooded for high return period floods and they will not contribute to the social risk when small return period floods occur.

5.5.3 Environmental Risk Maps

In Figure 5.28, the environmental risk maps are given. In Figure 5.28-a, the environmental risk map for pollution is given and in Figure 5.28-b, the environmental risk map for erosion is provided. The risk is getting smaller away from the river bed due to the reason explained under the social risk. In Figure 5.28-c, normalized overall environmental risk map is given.

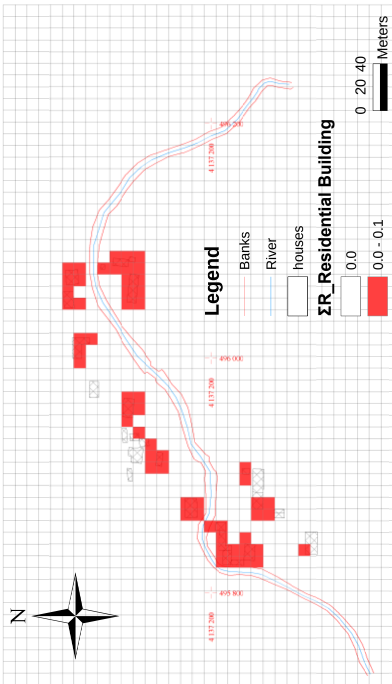

(a) Residential Buildings

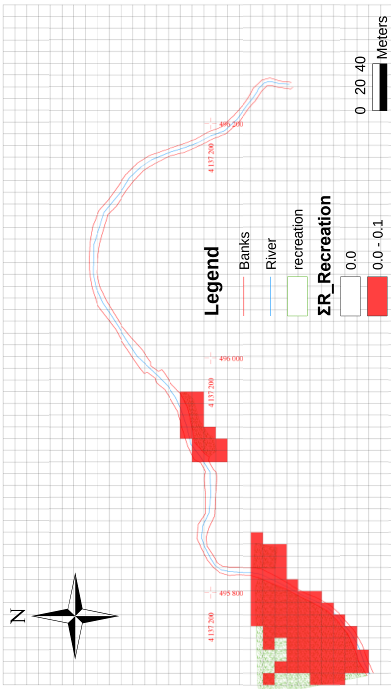

(b) Recreation Area

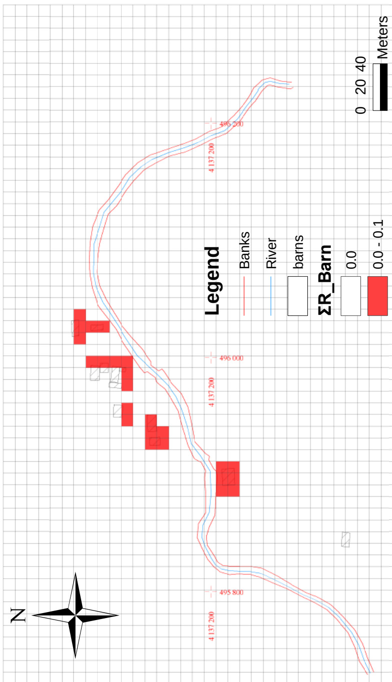

(c) Barns

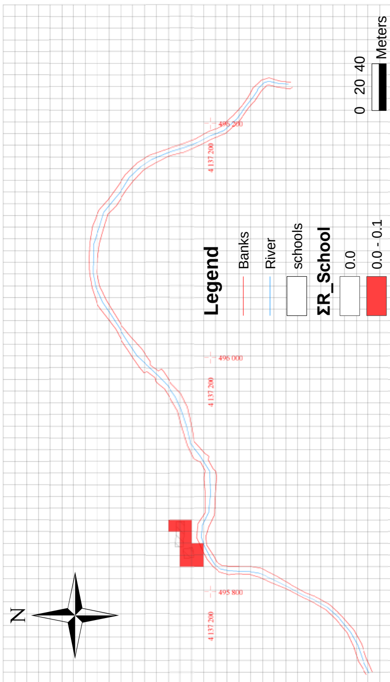

(d) Schools

Figure 5.25: Economic Risk Maps for (a) Residential Buildings (b) Recreation Area (c) Barns (d) Schools (e) Mosques (f) Rest Rooms (g) Earth Roads (h) Asphalt Roads

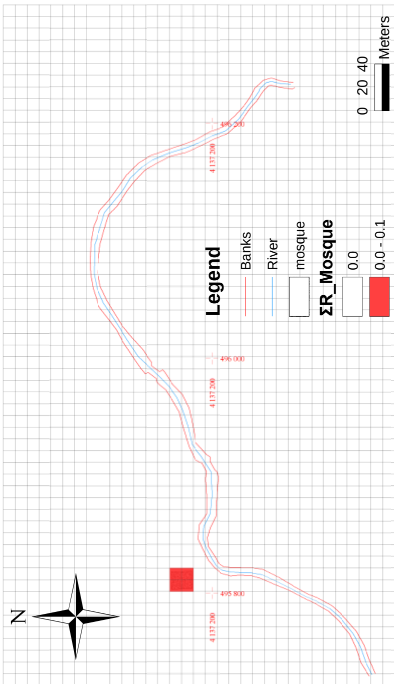

(e) Mosques

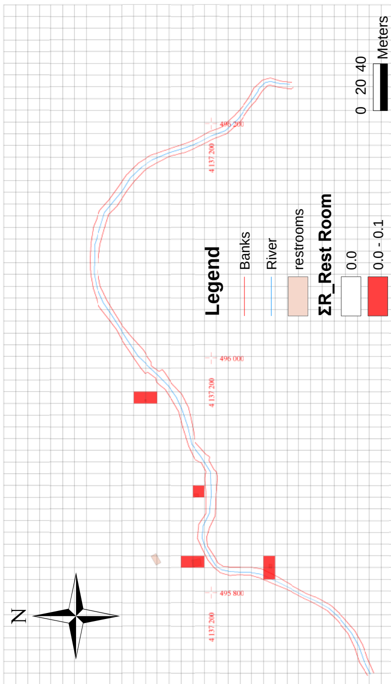

(f) Rest Rooms

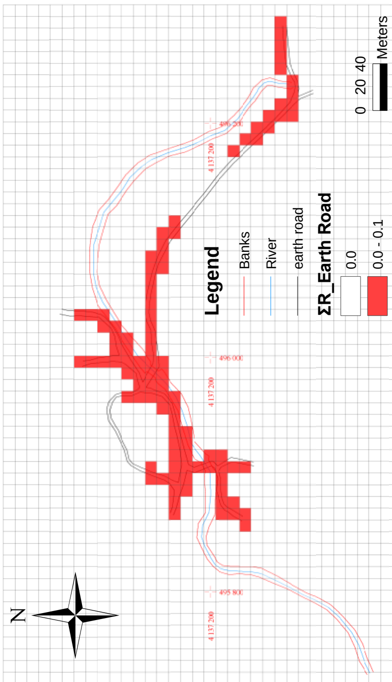

(g) Earth Roads

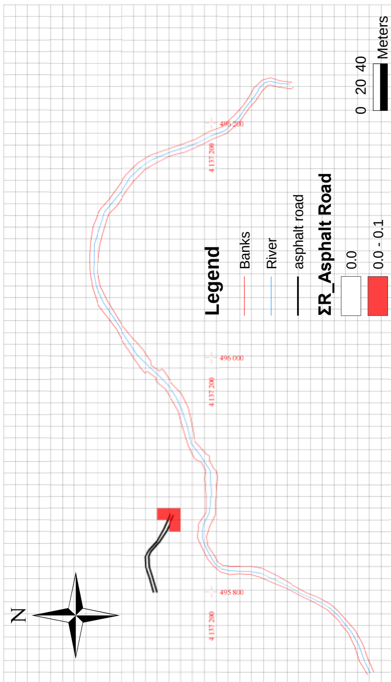

(h) Asphalt Roads

Figure 5.25 (cont'd)

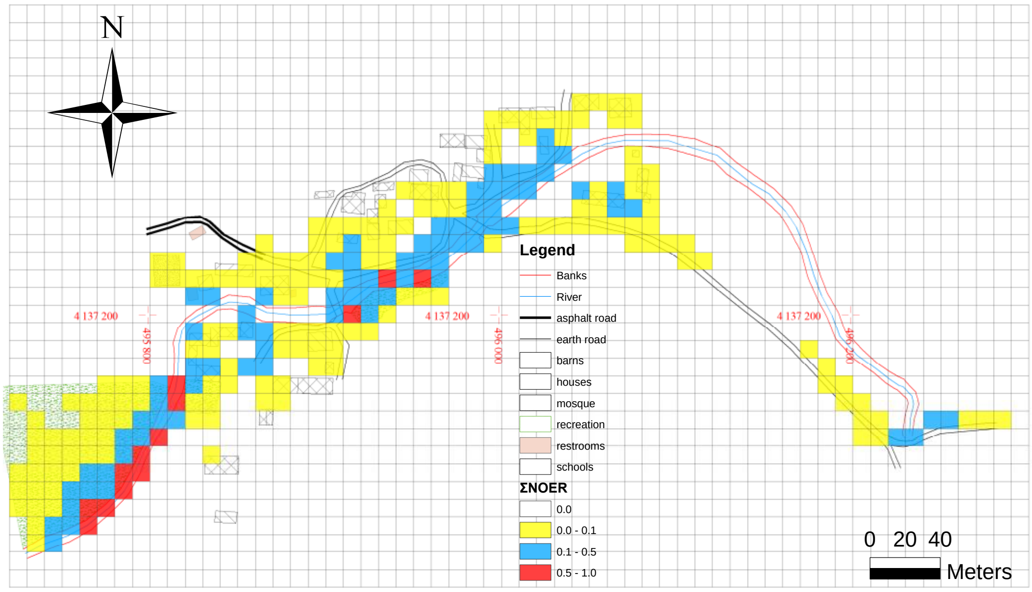

(a) Normalized Overall Economic Risk Map without Resilience Factor in ArcGIS Environment

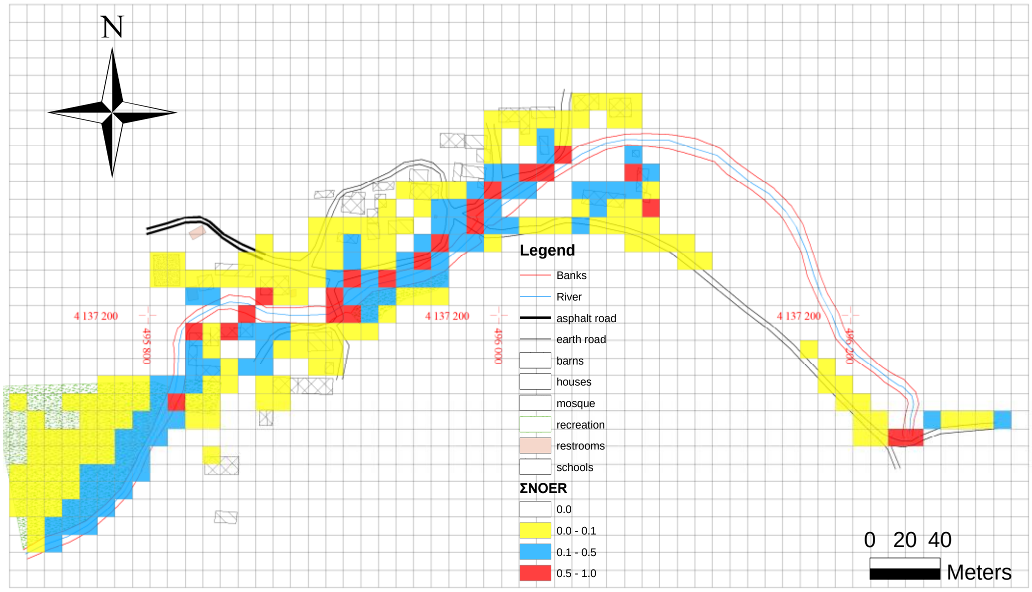

(b) Normalized Overall Economic Risk Map with Resilience Factor in ArcGIS Environment

Figure 5.26: Normalized Overall Economic Risk Maps in ArcGIS Environment (a) Without Resilience Factor (b) With Resilience Factor

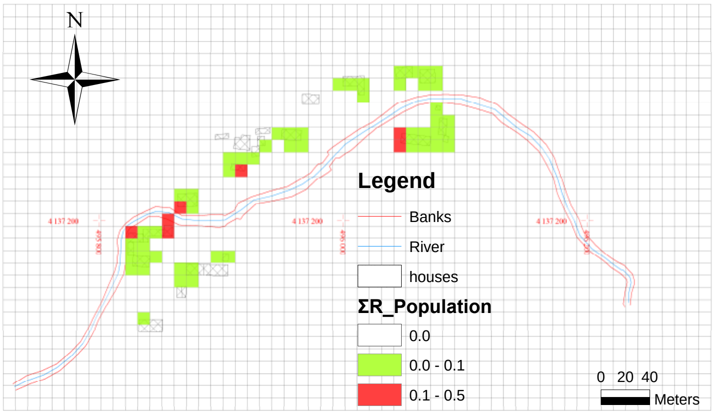

(a) Population

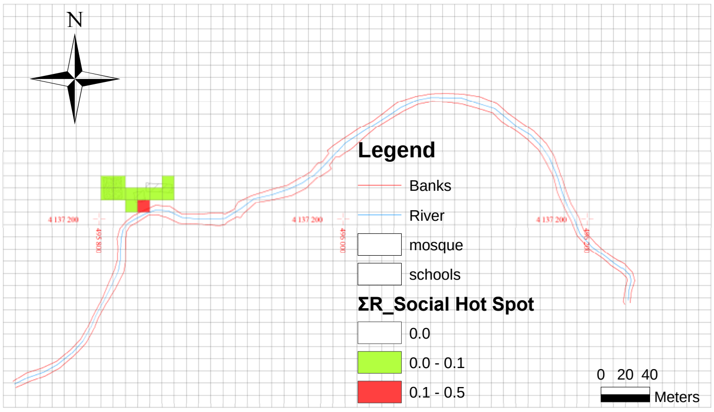

(b) Social Hot Spots

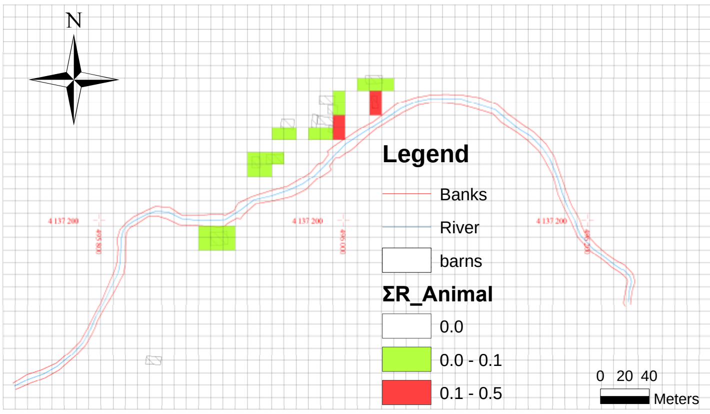

(c) Animals

Figure 5.27: Social Risk Maps (a) Population (b) Social Hot Spots (c) Animals (d) Normalized Overall Social Risk Map without Vulnerability Factor (e) Normalized Overall Social Risk Map with Vulnerability Factor

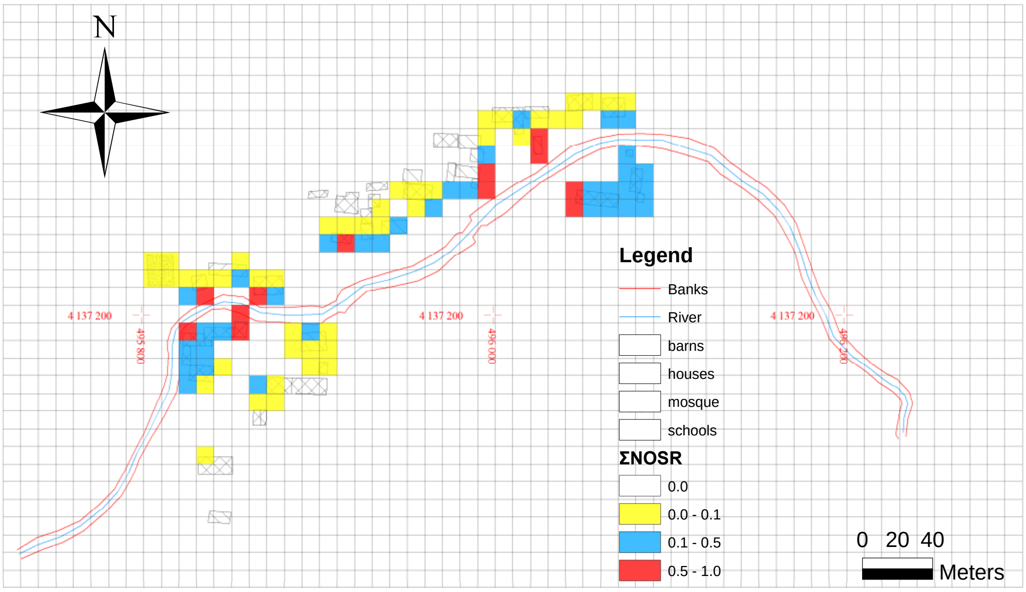

(d) Normalized Overall Social Risk Map without Vulnerability Factor

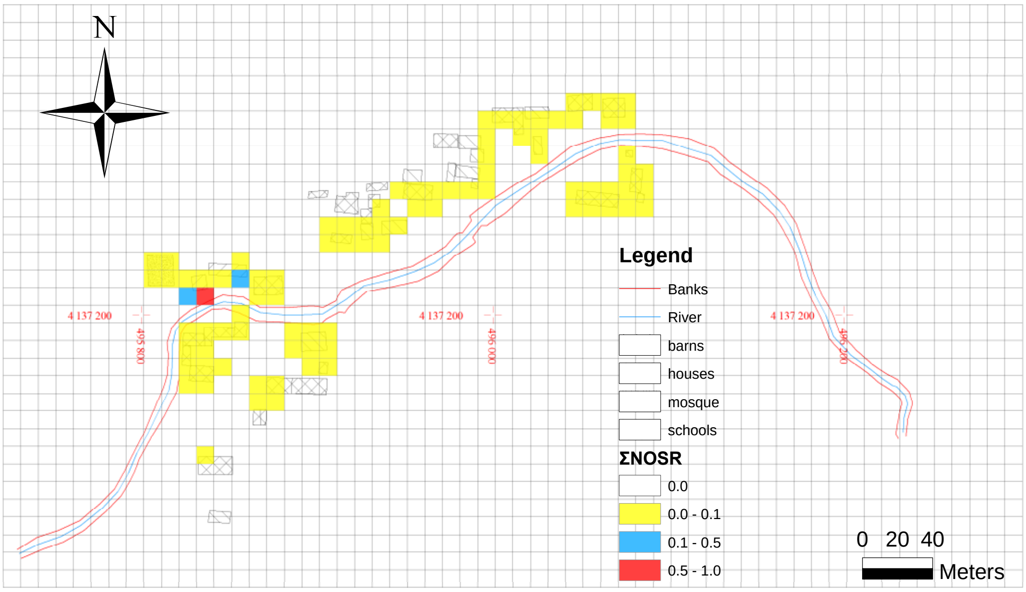

(e) Normalized Overall Social Risk Map with Vulnerability Factor

Figure 5.27 (cont'd)

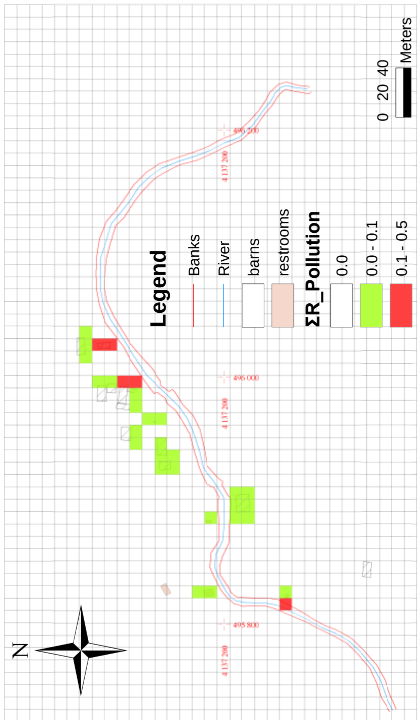

(a) Pollution

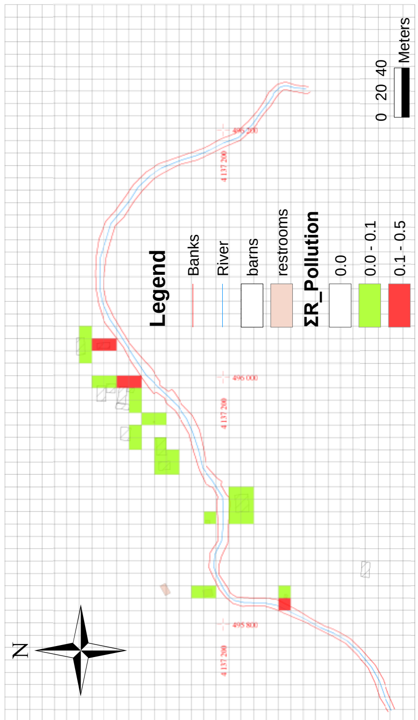

(b) Erosion

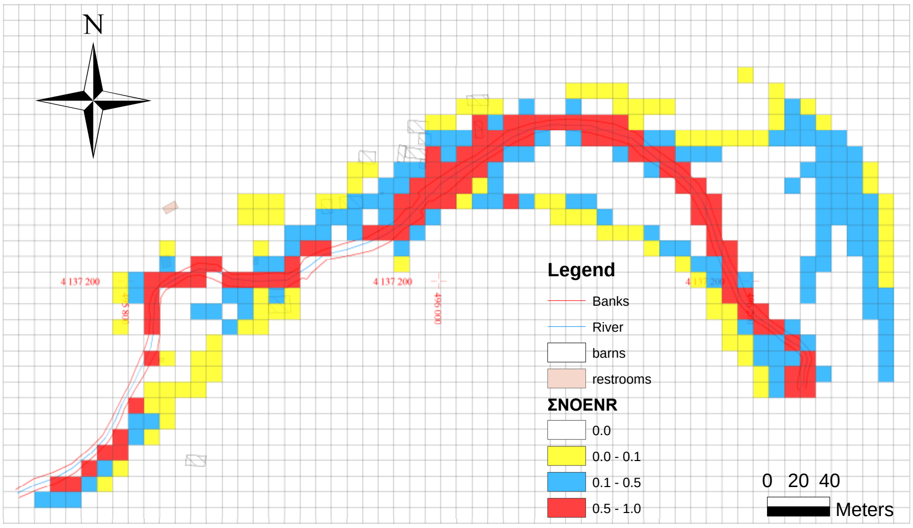

(c) Normalized Overall Environmental Risk

Figure 5.28: Environmental Risk Maps (a) Pollution (b) Erosion (c) Normalized Overall Environmental Risk

5.6 Multicriteria Risk Maps

Economic, social and environmental risk maps are aggregated into an overall risk map using weights. Nine different scenarios composed of different weights are generated and listed in Table 5.5. Economic risk map is referred to as the “Base” scenario. In the “Equal” scenario, all risk dimensions are weighted equally. In the “Economic” scenario, the economic loss is considered to be the most important than the others. In this scenario, environmental dimension and social dimension have same weights. In the “Social” scenario, social dimension is considered as the most critical dimension. Economic and environmental risks are given equal weights. Similarly, in the “Environmental” scenario, environmental assets in the study area are considered to be the most critical component of the risk. Furthermore, three extreme scenarios are also created. In addition to these, another scenario is created in which the economic risk map generated using resilience and the social risk map generated using vulnerability concepts are used.

The risk maps related to “Base”, “Equal”, “Economic”, “Social”, “Environmental”, “Extreme economic”, “Extreme social”, “Extreme environmental and “Equal with vulnerability factor and resilience factor” are given in Figures 5.26, 5.29, 5.30, 5.31, 5.32, 5.33, 5.34, 5.35 and 5.36, respectively.

Table 5.5: Weights of the Social, Environmental and Economic Dimensions in the Applied Sets

Scenario Name	Economic	Social	Environmental
Base	1.00	0.00	0.00
Equal	0.33	0.33	0.33
Economic	0.60	0.20	0.20
Social	0.20	0.60	0.20
Environmental	0.20	0.20	0.60
Extreme economic	0.90	0.05	0.05
Extreme social	0.05	0.90	0.05
Extreme environmental	0.05	0.05	0.90
Equal_res_vul	0.33	0.33	0.33

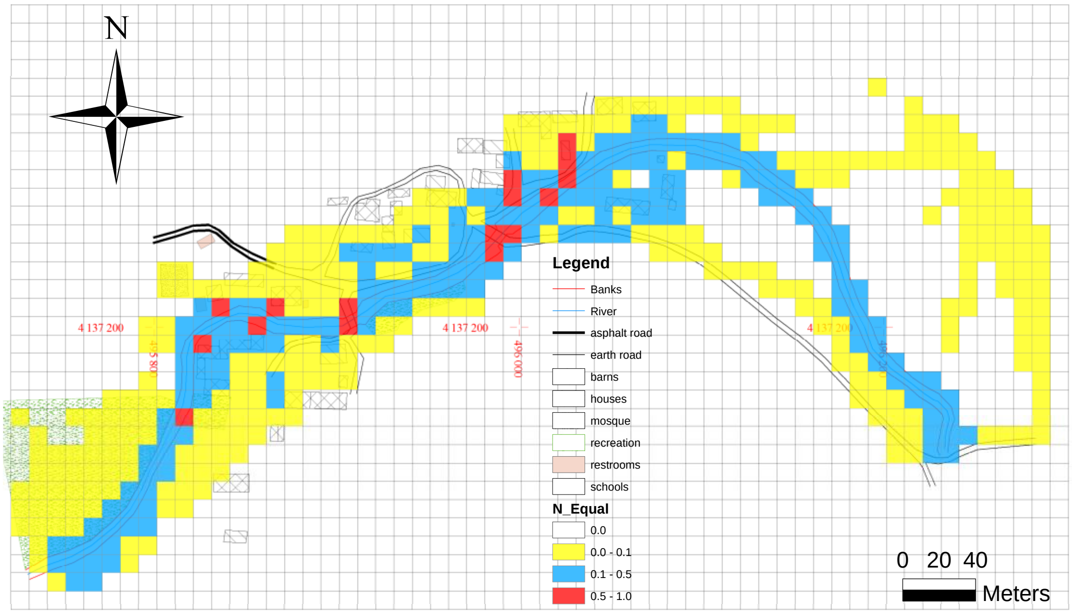

Figure 5.29: Aggregated Overall Multicriteria Flood Risk Map: "Equal" Scenario (0.33 Economic Risk + 0.33 Social Risk + 0.33 Environmental Risk)

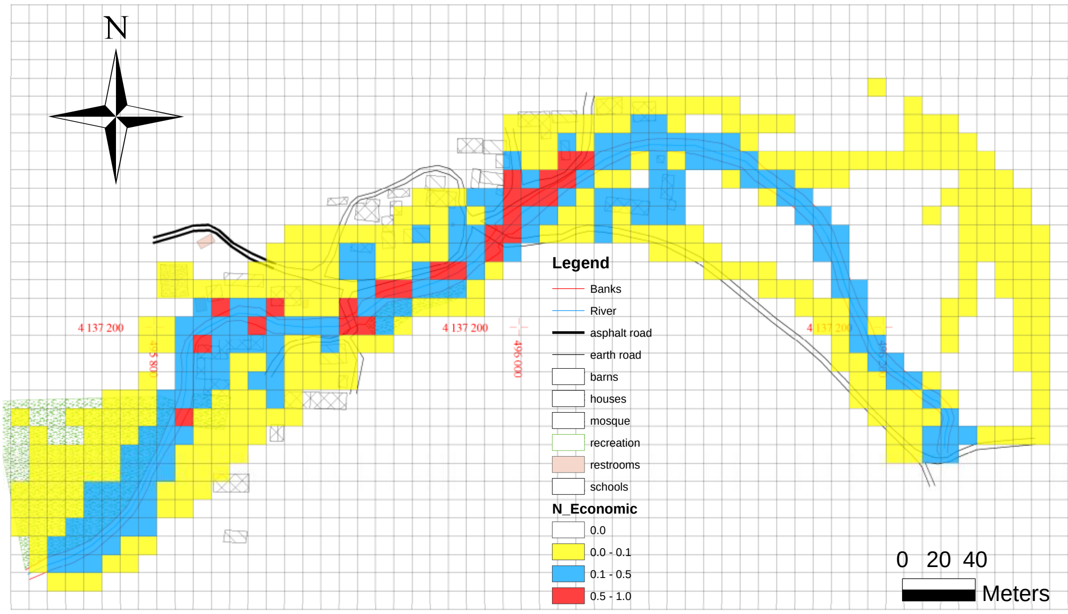

Figure 5.30: Aggregated Overall Multicriteria Flood Risk Map: "Economic" Scenario (0.60 Economic Risk + 0.20 Social Risk + 0.20 Environmental Risk)

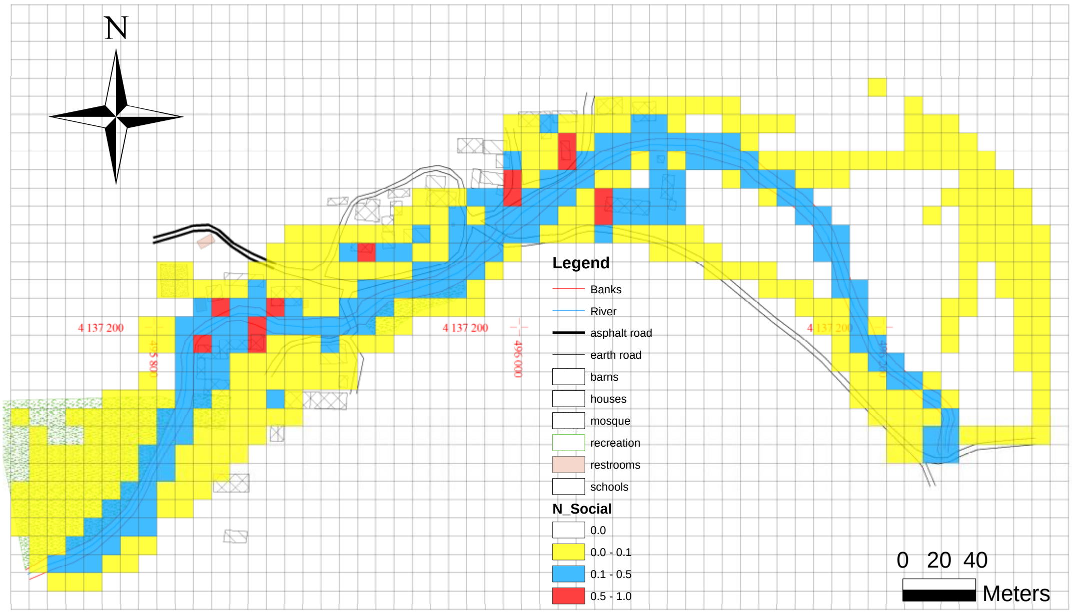

Figure 5.31: Aggregated Overall Multicriteria Flood Risk Map: "Social" Scenario (0.20 Economic Risk + 0.60 Social Risk + 0.20 Environmental Risk)

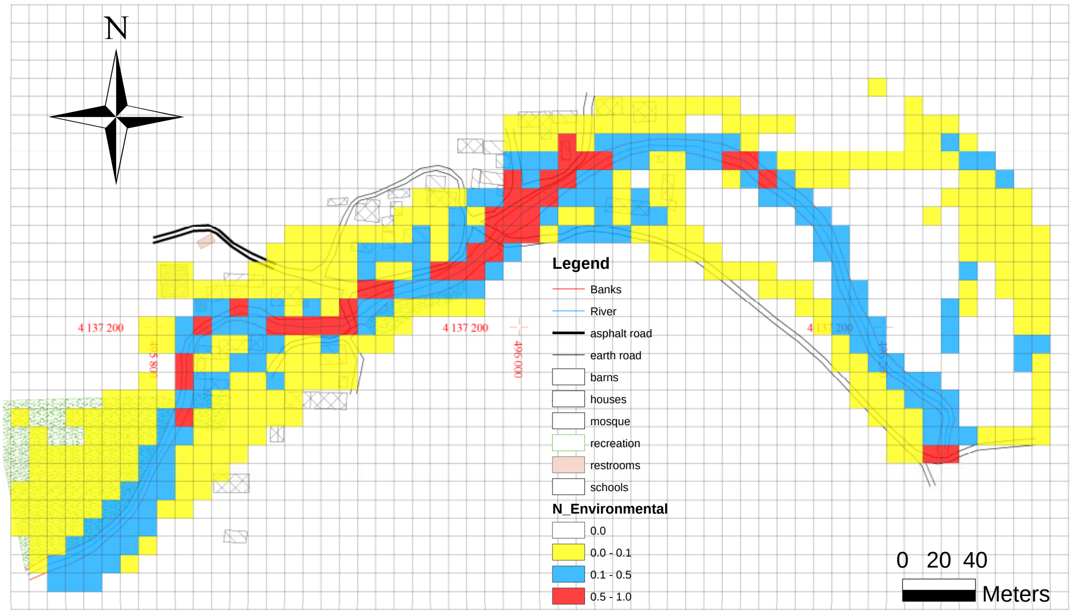

Figure 5.32: Aggregated Overall Multicriteria Flood Risk Map: "Environmental" Scenario (0.20 Economic Risk + 0.20 Social Risk + 0.60 Environmental Risk)

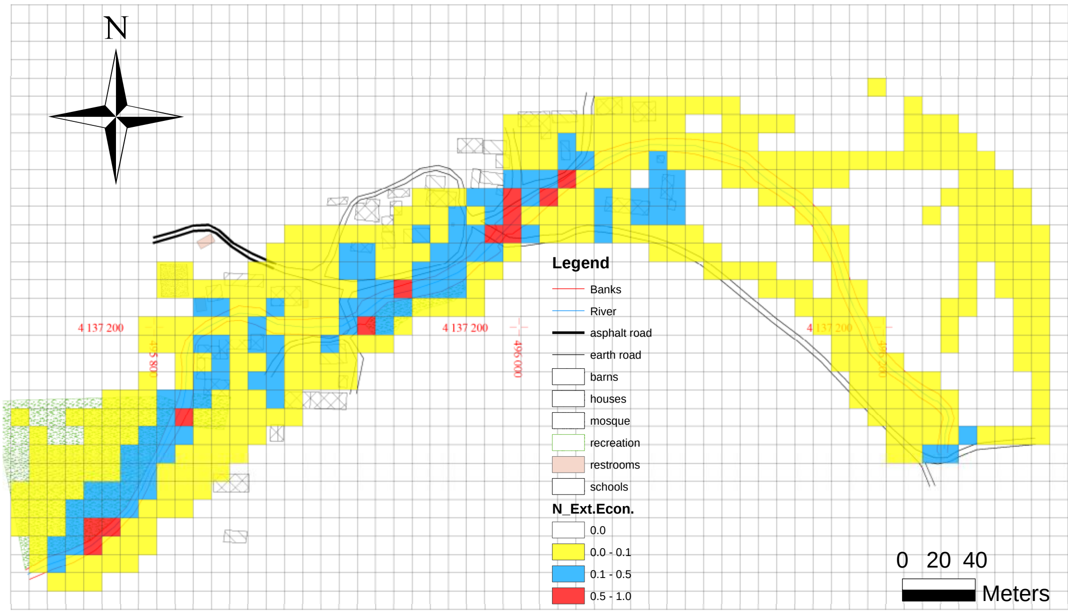

Figure 5.33: Aggregated Overall Multicriteria Flood Risk Map: "Extreme Economic" Scenario (0.90 Economic Risk + 0.05 Social Risk + 0.05 Environmental Risk)

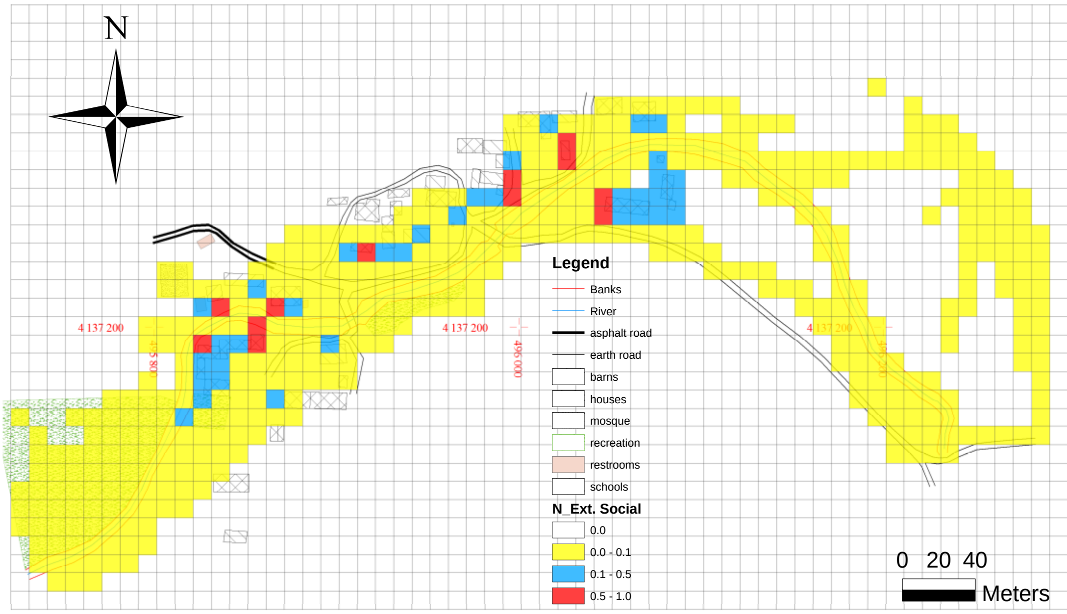

Figure 5.34: Aggregated Overall Multicriteria Flood Risk Map: "Extreme Social" Scenario (0.05 Economic Risk + 0.90 Social Risk + 0.05 Environmental Risk)

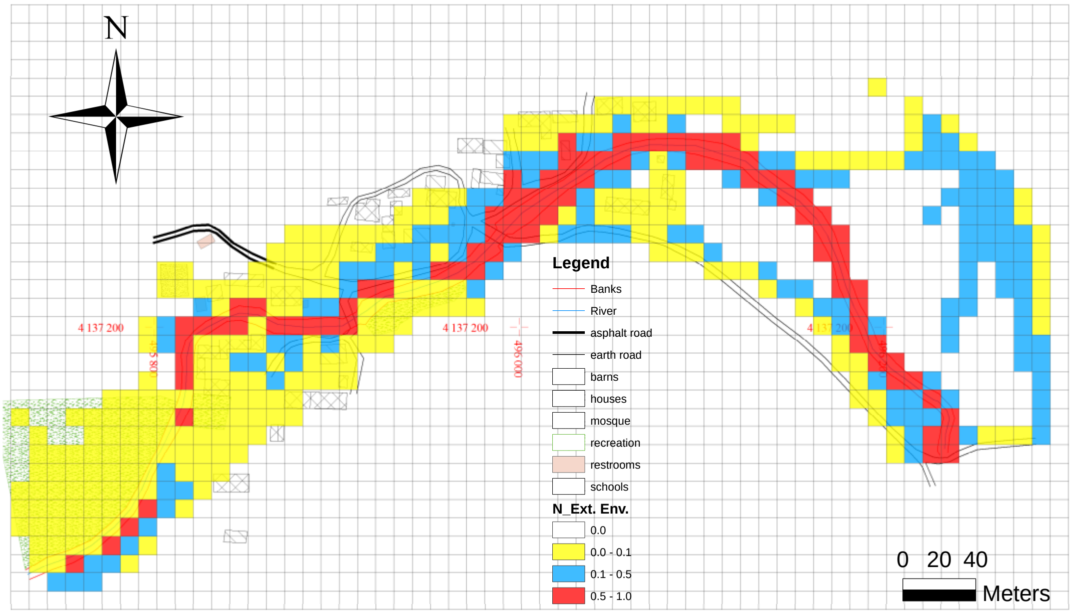

Figure 5.35: Aggregated Overall Multicriteria Flood Risk Map: "Extreme Environmental" Scenario (0.05 Economic Risk + 0.05 Social Risk + 0.90 Environmental Risk)

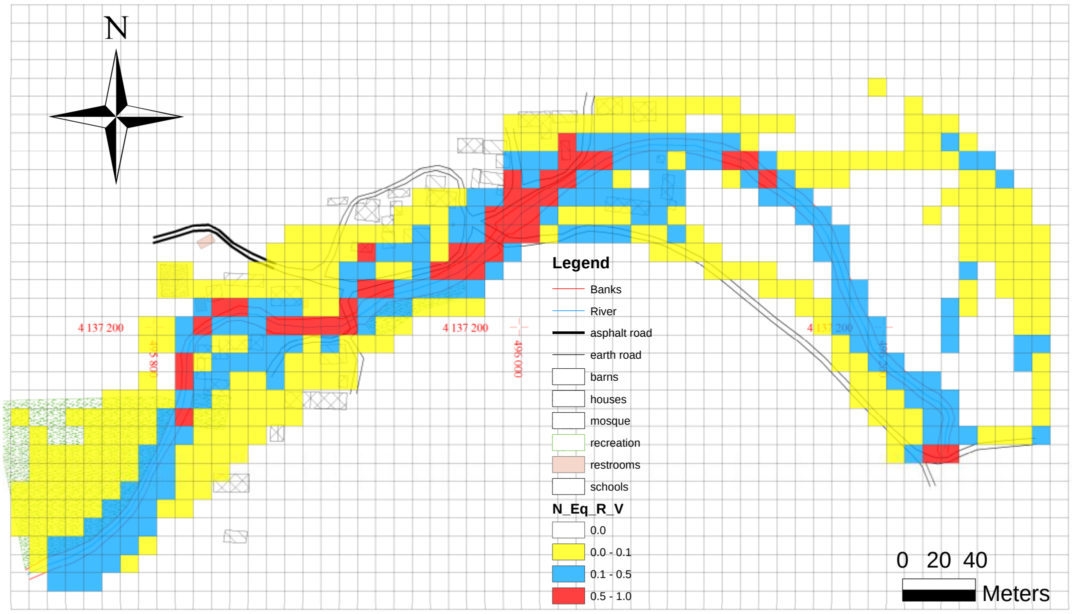

Figure 5.36: Aggregated Overall Multicriteria Flood Risk Map: "Equal" Scenario with vulnerability and resilience factor (0.33 Economic Risk + 0.33 Social Risk + 0.33 Environmental Risk)

After creating aggregated overall multicriteria risk maps for all the scenarios, overall risk values are divided into 4 groups: i) cells with an overall risk of zero are grouped together and referred to as the “no risk” group, ii) cells with overall risk values between 0 and 0.1 form the second group and are referred to as the “low risk” group, iii) cells with overall risk values between 0.1 and 0.5 form the “medium risk” group; and iv)cells with overall risk values between 0.5 and 1.0 are form the “high risk” group. The number of cells in each of these four risk groups for different scenarios are given in Table 5.6. It can be seen that “no risk” value distribution is the same for all scenarios except for the “base” scenario. The number of high risky cells in “equal” scenario with the vulnerability and the resilience factor is approximately 60% greater than the number of high risky cells in “equal” scenario without the vulnerability factor and the resilience factor. This is reasonable because more realistic representation of risk is achieved through integration of resilience and vulnerability concepts. Distribution of number of cells in each risk group is plotted and given in Figure 5.37. As can be seen from Figure 5.37, around 75% of all the cells are in no or low risk groups for all scenarios. The importance of including social and environmental dimensions into the risk analysis can be deduced from Table 5.6. The risky areas in the “base” scenario is approximately 10 percent less than the integrated multicriteria risk maps. Evaluation of only the economic dimension of flood risk cannot reflect the real situation. As can be seen from Table 5.6 depending on the weights assigned to social and environmental elements at risk, some cells change their risk groups. Hence, it is very important to integrate social and environmental dimensions of flood into the risk calculations.

Table 5.6: Risk Value Distribution of Scenarios

Set	No risk TR=0		Low Risk 0<TR<0.1		Medium Risk 0.1≤TR<0.5		High Risk 0.5≤TR≤1.0	
	# of Cells	%	# of Cells	%	# of Cells	%	# of Cells	%
Base	1664	86.94	161	8.41	76	3.97	13	0.68
Economic	1441	75.29	299	15.62	150	7.84	24	1.25
Social	1441	75.29	313	16.35	148	7.73	12	0.63
Environmental	1441	75.29	286	14.94	148	7.73	39	2.04
Extreme Econ.	1441	75.29	369	19.28	92	4.81	12	0.63
Extreme Social	1441	75.29	426	22.26	35	1.83	12	0.63
Extreme Env.	1441	75.29	251	13.11	136	7.11	86	4.49
Equal	1441	75.29	290	15.15	167	8.73	16	0.84
Equal_vul_res	1441	75.88	269	14.17	162	8.53	27	1.42

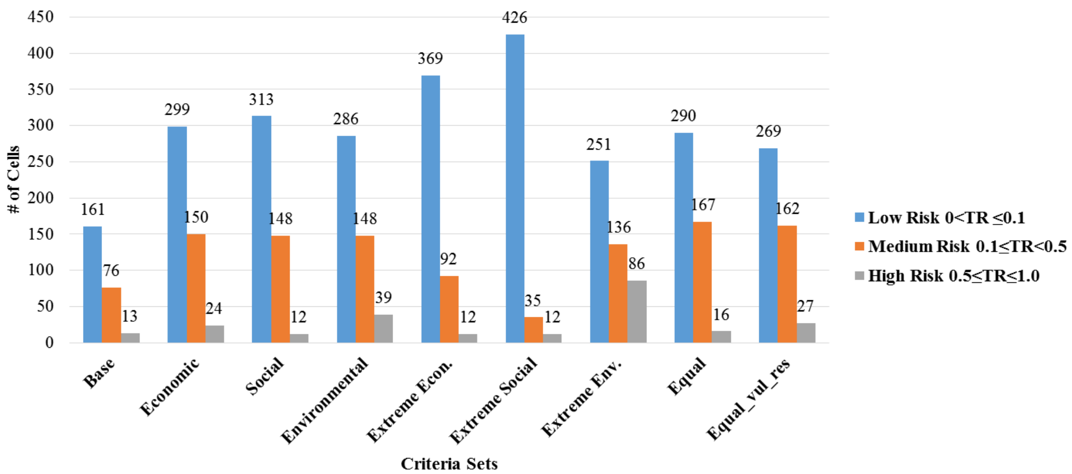

Figure 5.37: Risk Value Distribution

5.7 Economic Risk Map using Netherlands Later Curves

As an additional analysis, economic risk map of the study area is generated using Netherlands Later Curves (De Moel and Aerts, 2011) as depth-damage functions as well (see Figure 5.38). Three different curves are used: one for residential buildings, barns, restrooms and roads, one for the recreation area and one for schools and mosques. In Figure 5.39, the comparison of the economic risk map generated using HOWAS-database damage function and Netherlands Later Curves is provided. As can be seen from Figure 5.39, the number of cells in medium risk class decreases while the number of cells in low risk and high risk classes increase. It can be deduced that depth-damage curve may affect the results significantly, thus utilization of local depth-damage functions is very crucial to generate realistic risk maps. However, this analysis demonstrates that the proposed risk mapping approach is suitable for any depth-damage function. More realistic risk maps can be generated for Turkey if site specific depth-damage functions are created using data from past flood events.

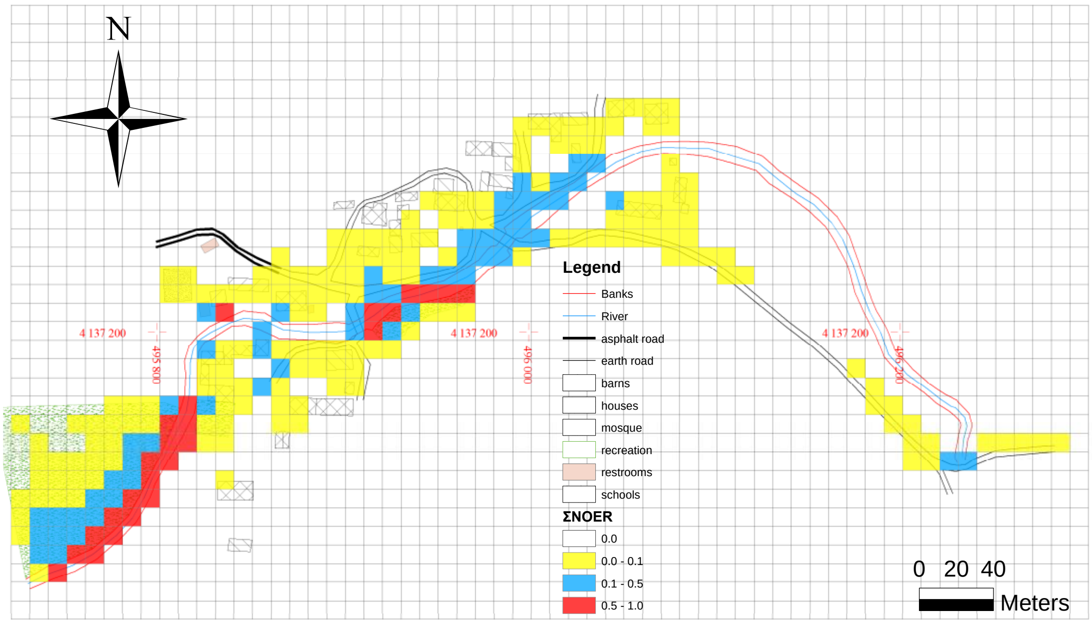

Figure 5.38: Aggregated Overall Economic Risk Map using Netherlands Later Curves

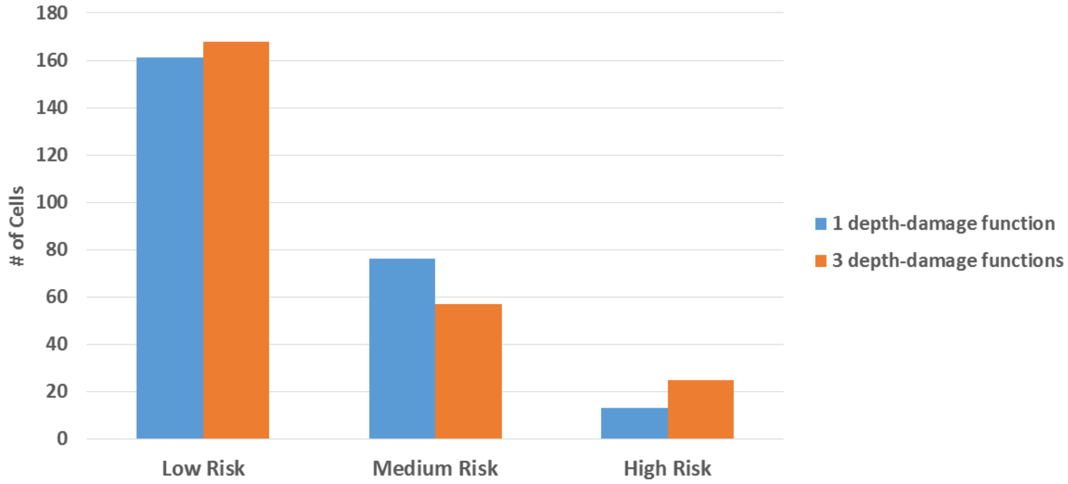

Figure 5.39: The Comparison of Overall Economic Risk Map with One Damage Function and Overall Economic Risk Map with Three Damage Function

5.8 Monetary Damage Calculations using Netherlands Depth-Damage Functions

Monetary damage calculations are carried out using Equations (4-25) – (4-28) provided in Section 4.8. These functions are frequently used in the Netherlands to estimate economic risk. Different depth-damage curves are used to estimate flood damage for different elements at risk. In this study, four different depth-damage functions are used to generate economic flood risk map (see Figure 5.40). The underlying assumption here is that similar depths cause similar damages in the Netherlands and in Turkey. This assumption is not very realistic; to obtain representative monetary damage estimates for Turkey, site specific depth-damage functions need to be used. Such depth-damage functions do not exist for Turkey, thus our goal here is to demonstrate the procedure. To obtain realistic estimates, it is very important to record past flood events' depths and associated damages to generate depth-damage curves which are specific for Turkey.

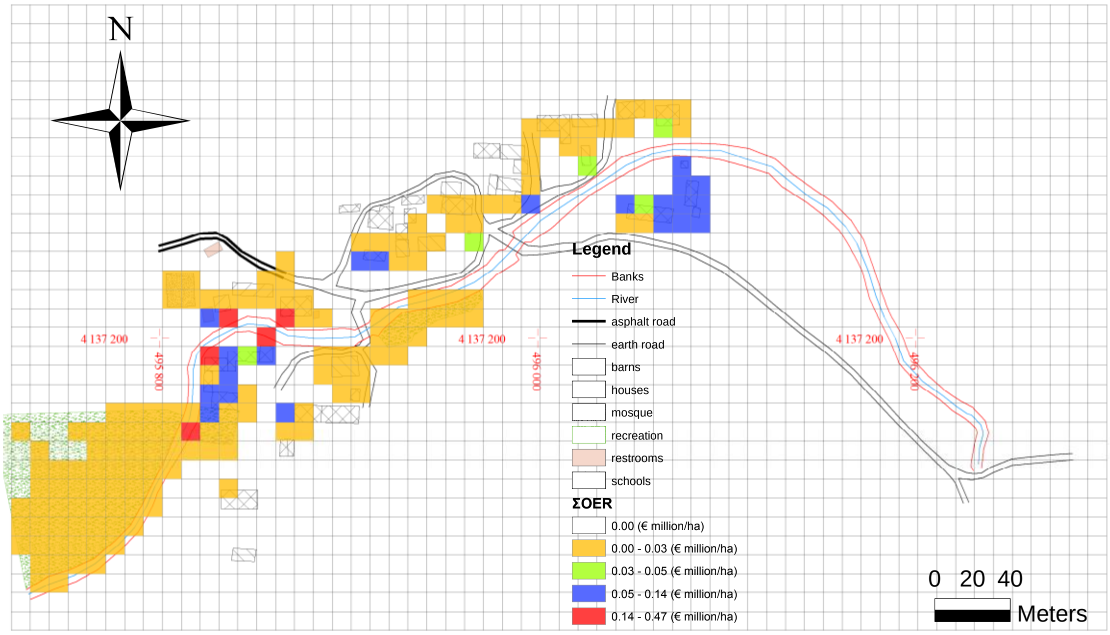

Figure 5.40: The Overall Economic Risk Map in € million / ha

CHAPTER 6

CONCLUSION

Floods are natural hazards that cannot be prevented. However, conducting risk analysis and taking necessary precautions based on the results of these analysis can minimize negative impacts of the floods. Thus, preparation of flood risk maps of all basins and sub-basins in Turkey is essential. This is also important for the process of adaptation to the European Union. European Union stipulates the member states to prepare different types of flood maps. This is a long, difficult and expensive process. However, initiating this process by collecting necessary data, generating flood extent maps and identifying gaps and missing information required to conduct risk analysis is crucial.

The main objective of this study was to demonstrate application of a methodology to prepare flood damage maps and flood risk maps for economic, social and environmental dimensions of risk. These maps were aggregated into an overall risk map using a simple multicriteria decision making approach.

Major findings of this study may be summarized as follows:

- Traditionally, economic risk maps are generated and used as guidance for flood mitigation. However, social and environmental elements at risk often exist at the study site and need to be considered. The overall risk map differs from the economic risk map. Thus integration of environmental and social dimensions of risk into the analysis is beneficial and conveys useful information. In this study, economic, environmental, social risk maps for a selected region in Turkey is generated for the first time.

- Elements at risk for economic, social and environmental dimensions should be selected taking into account site specific conditions. This requires collection of site specific data through site visits, surveys, existing maps and literature. Determination of the relative importance of social, environmental and economic risks should be guided by the authorities. In this study, a number of scenarios (i.e. combination of different sets of weights for each dimension of risk) are generated to demonstrate differences in overall risk maps. Evaluation of these scenarios demonstrated that relative importance of risk dimensions effect the overall risk considerably.
- Damage-exceedance probability curves need to be generated to carry out risk estimations. Water depths corresponding to various return period floods have to be calculated and used in damage-exceedance probability curves. Water depth map is a crucial component of the risk maps. Rasterization cell size of water depth maps should be selected low enough to avoid discontinuities in the results in the ArcGIS environment.
- Damages are calculated from depth-damage curves. Since depth-damage curves for Turkey are not available, curves developed for Germany and the Netherlands are used in this study and resulting overall risk maps are compared. Evaluation of these maps showed that depth-damage curve affect the overall risk map significantly. Unfortunately, environmental and social damages associated with flood events are not commonly studied in Turkey. Economic losses are usually available however water depths are hard or impossible to reach. Detailed studies of experienced flood events and proper recording are necessary in Turkey. This will allow development of a database and generation of depth-damage curves for Turkey. Local depth-damage curves will allow generation of realistic flood risk map of the country.
- The environmental and social dimensions of risk have not been studied as much as the economic dimension of risk. In this study, risk maps for environmental and social dimensions as well as economic dimension are prepared for the selected region in Turkey. Moreover, a simple approach is

proposed to include resilience and vulnerability concepts into the risk analysis in this study.

Flood risk maps highlight flood vulnerable areas and they can be used to identify and design necessary precautions and prioritize areas that need attention. Additionally, flood risk maps might be useful for preparing emergency planning for flood prone areas. There are examples where residential areas are built in the river bed in Turkey. Floods resulted in deaths because of this situation in the past in Turkey. Flood risk maps may provide guidance in city planning as well. Raising awareness about floods and their consequences is part of the solution and flood risk maps may be used as guidance tools for this purpose.

As future work, utilization of a two dimensional model such as MIKE11 or FLO-2D instead of HEC-RAS is suggested. HEC-RAS is a one dimensional hydraulic model and is used in this study because it is free, very fast and many previous studies found in literature showed that results from one and two dimensional models do not differ significantly. On the other hand, several researchers reported that there are unignorably differences between one and two dimensional models. In this study, a number of problems especially at the meandering sections of the river has experienced due to one dimensional water depth calculations. Hence, carrying out the hydraulic calculations with a two dimensional model might be beneficial to see how these models affect the risk maps. Using two-dimensional models will require more processing time and necessitate powerful computers.

REFERENCES

Abudeif, A.M., Moneim, A.A.A. and Farrag, A.F. (2015). Multicriteria decision analysis based on analytic hierarchy process in GIS environment for siting nuclear power plant in Egypt. *Annals of Nuclear Energy, 75*, 682-692.

Ackerman, C.T., Jensen, M.R. and Brunner, G.W. (2010). *Geospatial capabilities of HEC-RAS for model Development and mapping.* 2nd Joint Federal Interagency Conference, Las Vegas. Retrieved from http://acwi.gov/sos/pubs/2ndJFIC/Contents/1F_Ackerman_3_1_10(2).pdf

Adunlin, G., Diaby, V., Montero, A. and Xiao, H. (2014). Multicriteria decision analysis in oncology. Retrieved from http://www.researchgate.net/publication/260838171_Multicriteria_decision_analysis_in_oncology

Aerts, J.C.J.H., Botzen, W.J. and De Moel, H. (2013). *Cost Estimates for Flood Resilience and Protection Strategies in New York City*. In press: Annals of the New York Academy of Science (2013).

Ahmadi, H., Nilashi, M., Darvishi, M., Ibrahim, O., Zakaria, R., Zolghadri, A.H. and Alizadeh, M. (2014). Fuzzy Multi-Criteria Approaches for Evaluating the Critical Factors of Electronic Medical Record Adoption. *American Research Institute for Policy Development*, *3*(2), 01-24.

Akter, T. and Simonovic, S.P. (2005). Aggregation of fuzzy views of a large number of stakeholders for multi-objective flood management decision-making. *Journal of Environmental Management, 77*(2), 133-143.

Balica, S.F., Douben, N. and Wright, N.G. (2009). Flood vulnerability indices at varying spatial scales. *Water Science & Technology*. doi: 10.2166/wst.2009.183

Balica, S.F. (2012). *Applying the Flood Vulnerability Index as a Knowledge base for flood risk assessment* (Published Doctoral Dissertation). UNESCO-IHE, Delft, the Netherlands.

Balica, S.F., Popescu, I., Beevers, L. and Wright N.G. (2013). Parametric and physically based modelling techniques for flood risk and vulnerability assessment: A comparison. *Environmental Modelling and Software. 41*, 84-92.

Bana, E. and Costa C.A. (1990). Reading in multicriteria decision aid. Berlin: Springer.

Bana, E., Costa, C.A., Da Silva, P.A. and Nunes Correia, F. (2004). Multicriteria Evaluation of Flood Control Measures: The Case of Riberia do Livramento. *Water Resources Management, 18*(21), 263-283.

Bashar, K., Khudair, B.H. and Khalid, G.K. (2014). Inundation Map Development by Using HEC-RAS Hydraulic Simulation Modeling From Roseires to Khartoum Cities. *Indian Journal of Research, 3*(9). Retrieved from http://theglobaljournals.com/paripex/file.php?val=September_2014_1410775516__20.pdf

Begum, S., Stive, M.J.F. and Hall, J.W. (Eds.). (2007). *Flood Risk Management in Europe Innovation in Policy and Practice.* Dordrecht, the Netherlands: Springer.

Belton, V. and Stewart, T.J. (2002). Multiple criteria decision analysis – an integrated approach. Boston: Kluwer

Bozoğlu, B. (2015). *1-D and 2-D Flood Modeling Studies and Upstream Structural Measures For Samsun City Terme District. (*Unpublished Master Thesis). Ankara, Middle East Technical University.

Brouwer, R. and van Ek, R. (2004). Integrated ecological, economic and social impact assessment of alternative flood control policies in the Netherlands. *Ecological Economics*, *50*, 1-21.

Brych, K., Dittrt, F. and Elias, V. (2002). *Development of flood boundary maps of urban areas using HEC-RAS software.* Regional Hydrology: Bridging the Gap between Research and Practice: Fourth International FRIEND Conference, Cape Town, South Africa. Retrieved from
http://hydrologie.org/redbooks/a274/iahs_274_237.pdf

Cook, A.C. (2008). *Comparison of one-dimensional HEC-RAS with two dimensional FESWMS model in flood* inundation *mapping* (Unpublished master thesis). West Lafayatte, Indiana, Purdue University.

Cowan, W.L. (1956). Estimating Hydraulic Roughness Coefficients. *Agricultural Engg., 37(7),* 473-475.

De Moel, H., van Alphen, J. and Aerts, J.C.J.H. (2009). Flood maps in Europe – methods, availability and use. *Natural Hazards and Earth System Sciences, 9*, 289-301.

De Moel, H. and Aerts, J.C.J.H. (2011). Effect of uncertainty in land use, damage models and inundation depth on flood damage estimates. *Nat Hazards*, *58,* 407-425.

Directive 2007/60/EC of the European Parliament and of the council of 23 October 2007 on the assessment and management of flood risks. (2007). OJ L288/27.

Doğan, E., Sönmez, O., Yapan, E., Othan, K., Özdemir, S., Çitgez, T. (2013). Aşağı Sakarya Nehrinde taşkın yayılım haritalarının elde edilmesi. *Sakarya Üniversitesi Fen Bilimleri Enstitüsü Dergisi*, *17*(3), 363-369.

Eser Project & Engineering Co. Inc. (2012). *Şanlıurfa İli ve İlçeleri Taşkın Koruma Master Plan Mühendislik Hizmetleri İşi Şanlıurfa Merkez İlçesi Taşkın Hidrolojisi Raporu.* Ankara.

Eser Project & Engineering Co. Inc. (2013). *Şanlıurfa İli ve İlçeleri Taşkın Koruma Master Plan Proje Yapımı İşi Merkez Köyleri Harita Hesap Ciltleri*. Ankara.

European Environment Agency. (2010). *Mapping the impacts of natural hazards and technological accidents in Europe An overview of the last decade.* (No 13/2010). Luxembourg: Publications Office of the European Union.

European exchange circle on flood mapping. (2007). *Handbook on good practices for flood mapping in Europe.* Retrieved from http://ec.europa.eu/environment/water/flood_risk/flood_atlas/pdf/handbook_goodpractice.pdf

European Investment Bank. (2007). *Guide for preparation of flood risk management schemes.* Retrieved from http://www.eib.org/attachments/strategies/flood_risk_management_guide_en.pdf

European Spatial Planning Observation Network. (2006). *The Spatial Effects and Management of Natural and Technological Hazards in Europe – ESPON 1.3.1.* Retrieved from http://www.espon.eu/export/sites/default/Documents/Projects/ESPON2006Projects/ThematicProjects/NaturalHazards/fr-1.3.1_revised-full.pdf

FLOODsite. (2006). *Guidelines for Socio-economic Flood Damage Evaluation* (T9-06-01). European Community.

Fosu, C., Forkuo, E.K. and Asare, M.Y. (2012). *River Inundation and Hazard Mapping – a Case Study of Susan River – Kumasi*. Proceedings of Global Geospatial Conference, Québec City, Canada. Retrieved from http://www.gsdi.org/gsdiconf/gsdi13/papers/168.pdf

Goodell, C. and Warren, C. (2006). *Flood Inundation Mapping using HEC-RAS.* Retrieved from http://www.oyp.ucsc.cl/2/Goodell_ch_bn.pdf

Guilford Borough. (2010). *Flood Risk Reduction Measures.* Retrieved from http://www.guildford.gov.uk/media/7426/Flood-Risk-Reduction-Measures/pdf/FRRM_20document_20November_202010resize.pdf

Hicks, F.E. and Peacock, T. (2005). Suitability of HEC-RAS for Flood Forecasting. *Canadian Water Resources Journal*, *30*(2), 159-174.

Horritt, M.S. and Bates, P.D. (2002). Evaluation of 1D and 2D numerical models for predicting river flood inundation. *Journal of Hydrology, 268*, 87-99.

Ishizaka, A. and Nemery P. (2013). Multi-Criteria Decision Analysis Methods and Software. Chichester: John Wiley & Sons Ltd.

İrvem, A. and Topaloğlu, F. (2012). Identification of flood risk area in the Orontes river basin, Turkey, using multi-criteria decision analyses. *Food, Agriculture and Environment, 10*(3-4), 895-899.

Jongman, B., Kreibich, H., Apel, H., Barredo, J.I., Bates, P.D., Feyen, L., Gericke, A., Neal, J., Aerts, J.C.J.H. and Ward, P.J. (2012). Comparative flood damage model assessment: towards a European approach. *Natural Hazards and Earth System Sciences*, *12*, 3733-3752.

Jonkman, S.N., Bočkarjova, M., Kok, M. and Bernardini, P. (2008). Integrated hydrodynamic and economic modelling of flood damage in the Netherlands. *Ecological Economics*, *66*(2008), 77-90.

Kahn, M.E. (2003). *The Death Toll From Natural Disasters: The Role of Income, Geography, and Instutions.* Retrieved from http://eml.berkeley.edu/~webfac/quigley/e231_f03/kahn.pdf

Keskin, F. (2012). *Quantitative Flood Risk Assessment with Application in Turkey.* (Unpublished doctoral thesis). Ankara, Middle East Technical University.

Kienberger, S., Lang, S. and Zeil, P. (2009). Spatial vulnerability units – expert – based spatial modelling of socio – economic vulnerability in the Salzach catchment, Austria. *Natural Hazards and Earth System Sciences, 9*, 767-778.

Kubal, C., Haase, D., Meyer, V. and Scheuer, S. (2009). Integrated urban flood risk assessment – adapting a multicriteria approach to a city. *Natural Hazards and Earth System Sciences, 9,* 1881-1895.

Kute, S., Kakad, S., Bhoye, V. and Walunj, A. (2014). Flood Modelling of River Godavari Using HEC-RAS. *International Journal of Research in Engineering and Technology*, *3*(9). Retrieved from http://esatjournals.org/Volumes/IJRET/2014V03/I21/IJRET20140321017.pdf

Kutluay, E.S. (2010). *Adıyaman – Şanlıurfa – Diyarbakır Planlama Bölgesi 1/100.000 ölçekli çevre düzeni planı araştırma raporu.* Ankara.

Kühmaier, M. and Stampfer, K. (2012). Development of a Multi-Criteria Decision Support Tool for Energy Wood Supply Management. *Croatian Journal of Forest Engineering, 33*(2012), 181-198.

Lombard, P.J. (2011). Flood-Inundation Maps for the St. John and Fish Rivers in Fort Kent, Maine: U.S. Geological Survey Scientific Investigations Map 3157, 8 p. pamphlet, 29 map sheets, scale 1:17,500.

Malczewski, J. (1999). *GIS and Multicriteria Decision Analysis.* Canada: John Wiley & Sons Ltd.

Merz, B., Thieken, A. H. and Gocht, M. (2007). Flood risk mapping at the local scale: concepts and challenges, in: Begum, S., Stive, M. J. F., Hall, J. W. (Eds.), Flood Risk Management in Europe. Innovation in Policy and Practice, Advances in Natural and Technological Hazards Research 25, Dordrecht, pp. 231-251

Meyer, V., Scheuer, S. and Haase, D. (2009). A multicriteria approach for flood risk mapping exemplified at the Mulde river, Germany. *Nat Hazards, 48*(1), 17-39.

Musungu, K., Motala, S. and Smit, J. (2012). Using Multi-criteria Evaluation and GIS for Flood Risk Analysis in Informal Settlements of Cape Town: The Case of Graveyard Pond. *South African Journal of Geomatics, 1*(1).

Nimaev, A. (2015). *The Use Of Simple Inertial Formulation Of The Shallow Water Equations In 2-D Flood Inundation Modeling.* (Unpublished master thesis). Ankara, Middle East Technical University.

Nut, N. and Plermkamon, V. (2013). *Estimation of Flood Damages on Namphong River by HEC-RAS.* The 14th TSAE National Conference and the 6th TSAE International Conference. 179-186.

Ouma, Y.O. and Tateishi, R. (2014). Urban Flood Vulnerability and Risk Mapping Using Integrated Multi-Parametric AHP and GIS: Methodological Overview and Case Study Assessment. *Water, 6,* 1515-1545. doi: 10.3390/w6061515

Ozcan, O., Musaoglu, N., Seker, D.Z. and Tanık, A. (2008). Determination of Flood Risk in Sakarya Sub-basin Using Remotely Sensed Data and GIS. *Fresenius Environmental Bulletin, 17,* 1964-1970.

Penning-Rowsell, E., Johnson, C., Tunstall, S., Tapsell, S., Morris, J. Chatterton, J. Coker, A. and Green, C. (2003). *The Benefits of Flood and Coastal Defence: Techniques and Data for 2003.* Flood Hazard Research Centre, Middlesex University.

Porio, E. (2011). Vulnerability, Adaptation, and Resilience to Floods and Climate Change-Related Risks among Marginal, Riverine Communities in Metro Manila. *Asian Journal of Social Science, 39(2011),* 425-445.

Pornasdoro, K.P., Silva, L.C., Munárriz, M.L.T., Estepa, B.A. and Capaque, C.A. (2014). Flood Risk of Metro Manila Barangays: A GIS Based Risk Assessment Using Multi-Criteria Techniques. *Journal in Urban and Regional Planning.* Retrieved from http://journals.upd.edu.ph/index.php/19May2014_surp/article/view/4207/3817

PROMITHEAS-4. (2011). *Overview and selection of multi-criteria evaluation methods for mitigation/adaptation policy instruments.* Greece. Retrieved from http://www.promitheasnet.kepa.uoa.gr/Promitheas4/images/library/wp4.1%20overview%20and%20selection%20of%20multicriteria%20evaluation%20methods%20for%20mitigation-adaptation%20policy%20instruments.pdf

Raji, S.A., Adeniyi, P.O. and Odunuga, S. (2014). Multicriteria Flood Risk Analysis of Lower Ogun River Basin. *Journal of Environment and Earth Science* [Online] 4. Available at: http://www.iiste.org/Journals/index.php/JEES/article/view/14234/14542 [Accessed: 19 August 2015].

Roy, B. (1981). The optimisation problem formulation: Criticism and overstepping. *Journal of the Operational Research Sociey, 32*(6), 427-436.

Saini, S.S. and Kaushik, S.P. (2012). Risk and vulnerability assessment of flood hazard in part of Ghaggar Basin: A case study of Guhla block, Kaithal, Haryana, India. *International Journal of Geomatics and Geosciences, 3*(1). Retrieved from http://www.ipublishing.co.in/jggsvol1no12010/volthree/EIJGGS3104.pdf

Salajegheh, A., Bakhshaei, M., Chavoshi, S., Keshtkar, A.R. and Hajivar, M.N. (2009). Floodplain mapping using HEC-RAS and GIS in semi-arid regions of Iran. *DESERT, 14*(2009), 83-93.

Saville, D. (2011). *Flood Inundation Mapping and Economic Damages Modeling.* North Dakota GIS Conference, North Dakota, 13 October.

Selek, B. and Darama, Y. (2013). *Taşkın Strateji Eylem Planı Kapsamında DSİ Çalışmaları*. 3. Ulusal Taşkın Sempozyumu, İstanbul, Turkey. Retrieved from http://www.dsi.gov.tr/docs/sempozyumlar/ta%C5%9Fk%C4%B1n-strateji-eylem-plan%C4%B1-kapsam%C4%B1nda-dsi-%C3%A7al%C4%B1%C5%9Fmalar%C4%B1-(y-darama).pdf?sfvrsn=2

Sepetçioğlu, M.Y. (2013). Şanlıurfa İli Taşkın Sorunları ve Çözümleri. *e-Journal of New World Sciences Academy, 8, (1),* 21-38.

Silva, F.V., Bonumá, N.B. and Uda, P.K. (2014). *Flood Mapping in Urban Area Using HEC-RAS Model Supported by GIS.* 6th International Conference on Flood Management, São Paulo, September.

Sredojevic, D. and Simonovic, S.P. (2009). *Water Resources Research Report City of London: Vulnerability of Infrastructure to Climate Change Background Report #2 Hydraulic Modeling and Floodplain Mapping.* Retrieved from http://ir.lib.uwo.ca/cgi/viewcontent.cgi?article=1031&context=wrrr

Stepinski, E. (2011). *1D and 2D Methods for Modeling Floodplains under Storm Surge Conditions.* (Unpublished master thesis). Houston, Rice University.

Te Linde, A.H., Bubeck, P., Dekkers, J.E.C., De Moel, H. and Aerts, J.C.J.H. (2011). Future flood risk estimates along the river Rhine. *Natural Hazards and Earth System Sciences*, *11*, 459-473.

Thywissen, K. (2006). *Components of Risk A Comparative Glossary.* United Nations University UNU-EHS Institute for Environment and Human Security, Paffenholz, Bornheim: Germany.

Turkish State Meteorological Services, CDM, Riverside (2011) Final Feasibility Study Report: Flood Forecasting and Early Warning System Project Feasibility Study. Turkish State Meteorological Services, December 2011.

Uçar, İ. (2010). *Trabzon Değirmendere Havzası'nda Coğrafi Bilgi Sistemleri ve Bir Hidrolik Model Yardımıyla Taşkın Analizi Yapılması.* (Unpublished master thesis). Ankara, Gazi Üniversitesi.

US Army Corps of Engineers Hydraulic Engineering Center. (2010). *HEC-RAS River Analysis System Hydraulic Reference Manual.* (No. CPD-69). Davis: US.

Usul, N. and Turan, B. (2006). Flood forecasting and analysis within the Ulus Basin, Turkey, using geographic information systems. *Nat Hazards*, *39*, 213-229.

Usul, N. (n.d.). *Taşkın Çlaışmalarında Coğrafi Bilgi Sistemlerinin (CBS) Kullanılması*. Retrieved from http://www.imo.org.tr/resimler/ekutuphane/pdf/3933.pdf

Ünüvar, N. (n.d.). *Sel ve Su Taşkınlarında Ortaya Çıkan Sağlık Sorunları ve Yönetimi*. Retrieved from http://www.dsi.gov.tr/docs/sempozyumlar/5-6-task%C4%B1n-sonras%C4%B1-yasanab%C4%B1lecek-sagl%C4%B1k-problemler%C4%B1-n-unuvar-.pdf?sfvrsn=2

Vazifedoost, R.M., Nayyeri, M. and Barani, G.A. (2014). Floodplian Modeling Using HEC-RAS and MIKE11 Models. *Journal of River Engineering, 2*(5).

Velasco, M. (2014). *Flood damage assessment and estimation of flood resilience indexes Barcelona case study*. Workshop Collaborative research on flood resilience in urban areas, Cornellà de Llobregat, 19th of May 2014.

Velasquez, M. and Hester, P.T. (2013). An Analysis of Multi-Criteria Decision Making Methods. *International Journal of Operations Research, 10*(2), 56-66.

Vincke, P. (1992). Multicriteria decision-aid. Chichester: John Wiley & Sons Ltd.

Ward, P.J., De Moel, H. and Aerts, J.C.J.H. (2011). How are flood risk estimates affected by the choice of return-periods? *Natural Hazards and Earth System Sciences*, *11*, 3181-3195.

Yalcin, G. and Akyurek Z. (n.d.). *Analyzing Flood Vulnerable Areas with Multicriteria Evaluation.* Retrieved from http://www.isprs.org/proceedings/XXXV/congress/comm2/papers/154.pdf

Yerramilli, S. (2012). A Hybrid Approach of Integrating HEC-RAS and GIS Towards the Identification and Assessment of Flood Risk Vulnerability in the City of Jackson, MS. *American Journal of Geographic Information System, 1*(1), 7-16.

Younus, A.F. (2013). Community-Based Flood Vulnerability and Adaptation Assessment: A Case Study from Bangladesh. *Journal of Environmental Assessment Policy and Management, 15*(3). DOI: 10.1142/S1464333213500105

Zopounidis, C. and Pardalos, P.M. (Eds.). (2010). *Handbook of Multicriteria Analysis.* Berlin, Germany: Springer.

APPENDICES

A. HYDROLOGIC ANALYSIS

In flood risk mapping, water depth and water velocity are the main inputs. Peak flood discharges should be calculated to obtain these parameters. Moreover, for flood risk calculation, peak discharges with different return periods should be calculated to create depth-exceedance probability curves to calculate risk. The procedure of calculation of peak discharges can be seen in Figure A.1.

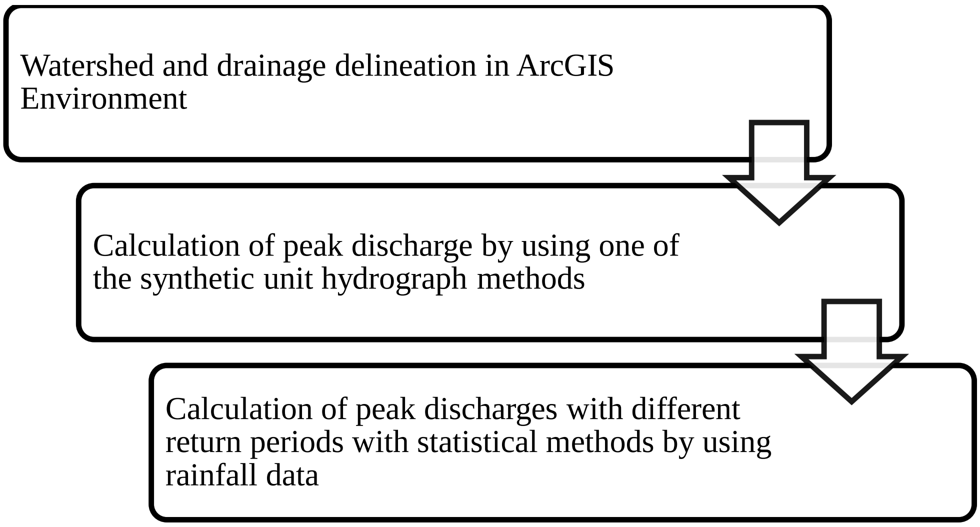

Figure A.1: Procedure of Peak Flood Discharge Calculation

A.1 Watershed and Drainage Delineation

Watershed area and river length are important parameters used in calculation of synthetic unit hydrographs. These parameters can be calculated using ArcGIS. The procedure of watershed and drainage delineation can be seen in Figure A.2.

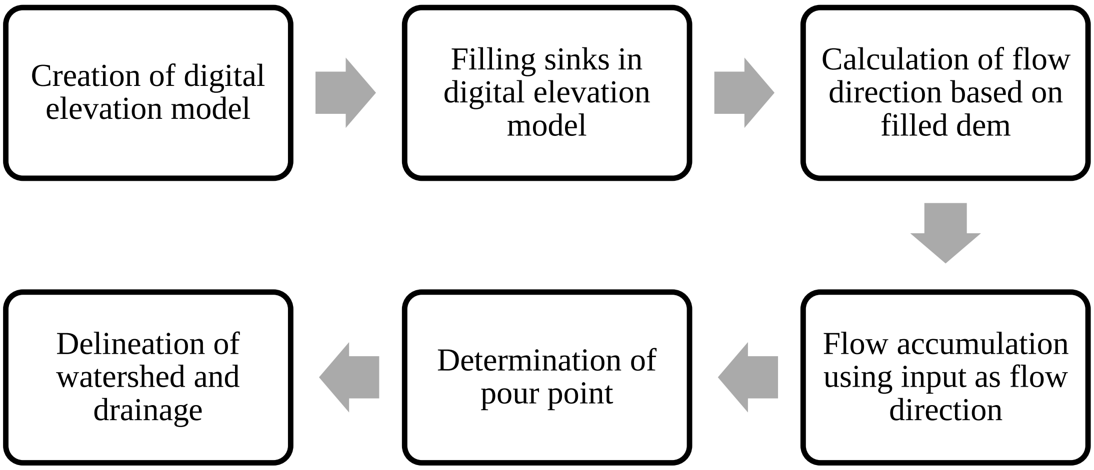

Figure A.2: Procedure of Watershed and Drainage Delineation

Firstly, the digital elevation model of study area is created by using 1/25000 scaled maps. After this step, the sinks in the digital elevation model is filled by "fill" under Hydrology tool in ArcGIS. Then, flow direction is calculated using filled digital elevation model as an input. In this step, the direction of water flow through is computed. Each direction is represented with a number. For example if flow is from center to north, it is represented with "64". These numbers and directions can be seen in Figure A.3.

32	64	128
16		1
8	4	2

Figure A.3: Numbers Showing the Direction of Water Flow in ArcGIS

After this step, flow accumulation is calculated using flow direction as an input. In this step, the number of cells flowing into a cell is calculated. The cells with higher values represent where water collects and drains. Next, the pour point is placed. The pour point is the cell which stream gage exists. It should be the cell which has highest flow accumulation value. Finally watershed is created using "watershed" under Hydrology tool using pour point and flow direction. The calculated watershed area is 25.39 km^2 and river length is approximately 11402 m. The created watershed and delineated drainage network can be seen in Figure A.4.

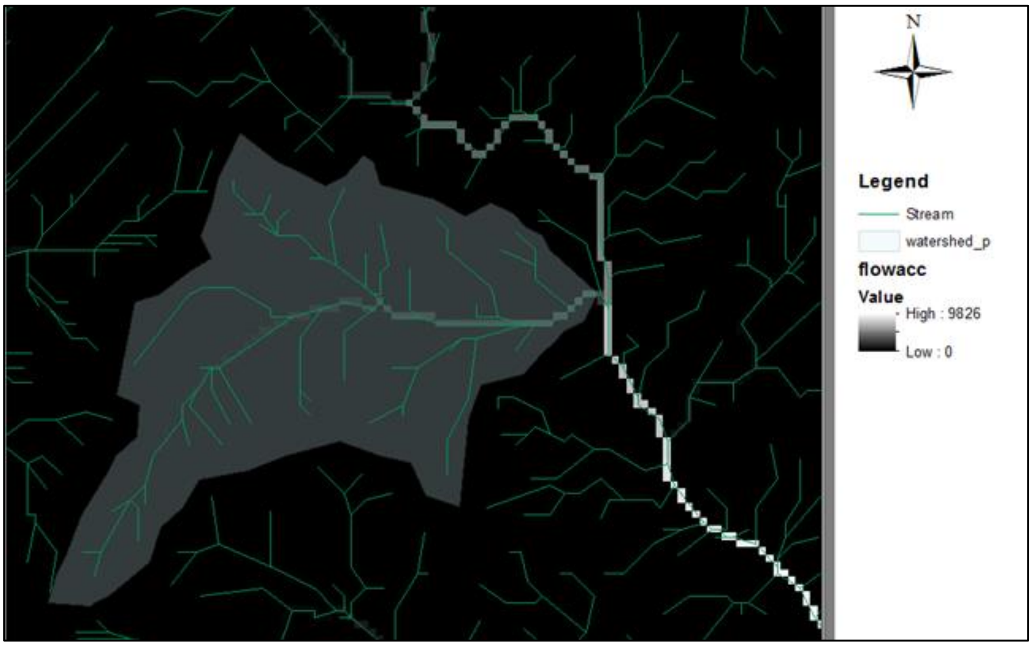

Figure A.4: Created Watershed and Delineated Drainage Networks in ArcGIS

A.2 Calculation of Peak Discharges

There is no stream gage on the studied river. Hence, unit hydrograph is created synthetically. There are many methods to derive synthetic unit hydrographs: Mockus Method, Snyder Method, DSI Synthetic Unit Hydrograph Method etc. In this study, Mockus Method is used to calculate peak discharge. In Mockus Method, the shape of the unit hydrograph is accepted as triangular. It is applied to basins which the time of concentration is less than 30 hours. Time of concentration is calculated with Equation (A-1):

$$T_c = 0.00032 * \frac{L_h^{0.77}}{S_h^{0.385}} \quad \text{(A-1)}$$

where T_c is time of concentration (hours), L_h is hydraulic length of the watershed (meters), S_h is harmonic slope of the channel.

Harmonic slope of the channel is determined by using Equation (A-2):

$$S_h = \left(\frac{P}{\Sigma \sqrt{\frac{1}{\sqrt{S}}}} \right)^2 \qquad \text{(A-2)}$$

Where p is the total number of divided segments and s is the slope of the divided segment. The river is divided into 10 parts and harmonic slope is calculated as 0.012. After these calculations, time of concentration is calculated as 2.31 hours. Excess rainfall duration in corresponding time of concentration (D) can be calculated with Equation (A-3):

$$D = 2 * \sqrt{t_c} \qquad \text{(A-3)}$$

D is calculated as 3.04 hours and it is taken as 3.0 hours. Time to peak, T_p , can be calculated with Equation (A-4):

$$T_p = 0.5 * D + 0.6 * T_c \qquad \text{(A-4)}$$

Time to peak is calculated as 2.89 hours and it is taken as 3.0 hours. Finally peak discharge, Q_p, is calculated with Equation (A-5):

$$Q_p = \frac{0.208 * A * h_a}{T_p} \qquad \text{(A-5)}$$

Where A is the drainage area in km^2 and h_a is unit rainfall depth which is 1 mm. Using Equation (A-5), peak discharge is calculated as 1.83 m^3/s/mm.

After calculating peak discharge, the peak rainfall values should be calculated by statistical methods. Firstly, the station(s) should be found which represent the studied area. For this reason, Thiessen Polygon created in ArcGIS environment. 53.7 % of studied area is represented by Şanlıurfa State Meteorological Station and remaining part of the studied area is represented by Hilvan State Meteorological Station. The past rainfall data is taken from these stations. Created Thiessen Polygon can be seen in Figure A.5:

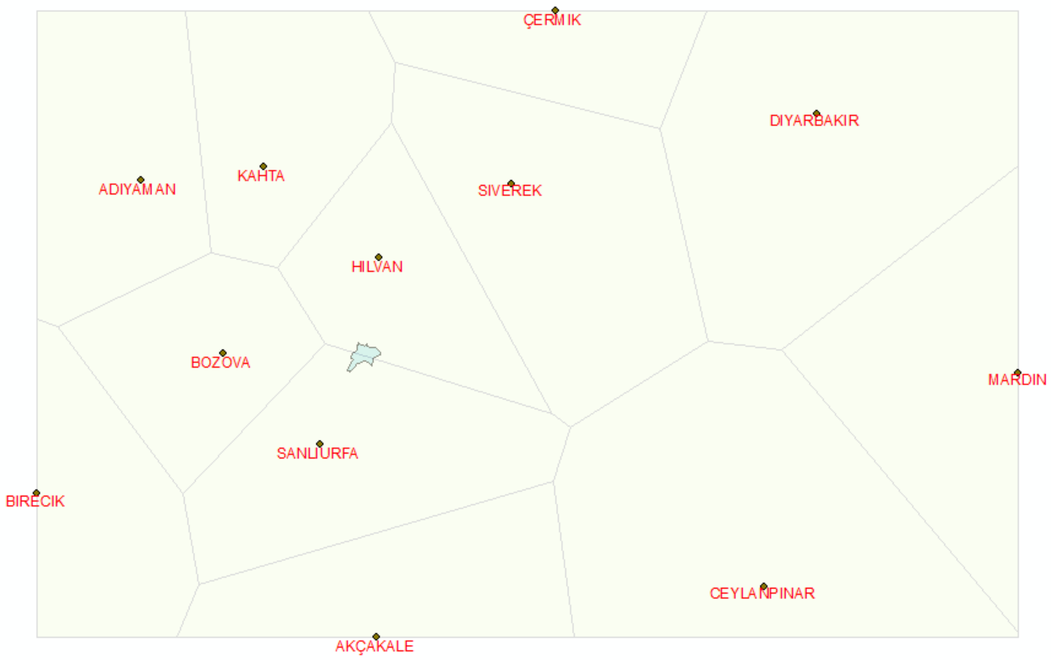

Figure A.5: Created Thiessen Polygon

A.3 Calculation of Rainfall with Different Return Periods

Using maximum rainfall data from mentioned stations, the probable maximum rainfall is calculated for different return periods. For carrying on these calculations, the statistical methods should be used such as Normal Distribution, Log-normal distribution, Log-Pearson Type III distribution etc. The rainfall data includes years from 1929 to 2010. Şanlıurfa State Meteorological Station maximum rainfall data is given in Table A.1.

Table A.1: Şanlıurfa State Meteorological Station Maximum Rainfall Data

Years	Maximum Rainfall (mm)	Years	Maximum Rainfall (mm)	Years	Maximum Rainfall (mm)	Years	Maximum Rainfall (mm)
1929	37.70	1952	73.60	1975	43.90	1998	33.80
1930	49.40	1953	67.30	1976	57.50	1999	43.50
1931	32.00	1954	54.00	1977	34.80	2000	59.30
1932	19.80	1955	42.20	1978	27.20	2001	34.60
1933	30.70	1956	21.00	1979	31.50	2002	39.80
1934	-	1957	28.80	1980	41.90	2003	30.80
1935	-	1958	46.60	1981	64.10	2004	41.10
1936	-	1959	39.30	1982	47.00	2005	28.90
1937	29.30	1960	119.50	1983	50.50	2006	29.40
1938	53.20	1961	47.80	1984	53.70	2007	33.00
1939	48.20	1962	31.70	1985	31.60	2008	42.30
1940	37.80	1963	99.70	1986	64.70	2009	43.00
1941	55.00	1964	35.30	1987	29.80	2010	28.50
1942	35.20	1965	37.60	1988	50.20		
1943	30.60	1966	29.90	1989	36.40		
1944	51.00	1967	55.90	1990	33.60		
1945	30.30	1968	36.50	1991	59.50		
1946	61.40	1969	117.10	1992	28.30		
1947	37.10	1970	40.40	1993	49.40		
1948	35.00	1971	64.70	1994	40.90		
1949	68.60	1972	31.60	1995	22.30		
1950	55.90	1973	23.70	1996	62.30		
1951	47.90	1974	38.80	1997	49.30		

Before fitting probability distributions, some parameters should be calculated: the mean (μ), the standard deviation (σ) and the skewness coefficient (g). The "n" term is the sample size. These parameters are calculated by equations (A-6)-(A-8). The mean is calculated as 44.65 mm, the standard deviation is calculated as 18.369 mm and the skewness coefficient is calculated as 2.01 mm.

$$\mu = \frac{1}{n} * \sum_{i=1}^{n} x_i \quad \text{(A-6)}$$

$$\sigma = \left[\sqrt{\frac{1}{(n-1)} * \sum_{i=1}^{n} (x_i - \mu)^2}\right] \quad \text{(A-7)}$$

$$g = \frac{1}{\sigma^3} * \frac{n}{(n-1)*(n-2)} * \sum_{i=1}^{n} (x(i) - \mu)^3 \quad \text{(A-8)}$$

The Normal Distribution is a symmetric distribution with skewness factor = 0. The normal distribution calculations are carried out by Equation (A-9). The "z" term is a standardizing score and using z score, the probability can be found. The corresponding 2, 5, 10, 25, 50, 100, 500 and 1000 years rainfall z scores are 0.00, 0.841, 1.282, 1.751, 2.054, 2.326, 2.875 and 3.09. The calculated rainfall values are given in Table A.2.

$$z = \frac{x-\mu}{\sigma} \tag{A-9}$$

Table A.2: Normally distributed rainfall values with corresponding return periods in mm

Q_2	Q_5	Q_{10}	Q_{25}	Q_{50}	Q_{100}	Q_{500}	Q_{1000}
44.65	60.11	68.19	76.82	82.38	87.38	97.46	101.04

In the Log-Normal Distribution, logarithm of the random variable is distributed normally. In contrast to the Normal Distribution, the Log-Normal Distribution has a lower limit 0 and this provides a better fit because many hydrologic variables physically cannot take negative values. After taking logarithm of the random variables, the mean is calculated as 1.621 using Equation (A-6) and the standard deviation is calculated as 0.154 using Equation (A-7). The z scores used in normal distribution can also be used with the log-normal distribution. The calculations are carried out with Equation (A-9). The calculated rainfall values are given in Table A.3.

Table A.3: Log-normally distributed rainfall values with corresponding return periods in mm

Q_2	Q_5	Q_{10}	Q_{25}	Q_{50}	Q_{100}	Q_{500}	Q_{1000}
41.77	56.28	65.80	77.71	86.52	95.28	115.76	124.93

The Gumbel Type Distribution has a constant positive skewness and it is commonly used for rainfall analysis because it fits the maximum rainfall data well. The calculations are carried out with Equation (A-10). K_t is a frequency factor and they are read from statistical tables. The frequency factor is based on sample size and recurrence interval. If the searching value does not exist in the table, linear interpolation is applied to calculate that value. The read frequency factors for sample size 79 and 2, 5, 10, 25, 50, 100, 500 and 1000 year return periods are -0.16, 0.791, 1.418, 2.199, 2.804, 3.39, 4.251 and 5.326. The calculated values are given in Table A.4.

$$x = \sigma * K_t + \mu \tag{A-10}$$

Table A.4: Rainfall values with corresponding return periods in mm (Gumbel Distribution)

Q_2	Q_5	Q_{10}	Q_{25}	Q_{50}	Q_{100}	Q_{500}	Q_{1000}
41.71	59.18	70.70	85.05	96.16	106.91	122.73	142.48

In addition to the mean and the standard deviation, the skewness coefficient is also used in the Pearson Type III Distribution. The frequency factor is taken from a table which is based on the skewness coefficient and recurrence interval. If the searching value does not exist in the table, linear interpolation is applied to calculate that value. The calculated frequency factors are -0.309, 0.607, 1.301, 2.22, 2.915, 3.610, 4.912 and 5.924 for 2, 5, 10, 25, 50, 100, 500 and 1000 year return periods. The extreme value calculations are based on Equation (A-10). The calculated rainfall values are given in Table A.5.

Table A.5: Rainfall values with corresponding return periods in mm (the Pearson Type III Distribution)

Q_2	Q_5	Q_{10}	Q_{25}	Q_{50}	Q_{100}	Q_{500}	Q_{1000}
39.00	55.81	68.56	85.43	98.20	110.97	140.63	153.41

The Log-Pearson Type III Distribution is frequently used in flood analysis. The natural logarithms of the maximum rainfall values are used. The procedure is same with the Pearson Type III Distribution. The Skewness coefficient is calculated as 0.606. The frequency factor is taken from the same table with the Pearson Type III

Distribution. If the searching value does not exist in the table, linear interpolation is applied to calculate that value. The calculated frequency factors are -0.01, 0.799, 1.328, 1.941, 2.362, 2.759, 3.449 and 3.968 for 2, 5, 10, 25, 50, 100, 500 and 1000 year return periods. The extreme value calculations are based on Equation (A-10). The calculated rainfall values are given in Table A.6.

Table A.6: Rainfall values with corresponding return periods in mm (Log-Pearson Type III Distribution)

Q_2	Q_5	Q_{10}	Q_{25}	Q_{50}	Q_{100}	Q_{500}	Q_{1000}
40.31	55.45	66.90	83.11	96.51	110.09	150.52	170.30

The calculations above are carried out for Hilvan State Meteorological Station too. The rainfall data includes years from 1956 to 2010. Hilvan State Meteorological Station maximum rainfall data is given in Table A.7.

Table A.7: Hilvan State Meteorological Station Maximum Rainfall Data

Years	Maximum Rainfall (mm)	Years	Maximum Rainfall (mm)
1956	-	1984	32.10
1957	26.80	1985	32.30
1958	58.90	1986	-
1959	70.30	1987	-
1960	126.70	1988	-
1961	41.70	1989	-
1962	40.20	1990	-
1963	53.80	1991	-
1964	68.10	1992	-
1965	38.30	1993	-
1966	30.70	1994	-
1967	45.80	1995	-
1968	-	1996	-
1969	-	1997	-
1970	38.80	1998	-
1971	35.60	1999	41.70
1972	43.50	2000	42.00
1973	28.50	2001	33.60
1974	-	2002	31.00
1975	28.20	2003	35.00
1976	-	2004	49.60
1977	-	2005	36.50
1978	-	2006	52.00
1979	-	2007	25.90
1980	-	2008	65.10
1981	50.50	2009	53.70
1982	-	2010	43.00
1983	-		

Using above approaches, the extreme value calculations for Hilvan are carried out and these values are summarized in Table A.8.

Table A.8: Rainfall values with corresponding return periods in mm

Statistical Distribution	Q_2	Q_5	Q_{10}	Q_{25}	Q_{50}	Q_{100}	Q_{500}	Q_{1000}
Normal Distribution	45.16	61.42	69.94	79.01	84.87	90.13	100.74	103.92
Log-Normal Distribution	42.37	56.43	65.59	76.95	85.32	93.61	112.86	121.44
Gumbel Distribution	42.07	61.85	74.85	91.29	103.5	115.57	142.52	155.87
The Pearson Type III Distribution	37.9	54.48	68.86	89.06	104.9	121.05	159.39	176.16
The Log-Pearson Type III Distribution	39.84	54.61	66.91	85.71	102.4	121.51	178.18	209.1

The Kolmogorov-Smirnov Test is used as a goodness of fit test. The results showed that majority of the statistical distributions are accepted at 0.1 significance level. The Log-Pearson Type III Distribution is selected as a statistical distribution.

Calculated discharges are given in Table A.9. Station rainfall values are the calculated values using Log-Pearson Type III Distribution. These values are converted to areal rainfall values using percentage area, maximize factor, rainfall-area factor and pluviograph factors. Maximize factor is usually taken as 1.13, rainfall-area factor is 0.973 for 3 hours rainfall and pluviograph factor is taken as 0.6 which is taken from Şanlıurfa State Meteorological Station. Then these rainfall values (mm) are converted to flow values (mm) using rainfall-flow curves. Curve number is chosen as 75 negotiating with State Hydraulic Works 15th Regional Directorate, Şanlıurfa. Then these values are multiplied with peak discharge value (m^3/s/mm) calculated with Equation A-5 to obtain peak discharge values (m^3/s).

Table A.9: Calculated peak discharges

Return Periods	Stations	Station Rainfall (mm)	Areal Rainfall (mm)	Areal Average Total Rainfall (mm)	Discharge (m^3/s)
2	Şanlıurfa	40.31	14.27	26.43	1.61
	Hilvan	39.84	12.16		
5	Şanlıurfa	55.45	19.63	36.30	6.85
	Hilvan	54.61	16.67		
10	Şanlıurfa	66.90	23.68	44.11	12.77
	Hilvan	66.91	20.42		
25	Şanlıurfa	83.11	29.42	55.58	22.97
	Hilvan	85.71	26.16		
50	Şanlıurfa	96.51	34.16	65.40	32.38
	Hilvan	102.35	31.24		
100	Şanlıurfa	111.09	39.33	76.42	43.19
	Hilvan	121.51	37.09		
500	Şanlıurfa	150.52	53.28	107.67	64.23
	Hilvan	178.18	54.39		
1000	Şanlıurfa	170.30	60.29	124.11	73.30
	Hilvan	209.10	63.82		